Author: Severin Lüps

Quality improvement of WegenerNet precipitation data and comparative analysis of precipitation extremes

Master's thesis

To obtain the academic degree

Master of Science
in Environmental Systems Sciences - Economics

submitted to the

University of Graz
Faculty of Environmental, Regional and Educational Sciences

Advisor: Univ.-Prof. Dr. Gottfried Kirchengast
Wegener Center for Climate and Global Change

Co-Advisor: Dipl.-Ing. Jürgen Fuchsberger
Wegener Center for Climate and Global Change

2022

Abstract

The WegenerNet Feldbach Region (FBR) climate station network in southeastern Austria comprises 156 meteorological stations covering an area of about 300 km^2. In addition to observing a variety of other meteorological parameters, ground precipitation data with a temporal resolution of 5 minutes are provided continuously since 2007. Due to the high spatial and temporal resolution, these data are particularly valuable for research on precipitation extremes at the regional scale. However, some inhomogeneities due to sensor changes, station re-locations, occasional clogging, and interpolations are inevitable. The main objective of this thesis is to find and quantify such errors stationwise, by comparing daily WegenerNet L2 v7.1 data (2007-2021) of each station with their respective neighbors' data. Turning points of the cumulative sum function of the normalized difference between the station and the median of its neighbors are used to detect breakpoints in the respective time series. A similar approach has been applied in different form to other WegenerNet parameters before. Based on the breakpoints found, the data are homogenized by determining correction factors through linear regression analyses for the relevant time periods and stations. The corrections are proposed as an improvement for the upcoming new data version of the WegenerNet, L2 v8, as they lead to a quality improvement by increasing homogeneity at stations affected. In addition to homogenization, the corrected data are compared in detail with respect to extreme precipitation with the uncorrected version v7.1 as well as with the standard data sets SPARTACUS, ERA5, ERA5-Land, and INCA. Findings include that individual extreme precipitation events in the FBR are not or inadequately represented in the analyzed data sets and that they tend to underestimate local precipitation amounts in the region.

Zusammenfassung

Das WegenerNet Feldbachregion (FBR) in der Südoststeiermark umfasst 156 Klimastationen, die eine Fläche von rund 300 km^2 abdecken. Neben der Messung von einer Reihe anderer meteorologischer Parameter werden seit 2007 kontinuierlich Bodenniederschlagsdaten mit einer zeitlichen Auflösung von 5 Minuten bereitgestellt. Aufgrund der hohen zeitlichen und räumlichen Auflösung sind diese Daten besonders wertvoll für die Erforschung von Niederschlagsextremen auf der regionalen Ebene. Einige inhomogenitäten aufgrund von Sensorwechseln, Stationsverlagerungen, zeitweiligen Verstopfungen und Interpolationen sind jedoch unvermeidlich. Das Hauptziel dieser Arbeit ist es, solche Fehler stationsweise zu finden und zu quantifizieren, indem die täglichen WegenerNet L2 v7.1 Daten (2007-2021) jeder Station mit den Daten der jeweiligen Nachbarstationen verglichen werden. Wendepunkte der kumulativen Summenfunktion der normalisierten Differenz zwischen einer Station und dem Median ihrer Nachbarn werden dabei verwendet, um "Breakpoints" in den jeweiligen Zeitreihen zu lokalisieren. Ein ähnlicher Ansatz wurde in abgewandelter Form bereits auf andere WegenerNet-Parameter angewandt. Auf der Grundlage der gefundenen Breakpoints werden die Daten homogenisiert, indem Korrekturfaktoren durch die Anwendung einer linearen Regressionsanalyse für die betreffenden Zeiträume und Stationen bestimmt werden. Die Korrekturen werden als Verbesserung für die kommende neue Datenversion des WegenerNet, L2 v8, vorgeschlagen, da sie zu einer Qualitätsverbesserung durch die Erhöhung der Homogenität bei betroffenen Stationen führen. Zusätzlich zur Homogenisierung werden die korrigierten Daten im Hinblick auf Extremniederschläge detailliert mit der unkorrigierten Version v7.1 sowie mit den Standarddatensätzen SPARTACUS, ERA5, ERA5-Land, und INCA verglichen. Die Ergebnisse zeigen, dass einzelne extreme Niederschlagsereignisse in der FBR in den Standarddatensätzen nicht oder nur unzureichend repräsentiert sind und diese dazu neigen, die lokalen Niederschlagsmengen in der Region zu unterschätzen.

Danksagung für Förderung

Diese Masterarbeit wurde durch ein Stipendium der Gemeinnützigen Privatstiftung zur Förderung der Forschung auf dem Gebiet der Versicherungswirtschaft sowie aus Mitteln des Wegener Center zur Nachwuchsförderung unterstützt.

Contents

List of Acronyms

AHYD Austrian Hydrographic Service

ANBS Agreeing Neighboring Station

BP Breakpoint

CRAS Command Receive Archiving System

DP-Flag Data Product Flag

DPG Data Product Generator

FBR Feldbach Region

PNBS Potential Agreeing Neighboring Station

QCS Quality Control System

WPS WegenerNet Processing System

ZAMG Central Institute for Meteorology and Geodynamics

1 Introduction

The relevance of high quality precipitation data emerges from the importance of being able to observe, model and forecast heavy precipitation both spatially and temporally. Mainly since in most regions of the northern hemisphere a climate change driven increase in e.g. one-day and five-day heavy precipitation can be observed since the 1950s, although the proportion of stations with a significant increase varies considerably between regions, with values of e.g. 6.6 % for Central end Western Europe compared to 14.4 % for Northern Europe and a total of 9.1 % (all values considering daily precipitation sums) (IPCC 2021, Sun et al. 2021).

At a global scale, a one-day event that happened once in ten years in 1850-1900 (seen as years without human influence) does already occur 1.3 times with 6,7 % relative increase in intensity (IPCC 2021). With 2 °C of global warming, such events are estimated to occur 1.7 times in 10 years with 14 % increase in intensity. At 4 °C, 2.7 events are expected, with an increase in intensity of 30.2 % (IPCC 2021). Under this premise, high-resolution precipitation data are highly valuable in the scientific community. However, due to potential high losses in assets, as seen after recent flooding events e.g. in Germany and Austria in summer 2021, such data become increasingly valuable in other areas as well. Next to the insurance and agricultural sector also e.g. in construction and urban planning data are needed. High quality precipitation data therefore play an important role in being a basis for risk assessments and subsequently in minimizing losses and enabling adaptation.

Precipitation data usually are obtained from direct gauge measurements or remote sensing by e.g. satellites and radar. While gauge measurement as a direct measurement method is less prone to systematic errors, remote sensing methods have the advantage of being less spatially limited in conducting measurements. However, since remote sensing is an indirect measurement technique, gauge data are also used as reference for evaluation and as input component to increase the overall quality of remote sensing data (O et al. 2017, Sharifi et al. 2016, Nerini et al. 2015). Ground monitoring gauge station networks with a high spatial and temporal resolution thus are highly valuable.

Such a high density ground weather station network is the WegenerNet in the Feldbach region (FBR), located in the southeast of the Austrian state of Styria (Kirchengast et al. 2014, Fuchsberger, Kirchengast & Kabas 2021). It includes 156 weather stations in an area of about 300 km^2. Designed to serve as a long-term monitoring and validation facility for weather and climate research and applications, it provides continuous precipitation data since 2007. However, providing data from many stations and at a high temporal resolution of 5 minutes, inhomogeneities can be expected. Mainly from clogging, sensor changes, station re-locations and interpolation of unreliable data by the WegenerNet Processing System (WPS).

The main objective of this thesis is to find and quantify such errors station-wise, by comparing daily WegenerNet L2 v7.1 data, documented by Fuchsberger, Kirchengast, Bichler, Leuprecht & Kabas (2021), of each station with their respective neighbors' data. Subsequently, found inhomogeneities are to be corrected by applying linear correction factors. Furthermore, the information content of precipitation extremes in the improved data set, denoted as WegenerNet L2 v8, is compared against the previous version (WegenerNet L2 v7.1), and other standard data sets. These are SPARTACUS ("SPARTACUS"), ERA5 ("ERA5"), & ERA5-Land ("ERA5 Land"), and INCA ("INCA") documented by Hiebl & Frei (2018), Hersbach et al. (2018, 2020), Muñoz Sabater (2019) and Haiden et al. (2011) respectively.

This thesis will address the above tasks in five sections. Chapter 2 focuses on the description of the study region and the WegenerNet FBR and outlines the research question. Chapter 3 describes the research setup, including data description and preprocessing, a variance analysis and a detailed method description. Two main methods are applied. For finding breakpoints in the data, a modified version of an algorithm described by Taylor (2000) is used. Confidence in biases is drawn by the level of agreement of daily precipitation amounts between the candidate station and selected neighboring stations. Second, for finding adequate correction factors for all breakpoints, a station wise linear regression analysis is applied. Results of both methods are discussed in detail in Chapter 4.

Next to documenting the correction factors and analyzing the changes in quality, using statistical parameters, the information content about extreme precipitation in the region and at example locations is compared to above mentioned data sets. This is done to evaluate possible improvements and highlight differences in the resolution and magnitude of extreme precipitation information content. Furthermore the limits of the used methods and results are described. The chapter closes with a re-correction, in which the methods are applied again on the corrected data, to allow for adjustments and to ensure that no overcorrections occurred. This re-correction ultimately determines the final proposed correction factors. We conclude by summarizing the main results in Chapter 5.

2 Study region and research aims

2.1 WegenerNet Feldbach Region

The WegenerNet FBR, a high resolution hydro-meteorological station network, that is located in the Raab river valley, southeast of the Austrian state of Styria (Kirchengast et al. 2014, Fuchsberger, Kirchengast & Kabas 2021). Regionally typical hills, known as riedel, with altitudes ranging from 250 m to 600 m, dominate the terrain. Summers are often hot, with heavy rainfall from thunderstorms, while winters are mild. This is due to the strong influence of Mediterranean climate systems from the south, as the region is surrounded by mountain ranges from north to west (O et al. 2018).

In total 156 meteorological stations are spread over an area of 300 km^2 measuring a wide range of meteorological parameters. The network provides continuous data starting from January 2007 with a temporal resolution of 5 min and an average spatial density of one station per 2 km^2. The allocation of the stations and their type is shown in Figure 2.1.
While all base stations measure the parameters air temperature, liquid precipitation and relative humidity, there are stations with additional sensors. Stations designated as Special Base Stations in addition measure soil parameters and so-called Primary Stations additionally measure solid precipitation and wind parameters. Furthermore, a reference station in the center of the network does measure the base parameters but also radiation, air pressure, solid precipitation and wind parameters (Scheidl et al. 2020).
Since 2020, also 3D atmospheric sensors, such as a precipitation radar, microwave and infrared radiometers, and GNSS ground stations, are in use at selected stations. However, the present thesis focuses on the 2D ground-station data data and the former will thus not be discussed in detail. As visible in Figure 2.1 the network also includes four external stations, two of which are operated by the Central Institute for Meteorology and Geodynamics (ZAMG) and two by the Austrian Hydrographic Service (AHYD).

The WPS is processing all raw data automatized and is divided in three main components. The Command Receive Archiving System (CRAS), the Quality Control System (QCS) and the Data Product Generator (DPG).
These components have already been described in detail by Kirchengast et al. (2014) and in a recent update, by Fuchsberger, Kirchengast & Kabas (2021). Therefore, we will discuss only the basic functions and provide details about the collection of precipitation data, which is the main subject of this thesis.
Raw data are sent hourly to the WegenerNet servers by the CRAS as Level 0 data. Next, the QCS applies reliability checks on the Level 0 data, mainly by comparing stations

with each other and climatological plausibility testing (Scheidl et al. 2020). The data is then stored as Level 1 data and serve as input for the DPG. The DPG allows to interpolate QCS flagged values, generate time series data with larger periods and interpolate values for grid data products. Hence, data that are output of the DPG are considered Level 2 data and carry a Data Product Flag (DP-Flag), indicating whether and how the value was interpolated (Scheidl et al. 2020).
Regarding precipitation measurement, at each station the integrated amount of every 5 min is sampled and transmitted every hour. After being checked by the QCS, the data are fed into the DPG and values are interpolated and flagged if necessary. As output, data are available as Level 2 time series data, ranging from sub-daily, starting at 5 min, to annual (O et al. 2018, Fuchsberger, Kirchengast & Kabas 2021).

In this analysis, daily level 2 data are used for the determination of breakpoints and the calculation of correction factors. For the comparative analysis of the results, hourly and daily data are used.

Three different sensor types have been installed in the WegenerNet so far. Therefore, all three types are in operation at the reference station. The primary stations are additionally equipped with a heating system to be able to measure solid precipitation (O et al. 2018). Since 2013, the MeteoServis type MR3H ("Meteoservis") is used fore this purpose, which replaced the R.M. Young type 52202 ("Young"). The base stations and thus the majority of the stations were, until 2016, all equipped with unheated Theodor Friedrichs & Co type 7041.2000 ("Friedrichs")(O et al. 2018). They were however, successively replaced with unheated Meteoservis sensors. Which has thus become the primary sensor used in the network. All sensors operate according to the tipping bucket principle and specifications are provided by Young (2022), Meteoservis (2022) and Theodor Friedrichs & Co (2022) respectively. Whereas a detailed description of implementation and usage in the WegenerNet FBR is provided by Szeberényi (2014) & Kabas (2012).

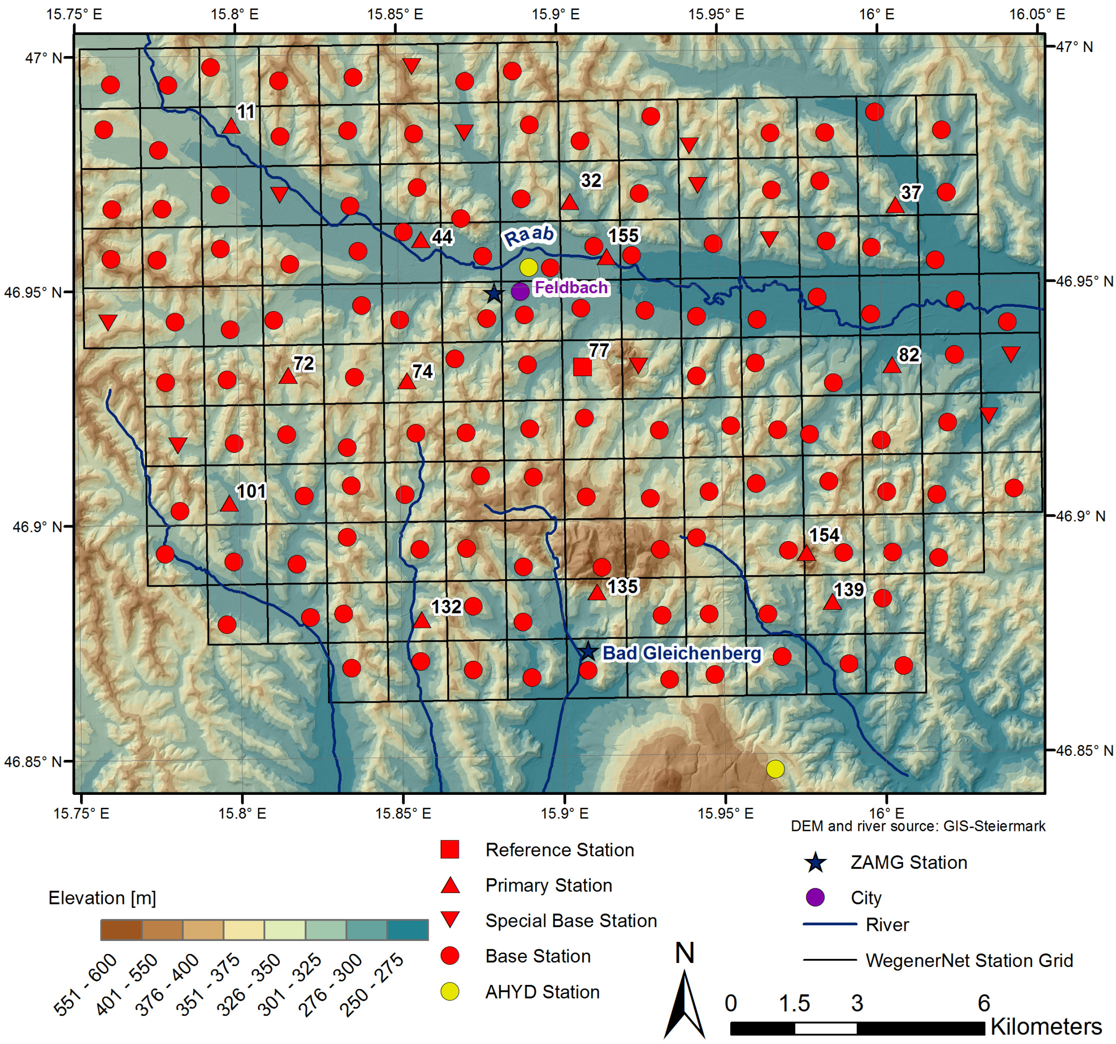

Figure 2.1: Region overview, locations, and types of the WegenerNet FBR stations.

2.2 Motivation and aims

Providing long-term data from a large number of sensors at a high spatial and temporal resolution comes with the potential for breakpoints in the data and the need to homogenize. Breakpoints can occur primarily due to sensor changes, sensor relocation, clogging and false interpolations of unreliable data by the WPS. Since different sensors are used, systematic sensor type specific errors are also possible.
The latter has already been investigated and corrected in detail for the Friedrichs and Young sensors by O et al. (2018). Finding a relative bias for both, when compared to external stations (ZAMG and AHYD) of around 12 % (O et al. 2018). However, since a breakpoint analysis has not yet been performed on a station-by-station basis and the time series has been too short for O et al. (2018) to check for systematic errors concerning the now primarily used Meteoservis sensors, there is room for further quality improvement.

This thesis aims to close this gap and improve the quality of the WegenerNet FBR precipitation data, in view of the release of the upcoming data version v8.
Thus, each station is checked for breakpoints individually and is corrected if applicable and it is analyzed if systematic errors with Meteoservis sensors are present.
As mentioned above, for the scientific community and others the value of high quality precipitation data lies mainly in the information content about extreme precipitation. Therefore, the second objective, evaluating the improvements and comparing them to other data sets, will be conducted with a focus on heavy precipitation. Thereby, the previous WegenerNet L2 v7.1 and the above introduced standard data sets SPARTACUS, ERA5 & ERA5 Land and INCA are used as comparison and analyzed in respect to heavy precipitation by e.g. providing the differences in the 95th percentile exceedance time series (daily and hourly).

3 Data and methods

3.1 Data and preprocessing

The data basis for homogenization is the WegenerNet L2 v7.1 dataset. Full documentation is provided by Fuchsberger, Kirchengast, Bichler, Leuprecht & Kabas (2021) and data can be accessed via the WegenerNet data portal on the website at wegenernet.org. The daily precipitation amount subset for the fifteen year period from 2007 to 2021 is used in this study. Based on 5 min precipitation amounts, this dataset contains aggregated 24-hour precipitation amounts for each station in the network with the day beginning at 6 am UTC.

For the breakpoint analysis the data set is limited to wet days with a precipitation amount of at least $2\,\mathrm{mm\,d^{-1}}$. This is done to optimize the adapted breakpoint detection algorithm described by Taylor (2000) which is discussed in detail in Section 3.3. For the regression analysis and hence the determination of correction factors, the data set is limited to periods from April to October to prevent solid precipitation and associated distortions to influence the factors. Further, it is restricted to wet days with at least $1\,\mathrm{mm\,d^{-1}}$ and a DP-Flag of $\leq 10\ \%$. This serves to minimize the influence of days with very low intensities and allows to improve on accuracy regarding significant precipitation amounts.

3.2 Variance analysis

Before homogenizing the data station wise, a general variance analysis appears useful to assess the data. Figure 3.1 shows a box-and-whisker plot of the relative deviation of each station from the mean annual precipitation amount in the WegenerNet FBR (2007-2021). It can be observed that for most years, a symmetrical distribution can be assumed. The interquartile range lies for most years in between $\pm 5\,\%$ relative deviation and is never exceeding $\pm 10\,\%$. Maxima and minima vary over the years, but except in the years 2009, 2012, 2015 and 2018, do not exceed $\pm 20\,\%$ of relative deviation. Every year shows outliers, most of which underestimate precipitation and reinforce the assumption that there is room for homogenization.

It is conceivable that stations that deviate strongly from the mean value might do so due to their location and exposure, and are not necessarily subject to breakpoints or systematic errors. Therefore, in the following we will consider if location and altitude

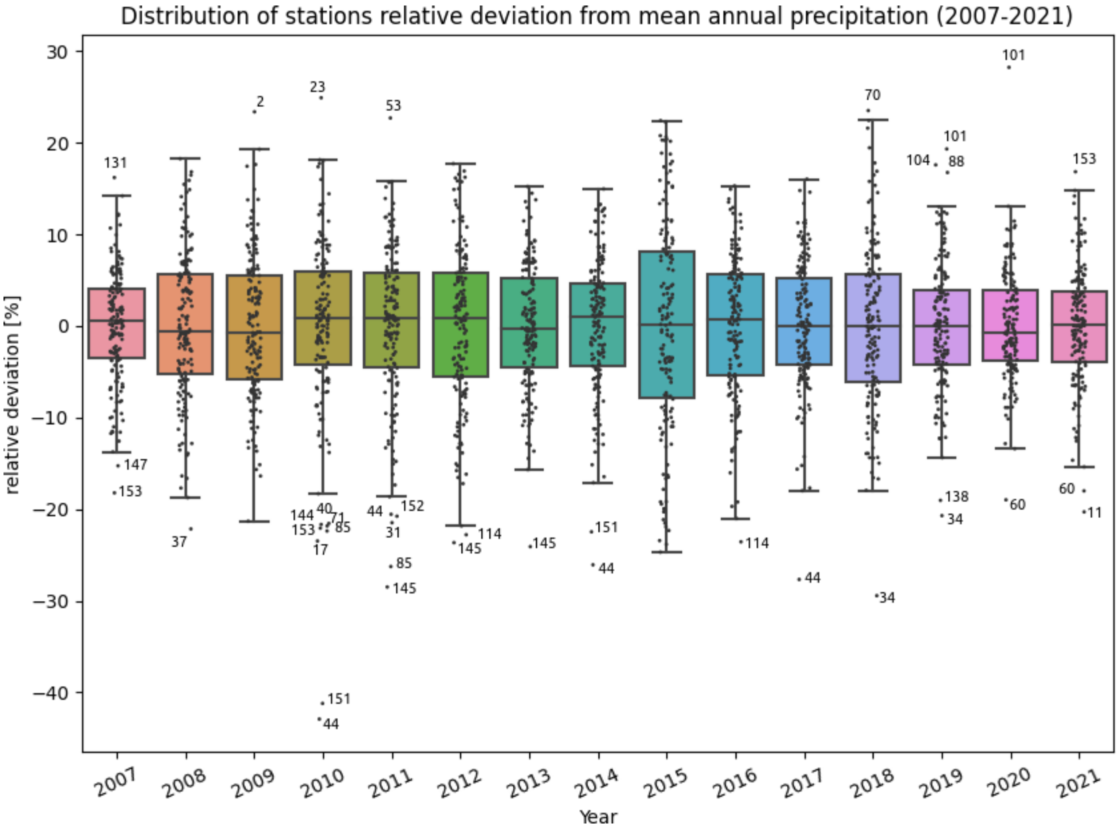

Figure 3.1: Relative deviation of station precipitation amounts from the WegenerNet L2 v7.1 regional-mean annual precipitation amount.

influence the measurement. Regarding location, Figure 3.2 shows the mean annual precipitation amount over 15 years (2007-2021) and for the years 2019 and 2020 separately. Regarding the average over the last 15 years it can be observed that there is a gradient from northwest to southeast, with highest precipitation amounts in the northwest. Part of the variance therefore can be explained by the positioning of the stations. However, this correlation occurs to varying degrees over time. While exemplary in the year 2019 location variation appears to be quite strong, this is not the case for 2020 (see Figure 3.2). A possible further explanation, as stated above, could be the stations altitude. When the mean annual precipitation is plotted against the stations' altitude, Figure 3.3, no clear relationship can be found.

In summary, positioning of stations in the network indeed plays a role in explaining the variance, albeit fluctuating over time. However, the altitude of the stations does not. Systematic errors and breakpoints are further explanations. Those, unlike the location bias, must be homogenized.

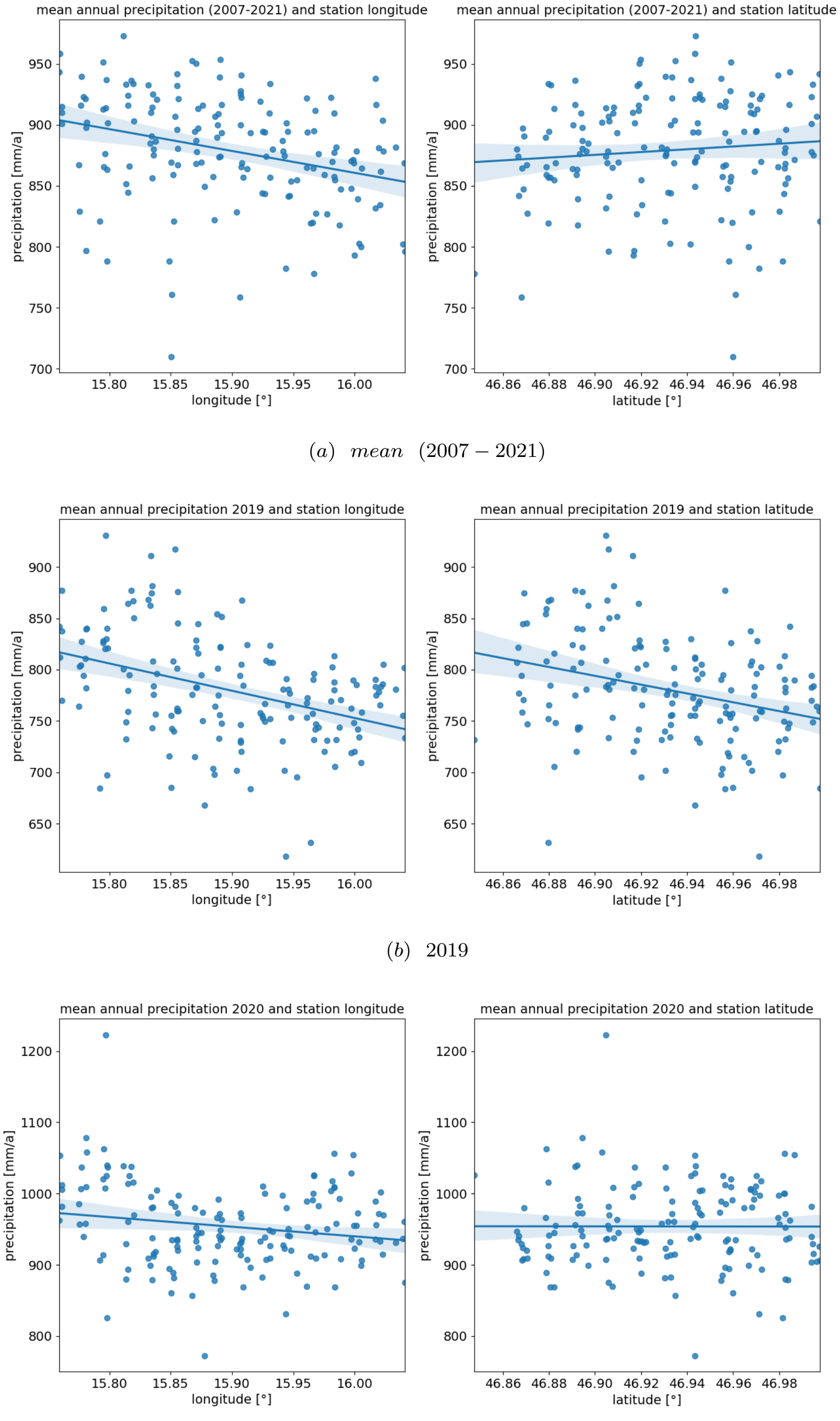

(a) *mean* (2007 − 2021)

(b) 2019

(c) 2020

Figure 3.2: Annual precipitation amount (long-term mean and example years 2019 and 2020) in dependence of the station location (longitude left, latitude right).

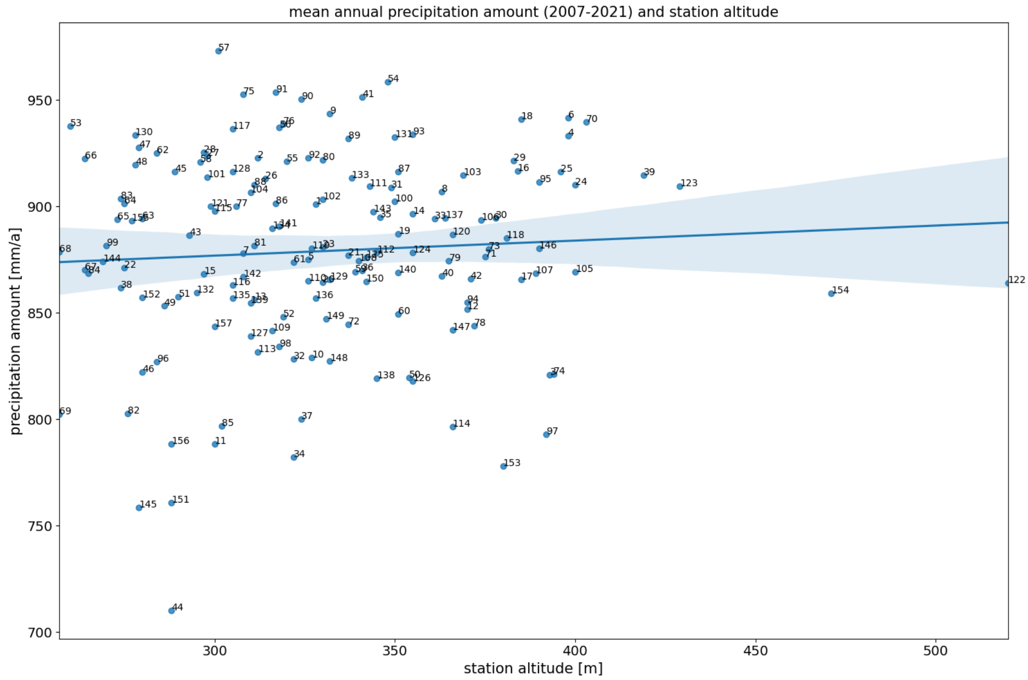

Figure 3.3: Annual precipitation amount of the WegenerNet FBR stations (identified by station number) in dependence of station altitude.

3.3 Breakpoint detection algorithm

The breakpoint detection is based on an algorithm described by Taylor (2000), which is using turning points of the cumulative sum function to detect breakpoints in timeseries data. In the present case, the normalized cumulative sum of the increment is used. The increment is given by the difference between the daily mean precipitation amount of the station and the median of prior selected neighboring stations. This approach was also used by Ebner (2017) and Scheidl et al. (2020) to homogenize WegenerNet relative humidity and air temperature data. In the present case however, the increment is calculated as the relative difference (rather than the absolute difference used in the above cited works) between measurements of the candidate station and its neighbors. While this, in addition to the adjustment of other parameters, can be seen as the main structural difference in the usage of the algorithm, in selecting neighboring stations and deciding on breakpoints we follow closely the work by Scheidl et al. (2020) which built up on and improves the implementation by Ebner (2017).
In the following we describe how the increment value is calculated and how the algorithm is detecting the breakpoints.

For each candidate station, Agreeing Neighboring Stations (ANBS) are selected. To be selected as ANBS, the Potential Agreeing Neighboring Stations (PNBS), which are all stations within a 5 km radius of the candidate station, must fulfil the following condition:

$$\sqrt{\frac{1}{n}\sum_i\left(\frac{p_i-c_i}{c_i}-\frac{\bar{p}-\bar{c}}{\bar{c}}\right)^2} < t\cdot\sqrt{\frac{1}{n}\sum_i\left(\frac{c_i-\bar{c}}{\bar{c}}\right)^2} \tag{3.1}$$

where

$$\begin{aligned}
n &= \text{number of available days}\\
p_i &= \text{precipitation amount of PNBS on day i}\\
c_i &= \text{precipitation amount of the candidate station on day i}\\
\bar{p} &= \text{daily mean precipitation amount of the PNBS}\\
\bar{c} &= \text{daily mean precipitation amount of the candidate station}\\
t &= \text{accordance level}\begin{cases}0.7 \text{ for breakpoint detection}\\ 0.8 \text{ for regression analysis}\end{cases}
\end{aligned}$$

Thus the PNBS is accepted as ANBS if the standard deviation of the relative difference between the PNBS and the candidate station is smaller than 70 % of the coefficient of variation of the candidate station.
The increment I_i of the candidate station on day i is calculated as follows, where a_i denotes the data of the corresponding ANBS stations:

$$I_i = \frac{c_i - \text{median}(a_i)}{\text{median}(a_i)} \tag{3.2}$$

Note that in order to calculate the increment at day i, only ANBS stations with a DP-Flag ≤ 20 % are allowed and at least 5 ANBS stations must be available.

Aiming to find the breakpoints in the candidate station data, the cumulative sum of the normalized increment for each day i needs to be calculated:

$$C_i = \sum_{k=1}^{i} I_{norm,k} \tag{3.3}$$

where

$$\begin{aligned}
I_{norm,i} &= I_i - \bar{I}\\
C_0 &= 0
\end{aligned}$$

Using the cumulative sum as a function C of the time (days), the potential first order breakpoints are found at the minimum and maximum value of C:

$$\begin{aligned}
cp_{min} &= \text{argmin}(C)\\
cp_{max} &= \text{argmax}(C)
\end{aligned}$$

To be accepted as a significant breakpoint however, the potential breakpoints must fulfil the following condition:

$$|C(cp)| > 1.96 \cdot \mathrm{std}[CB(cp)] \tag{3.4}$$

where CB are the cumulative sum values of 1000 bootstraps at the breakpoint day cp. Thereby, a bootstrap is the normalized increment of the candidate station but randomly rearranged. The confidence is given with lying outside 1.96 standard deviations which is equivalent to 95 %.

The algorithm is applied stations wise three times recursively, searching the time span before, between and after the found breakpoints. Periods that are smaller than 21 days are not processed. The algorithm also skips the first and the last 7 days of the processed interval as implemented by Scheidl et al. (2020).
As output, the algorithm provides the dates of significant first, second, and third order breakpoints for each station as output. These dates are used as reference points for the regression analysis in order to quantify the discrepancies and calculate the correction factors.

3.4 Regression analysis

The regression analysis is carried out station wise and examines the relationship between the candidate stations' daily data and the median of the corresponding ANBS set, using regression through the origin. Two purposes are fulfilled. On the one hand, it is checked if significant slope differences between sensor types are present, by analyzing time series in which different sensor types were mounted separately. This allows to check for sensor change discrepancies which are not detected by the breakpoint detection and to determine correction factors for all sensor change induced inhomogeneities. On the other hand, the time series before, after, and between all other dates found by the breakpoint detection are analyzed. This enables the quantification of all other found inhomogeneities and the determination of adequate correction factors.

In order to reinforce reasoning for this approach, the regression analysis was also carried out against the data of the external ZAMG stations for close by WegenerNet stations. This was done to verify that using the ANBS median as a reference does not involve any internal biases. The slopes showed only marginal differences when plotted against ZAMG or ANBS data such that the approach seems robust. Furthermore, it has the advantage over the single use of spatially poor distributed external data, that spatial differences are preserved after correction, since locally close reference data become available for every station investigated.

The correction factors are defined as the difference of the respective regression line slope to the slope of the reference time span, which, as reasoned in Section 4.1, is the slope of the Meteoservis time series of the respective station. Only differences with the absolute amount being ≥ 0.05 are considered worthy of correction. If the reference slope

is not feasible due to strong inhomogeneities, the difference to 1 or, if available, to a slope of another homogeneous time span of the station is utilized. This procedure is used to reduce possible distortions of the spatial characteristics of the stations' due to the correction.
The ANBS stations are determined in the same way as the breakpoint detection algorithm, but with different parameters. PNBS stations are all stations in a 3 km radius of the candidate station and become an ANBS if they fulfil the condition 3.1. Note that the accordance level is set to 0.8. In order to calculate the ANBS median, ANBS stations must have a DP-Flag $\leq$ 20 % and at least 5 ANBS stations must be available.
The regression line *slope* is calculated as follows:

$$slope = \frac{\sum_{i=1}^{N}(C_i \cdot A_i)}{\sum_{i=1}^{N} A_i^2} \tag{3.5}$$

where

$$\begin{aligned} N &= \text{number of paired daily datasets available} \\ i &= \text{the } i\text{th day} \\ C_i &= \text{data from candidate station} \\ A_i &= \text{ANBS median data} \end{aligned}$$

Note that for the fit of the linear regression line the increment is forced to 0. The corresponding correlation coefficient r is calculated according to the following equation:

$$r = \sqrt{\frac{\sum_{i=1}^{N} \widehat{C_i}^2}{\sum_{i=1}^{N} C_i^2}} \tag{3.6}$$

where

$$\widehat{C_i} = i\text{th fitted value of the candidate station data}$$

To provide further information and to evaluate the improvement after homogenization, the following statistical parameters are calculated for each candidate station. In the selection, we followed closely the homogenization work by O et al. (2018). The $bias$ (eq. 3.7), mean absolute error MAE (eq. 3.8), relative bias $rbias$ (eq. 3.9), relative mean absolute error $rMAE$ (eq. 3.10), and the root mean squared error $RMSE$ (eq. 3.11):

$$bias = \frac{\sum_{i=1}^{N}(C_i - A_i)}{N} \tag{3.7}$$

$$MAE = \frac{\sum_{i=1}^{N} |C_i - A_i|}{N} \tag{3.8}$$

$$rbias = \frac{\sum_{i=1}^{N}(C_i - A_i)}{\sum_{i=1}^{N} A_i} \cdot 100 \tag{3.9}$$

$$rMAE = \frac{\sum_{i=1}^{N} |C_i - A_i|}{\sum_{i=1}^{N} A_i} \cdot 100 \tag{3.10}$$

$$RMSE = \sqrt{\frac{\sum_{i=1}^{N}(C_i - A_i)^2}{N}} \tag{3.11}$$

4 Results and discussion

4.1 Breakpoint analysis

Figure 4.1 shows an example of the output of the breakpoint detection analysis for station 10. The first panel provides the temporal course of the increment, the mean increment, the offset between the mean increment before and after a breakpoint (BP), and dates of sensor and location changes. The second panel contains the cumulative sum function, the respective bootstraps, and the found BP's. Panel three supplies the data availability for each day. The last panel provides the DP-Fag percentage value of the respective data point (days).

Two noticeable inhomogeneities can be observed in this example. Next to a temporary change in measurement during a short period in 2011, between the tertiary BP and the secondary BP (see Figure 4.1), a significant primary BP at the visible inflection point of the cumulative sum function was detected. It coincides with the sensor change to Meteoservis on July 5, 2016. A noticeable difference in the time series before and after the sensor change is thus detected, which is then quantified in the regression analysis where the correction factors are obtained using the respective slopes.
Figure 4.2 shows the results for station 4 as another example that shows many BPs. In this case, next to a sensor change induced primary BP and secondary and tertiary BP's, another primary BP on April 12, 2011 is detected. However, the cause of this primary BP remains unknown. A change in exposure, sensor malfunction, or unnoticed clogging are potential causes.

These two examples demonstrate the functionality of the detection. While the sensor change dates are documented and the breakpoint detection gives a first indication if it is conspicuous, it is first and foremost dates of such other primary BP's that are searched for station by station. Subsequently all documented sensor change dates and all found primary BP dates are used as input in the regression analysis and correction factors are obtained if required. A list of all found primary breakpoint is provided in Table 4.1. Dates of secondary and tertiary BP's are only passed into the regression analysis, if the respective time series of the station appears to be especially worthy to break down further. However, this remains an exception. In the case of station 10, for example, this was omitted because the corrected time series obtained is considered too short.
While station 4 is an example of strong inhomogeneity with primary and many third and tertiary BPs, station 56 in Figure 4.3 demonstrates the opposite, a very homogeneous time series. In this case only a tertiary BP is detected and the sensor exchange did not

have any significant influence on the series.

In general, each station shows a differently homogeneous pattern, which is to be expected. In addition to the expected differences in frequency and type of BPs, only for about 37 % of the stations, the sensor changes to Meteoservis is detected as a BP. Note that an exact assignment of the relevant BP to the sensor change day is sometimes difficult. They do not always match perfectly, as there may be dry periods between the change and the first measurement of the new sensor. However, this gives a first indication that the Meteoservis sensors do not require any systematic correction. As pointed out in Chapter 2, the previous sensors Friedrichs and Young are already subject to a linear systematic correction, introduced by O et al. (2018).

In addition, the breakpoint detection graphically shows that the Meteoservis time series for most stations tends to be more homogeneous than the time spans of the previous sensors. This impression is affirmed and quantitatively substantiated by the regression analysis and underpins that a general correction of the Meteoservis sensors seems not to be necessary. Furthermore, this gives reason to use the Meteoservis time series as reference period for the station-specific corrections. This was realized, apart from a few exceptions where a visibly more homogeneous time series was available as reference.

Station	primary BP	Station	primary BP	Station	primary BP	Station	primary BP
2	2015-05-01	47	2015-03-02	81	2016-09-17	119	2008-11-30
3	2016-07-13	47	2021-05-27	82	2009-06-27	119	2018-02-08
4	2011-04-12	48	2017-06-25	82	2019-06-27	120	2007-07-07
4	2016-07-31	49	2008-12-01	83	2008-03-24	120	2014-02-11
5	2011-05-15	49	2016-08-21	83	2016-06-19	121	2011-09-18
6	2016-08-29	50	2007-08-18	84	2017-06-10	123	2019-07-17
7	2016-07-16	50	2016-07-26	85	2013-05-05	124	2017-07-24
8	2009-05-24	51	2016-01-06	86	2012-05-21	125	2007-08-10
9	2016-07-28	52	2012-07-14	87	2012-10-29	126	2008-06-23
10	2016-06-30	52	2021-05-27	88	2016-01-06	126	2017-07-24
11	2017-07-23	53	2016-07-31	89	2012-10-29	127	2017-06-25
13	2016-06-05	54	2011-06-14	90	2016-08-21	128	2016-07-16
14	2016-02-09	55	2010-12-03	93	2018-07-15	129	2011-09-18
15	2016-05-14	57	2007-06-07	94	2012-05-28	131	2009-12-22
16	2009-05-22	57	2016-06-30	94	2018-07-15	132	2013-08-28
16	2016-06-15	58	2014-04-14	95	2011-06-23	133	2016-09-04
17	2011-07-02	59	2016-02-09	95	2018-06-12	134	2014-06-03
19	2011-08-09	60	2018-05-29	96	2016-07-31	135	2010-08-15
20	2014-07-10	61	2013-05-05	97	2016-09-06	136	2019-06-05
23	2011-08-27	62	2012-11-12	98	2016-10-10	137	2017-12-10
24	2015-04-28	63	2016-08-10	99	2019-08-02	138	2013-06-02
25	2015-03-26	64	2007-08-18	101	2018-09-23	139	2012-04-22
27	2016-07-06	64	2013-04-12	104	2012-11-28	140	2016-09-16
30	2010-05-13	65	2017-06-25	105	2007-06-06	141	2017-08-27
31	2014-10-01	66	2017-07-24	105	2017-06-24	142	2016-08-16
32	2008-04-29	67	2019-06-27	106	2017-06-28	143	2007-08-10
32	2016-05-23	68	2011-04-12	107	2017-07-01	143	2014-02-11
33	2013-12-29	69	2016-11-19	108	2008-07-26	144	2018-03-05
34	2014-09-14	70	2012-03-19	108	2014-07-22	145	2009-01-16
36	2015-02-22	71	2011-06-23	109	2016-05-13	145	2016-05-23
37	2013-09-17	72	2013-07-11	110	2010-02-26	146	2019-08-24
38	2015-07-17	73	2011-05-21	110	2018-03-06	147	2012-03-19
39	2019-05-09	74	2013-04-02	112	2008-06-20	148	2013-08-09
40	2009-07-05	75	2016-08-09	113	2008-06-30	149	2009-07-15
40	2016-06-26	76	2021-07-17	113	2016-05-23	150	2017-04-14
42	2013-08-24	78	2014-07-25	114	2007-08-07	151	2016-05-14
44	2011-07-22	78	2018-02-04	114	2016-10-02	152	2013-05-06
44	2018-06-12	79	2017-06-24	116	2016-05-23	154	2017-12-29
45	2013-04-12	80	2018-06-06	117	2011-07-02	155	2020-09-27
46	2015-05-15	81	2008-06-06	118	2012-09-19		

Table 4.1: Overview of Primary Breakpoints (BP) found.

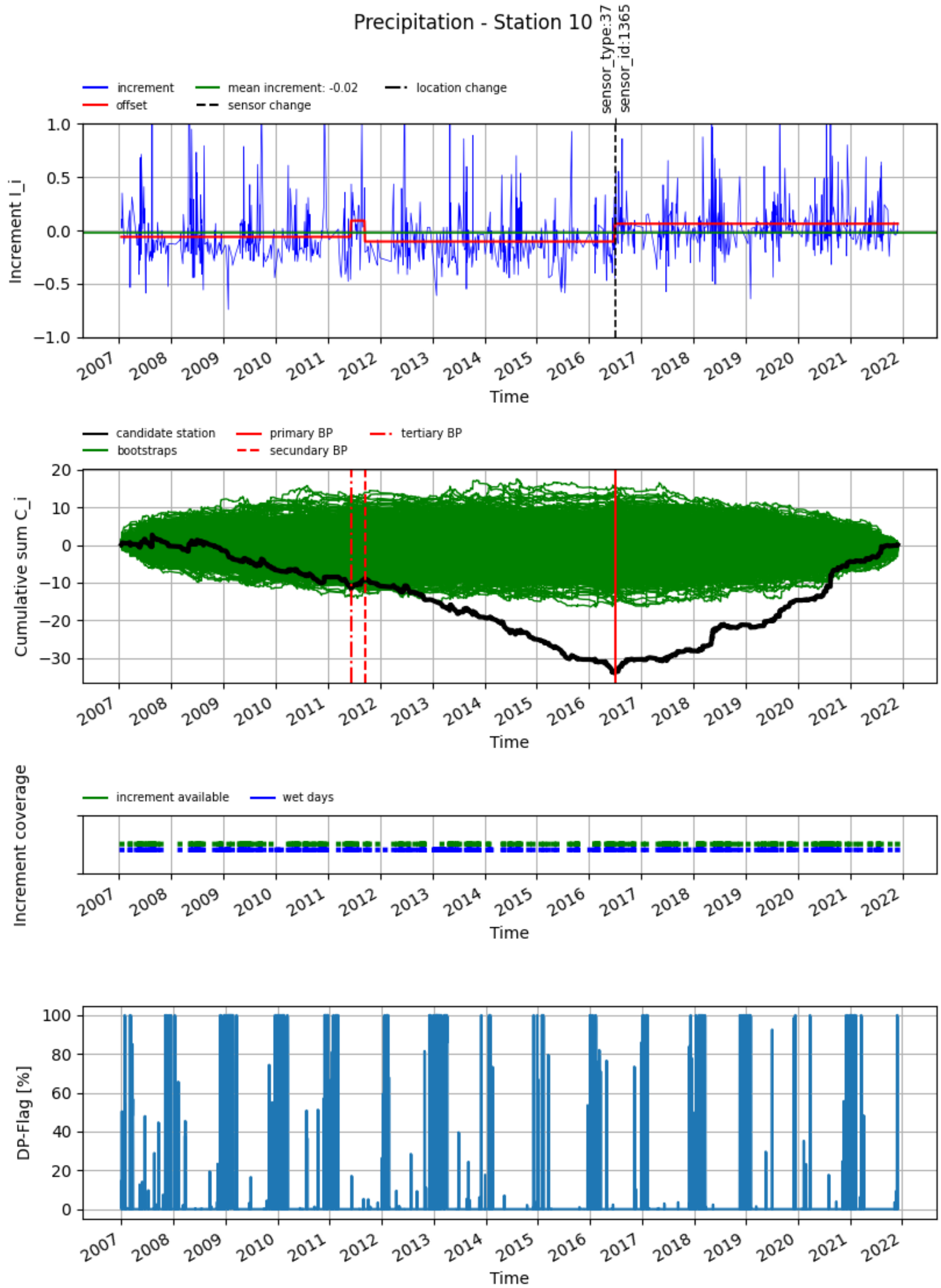

Figure 4.1: Result of breakpoint detection for example station 10.

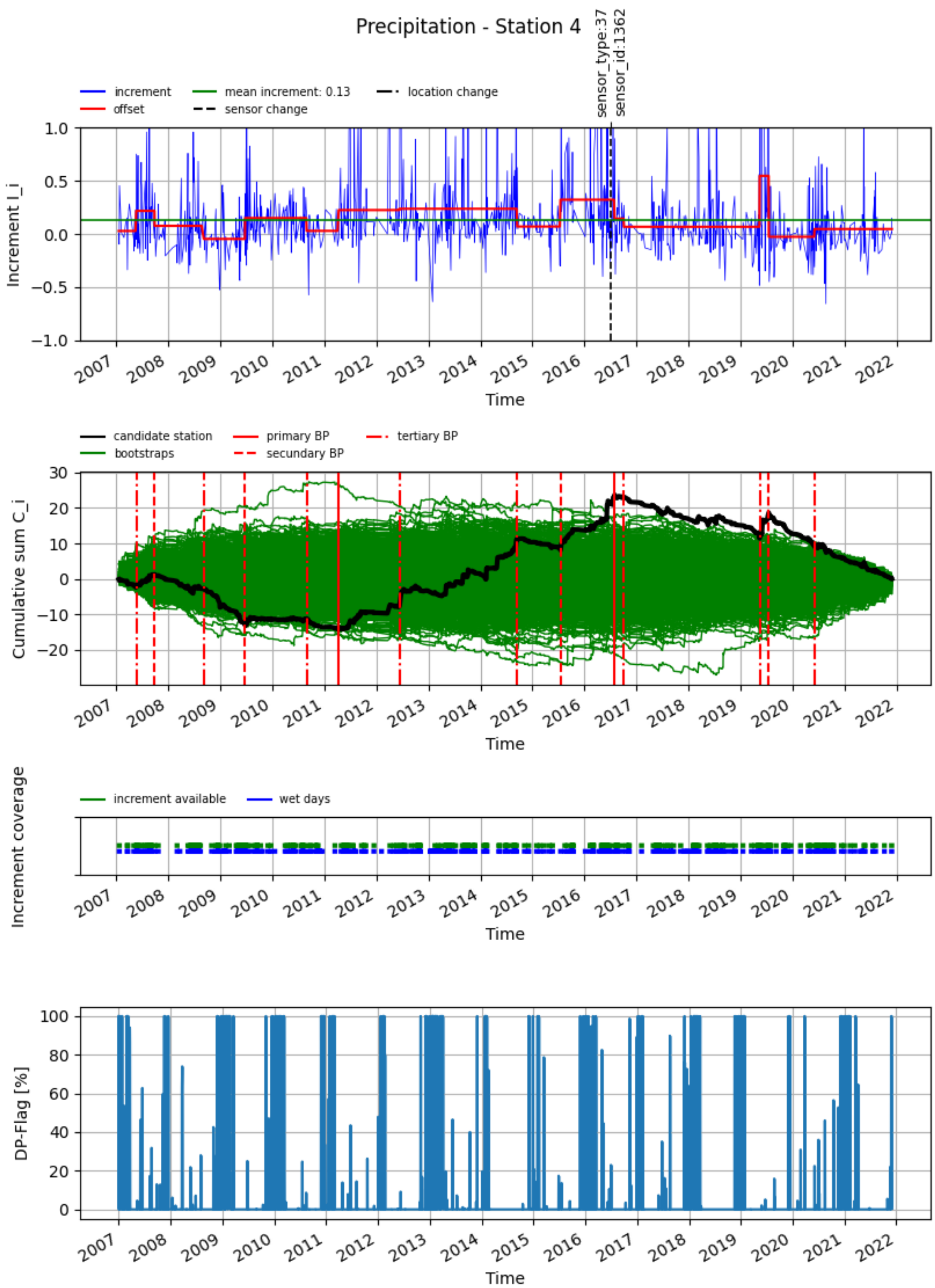

Figure 4.2: Result of breakpoint detection for example station 4.

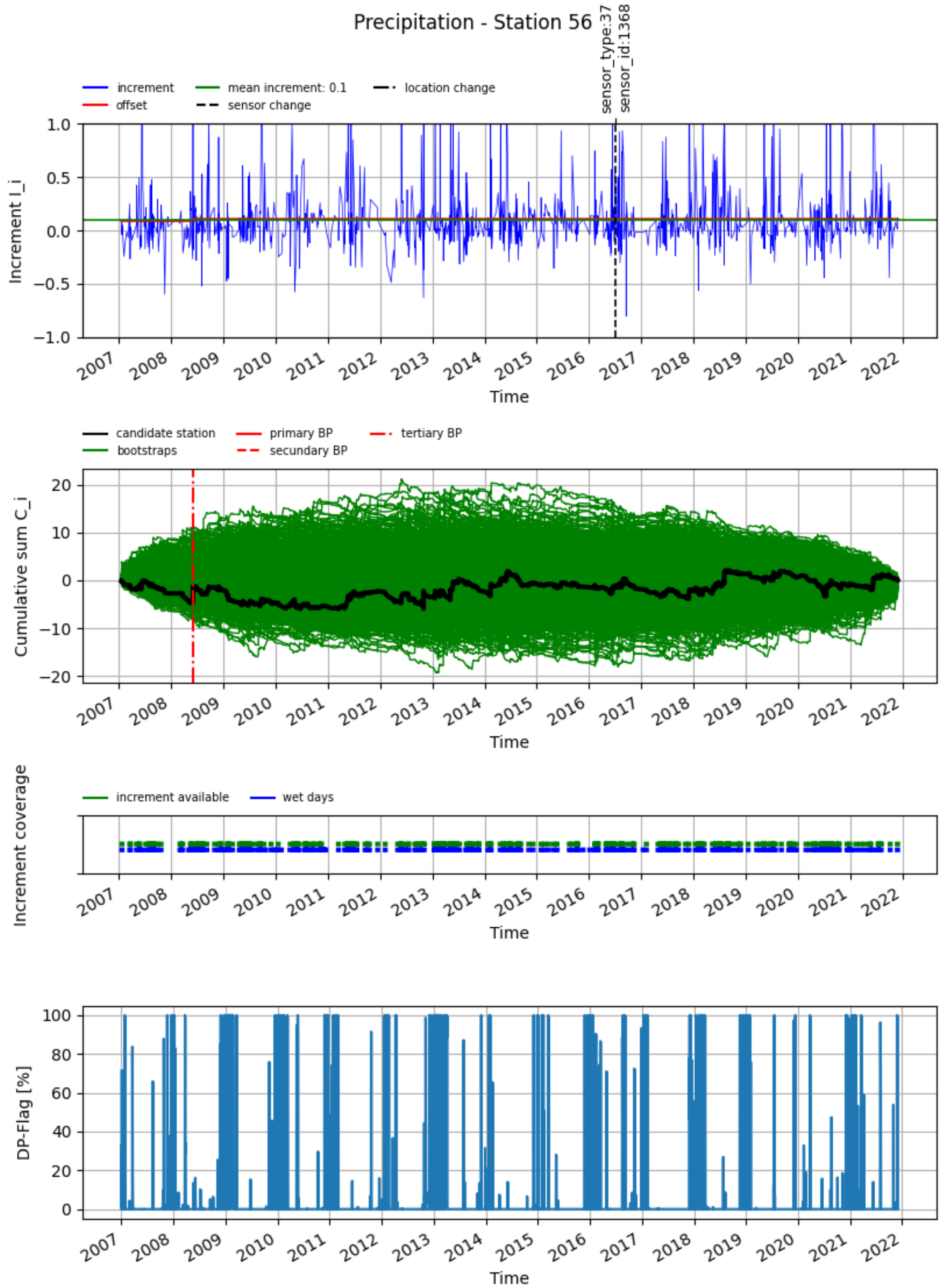

Figure 4.3: Result of breakpoint detection for example station 56.

4.2 Correction factors from regression analysis

Figure 4.4 shows an example of the regression analysis for the above described time series of station 10. In this case, as seen in in Figure 4.1, only one primary BP which is inline with the sensor change date was found. Note that the BP, as documented in Table 4.1, is on June 30, 2016. However, the exact senor change was documented on July 5, 2016. Since the latter date is more accurate, it is this date which is used for the analysis.

Two time spans are analyzed. Before the sensor change on July 5, 2016, in which the Friedrichs sensor operated, and after, where the Meteoservis sensor is operational. The latter is taken as the reference as outlined in Section 4.1 and Section 3.3. The absolute slope difference of 0.16 between the first time span (0.89) and the reference (1.05) is $\geq$ 0.05. Therefore, the value 0.16 is accepted as the correction factor for the period before the sensor replacement.

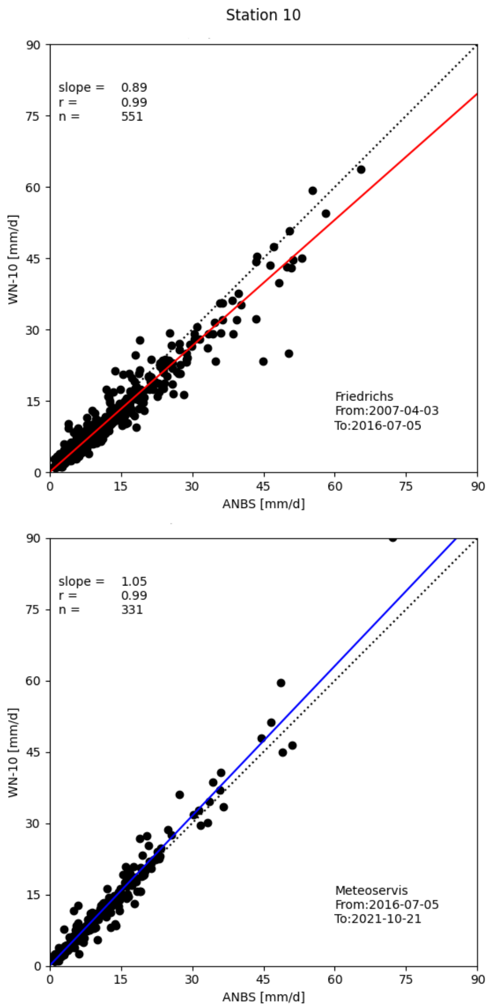

Figure 4.4: Regression analysis - result for example station 10.

In the case of multiple BPs, as it is the case for station 4 described above, multiple time periods are analyzed. In this case, from the beginning of the measurement series to the first breakpoint, from the first breakpoint to the sensor change date (second primary BP), and from the change date to the end of the time series.

All slopes of the respective time periods are provided in Figure 4.5. The reference slope value equals to 1.03 (bottom right panel). For the first period, from start to the first BP (top left panel) with a slope of 1.09, the difference to the reference slope results in a correction factor of -0.06. For the second period, from the first BP to the sensor change (bottom left panel) with a slope of 1.15, a correction factor of -0.12 is obtained analogously.

Following this procedure, all stations were checked with regard to the time span before and after the documented sensor change. For those stations where the breakpoint detection provided additional primary breakpoints, cf. Table 4.1, additional slopes for the respective periods were calculated. The obtained correction factors and the begin and end date of the periods to which they were applied are listed in Table 4.2. Note that corrections listed in Table 4.2 as station 7730, -31 and -32 correspond to the Friedrichs, Young and Meteoservis sensor at station 77 respectively.

As the reference station of the network, all sensor types used work in parallel at this station and were therefore analyzed and corrected individually. Note that due to limitations described in Section 4.6, changes will be made to the correction factors and the below factors are therefore preliminary. The final correction factors are documented in Table 4.5.

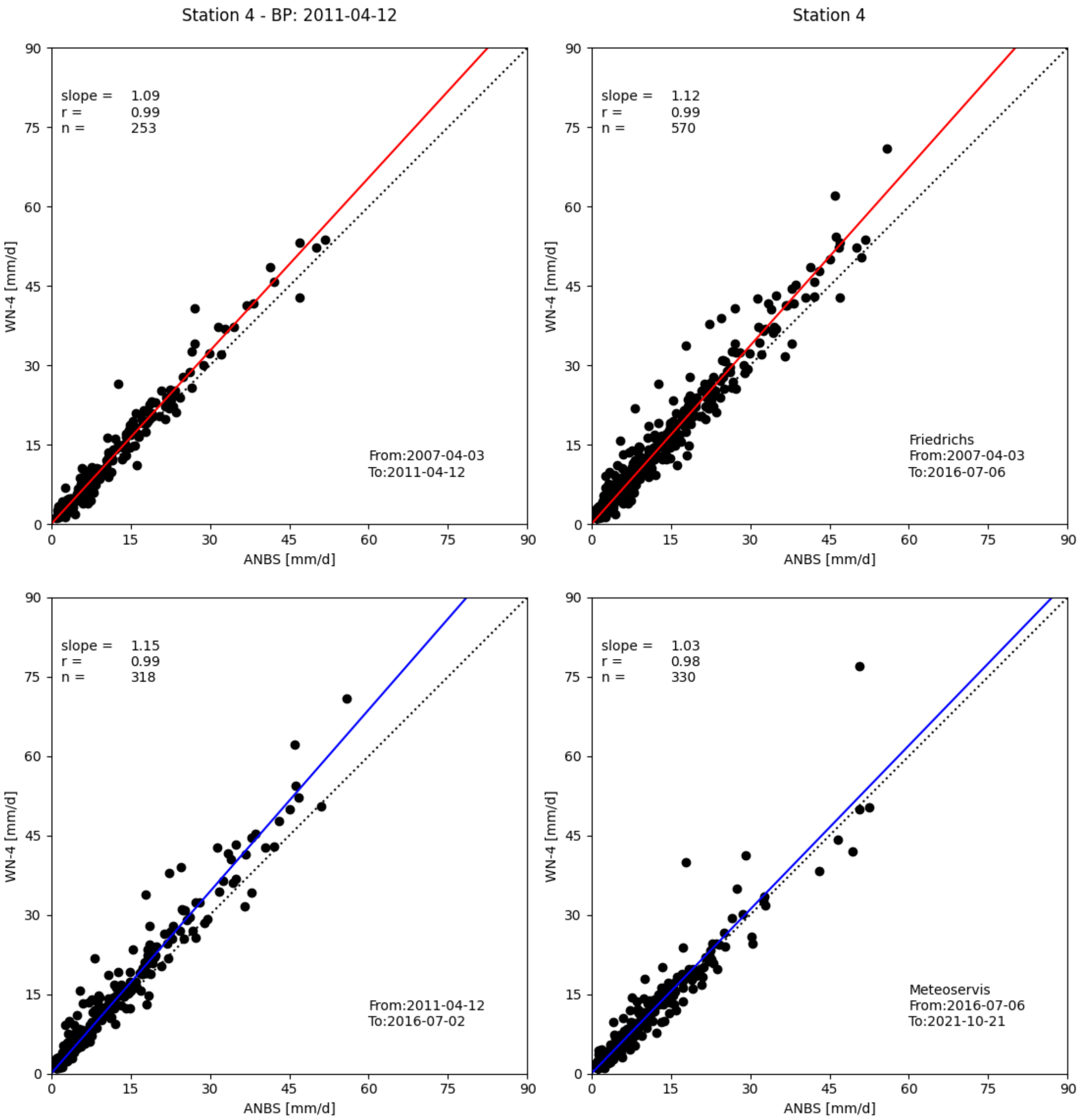

(a) Start - first BP - second BP (sensor change)

(b) Start - sensor change - end

Figure 4.5: Regression analysis - result for example station 4.

Station	Begin	End	Correction factor
3	2007-01-01	2016-07-05	0.09
4	2007-01-01	2011-04-12	-0.06
4	2011-04-12	2016-07-06	-0.12
5	2007-01-01	2011-05-15	0.09
6	2007-01-01	2016-07-08	-0.09
7	2007-01-01	2016-07-08	0.08
8	2009-05-24	2016-07-08	-0.05
10	2007-01-01	2016-07-05	0.16
11	2007-01-01	2013-10-07	0.05
13	2007-01-01	2016-07-06	0.05
15	2007-01-01	2016-07-08	0.12
16	2009-05-22	2016-07-08	-0.08
17	2007-01-01	2011-07-02	0.06
19	2007-01-01	2011-08-09	-0.09
20	2014-07-10	2016-08-08	-0.06
22	2018-06-08	2018-09-01	-0.15
22	2018-09-01	2099-12-31	-0.08
23	2007-01-01	2011-08-27	-0.16
24	2007-01-01	2016-07-05	0.06
25	2016-07-05	2099-12-31	-0.06
27	2007-01-01	2016-07-04	-0.13
30	2007-01-01	2010-05-13	0.03
31	2014-10-01	2016-07-09	-0.08
32	2008-04-29	2013-10-07	0.06
34	2007-01-01	2014-09-14	-0.06
36	2015-02-22	2016-08-09	-0.05
37	2007-01-01	2011-07-17	-0.09
37	2011-07-17	2012-04-23	-0.12
37	2012-04-23	2013-10-08	-0.06
38	2007-01-01	2015-07-17	0.09
39	2016-07-05	2019-05-09	0.14
40	2007-01-01	2009-07-05	-0.08
40	2009-07-05	2016-07-05	0.12
42	2007-01-01	2013-08-24	0.18
42	2013-08-24	2016-07-06	0.1
44	2007-01-01	2011-07-22	0.1
44	2011-07-22	2013-10-08	0.24
44	2013-10-08	2018-06-12	0.1
46	2007-01-01	2015-05-15	0.06
47	2007-01-01	2015-03-02	-0.07
48	2007-01-01	2016-07-05	-0.09
50	2007-01-01	2016-08-29	0.08
51	2007-01-01	2016-08-09	0.07
52	2012-07-14	2015-03-02	0.05
53	2007-01-01	2016-08-09	-0.11
59	2007-01-01	2016-08-22	0.12
60	2018-05-29	2021-12-17	0.14
61	2007-01-01	2013-05-05	0.06
61	2013-05-05	2016-08-28	0.05
62	2012-11-12	2016-08-27	0.05
64	2007-01-01	2016-07-05	0.05
66	2007-01-01	2016-08-29	-0.08
68	2011-04-12	2016-08-09	-0.06
69	2007-01-01	2016-08-09	0.07
70	2007-01-01	2012-02-19	0.06
71	2007-01-01	2011-06-23	0.12
71	2011-06-23	2016-08-22	0.05
72	2007-01-01	2013-10-05	-0.05
75	2007-01-01	2016-08-24	-0.13
78	2007-01-01	2014-07-25	0.07
78	2014-07-25	2016-08-27	0.25
80	2018-06-06	2099-12-31	-0.05
82	2007-01-01	2009-06-27	-0.07
83	2007-01-01	2016-08-10	-0.1
84	2017-06-10	2099-12-31	-0.06
85	2007-01-01	2013-05-05	0.15
87	2012-10-01	2016-08-22	-0.08
88	2016-01-06	2016-08-22	-0.05
88	2016-08-22	2099-12-31	-0.07
89	2012-10-29	2016-08-24	-0.08
90	2007-01-01	2016-08-28	-0.09
93	2016-08-29	2018-07-15	-0.08
96	2007-01-01	2016-08-27	0.08
98	2007-01-01	2016-08-23	0.07
101	2018-09-23	2099-12-31	-0.19
104	2016-08-24	2099-12-31	-0.06
105	2007-01-01	2016-06-28	0.05
106	2007-01-01	2016-08-28	0.08
107	2007-01-01	2014-09-26	0.05
107	2017-07-01	2099-12-31	-0.07
109	2007-01-01	2016-08-29	0.12
111	2007-01-01	2016-08-26	-0.05
112	2007-01-01	2008-06-20	-0.05
113	2008-06-30	2014-11-14	0.05
113	2014-11-14	2016-08-23	0.17
116	2007-01-01	2016-08-23	0.08
119	2007-01-01	2008-11-30	-0.13
119	2018-02-08	2019-09-02	-0.13
119	2019-09-02	2099-12-31	-0.08
121	2007-01-01	2016-08-25	-0.06
123	2007-01-01	2016-08-29	-0.05
126	2008-06-23	2016-08-23	0.1
126	2017-07-24	2099-12-31	-0.07
127	2007-01-01	2016-08-23	0.08
128	2007-01-01	2016-08-23	-0.06
129	2011-09-18	2016-08-08	0.08
134	2014-06-03	2016-08-25	-0.06
135	2007-01-01	2010-08-15	-0.16
137	2016-08-26	2017-12-10	-0.06
139	2007-01-01	2012-04-22	-0.3
139	2012-04-22	2013-10-21	-0.09
142	2007-01-01	2016-08-25	0.12
143	2007-01-01	2007-08-10	-0.13
143	2014-02-11	2016-08-25	-0.07
145	2007-01-01	2009-01-16	0.09
145	2009-01-16	2016-08-26	0.2
148	2007-01-01	2016-08-24	0.05
7730	2015-07-10	2018-08-10	0.06
7730	2018-08-10	2099-12-31	-0.06
7731	2007-01-01	2013-10-16	-0.29
7732	2007-01-01	2014-01-14	-0.08
7732	2017-10-11	2099-12-31	-0.11

Table 4.2: Overview of preliminary correction factors from the regression analysis.

4.3 Quality parameters for results assessment

A comparison of the quality parameters described in Section 3.4, before and after the correction, reveals and quantifies the homogeneity improvements achieved. Two analyses were performed. A comparison of all WegenerNet stations before and after correction, see Table 4.3, and a comparative comparison where only the corrected stations were considered, see Table 4.4.

In both cases the parameter values of all respective stations were grouped by sensor type and the mean value of the respective parameter was calculated. In the *after correction* panel of both tables, parameters that have improved compared to the respective *before correction* panel are marked in green, if they have worsened in red, and if they have remained the same in gray.

Before correction:

Sensor group	*bias* [mm/d]	*MAE* [mm/d]	*rbias* [%]	*rMAE* [%]	*RMSE* [mm/d]
Young	0.13	1.8	1.05	18.28	3.2
Friedrichs	0.24	1.37	2.39	13.26	2.37
Young+Friedrichs	0.23	1.4	2.26	13.62	2.43
Meteoservis	0.24	1.25	2.66	13.42	2.53

After correction:

Sensor group	*bias* [mm/d]	*MAE* [mm/d]	*rbias* [%]	*rMAE* [%]	*RMSE* [mm/d]
Young	-0.38	1.6	-3.87	15.92	2.88
Friedrichs	0.25	1.3	2.41	12.56	2.27
Young+Friedrichs	0.21	1.32	1.99	12.79	2.31
Meteoservis	0.24	1.24	2.65	13.3	2.49

Table 4.3: Quality parameters for all WegenerNet stations (average), grouped by sensor type.

Before correction:

Sensor group	*bias* [mm/d]	*MAE* [mm/d]	*rbias* [%]	*rMAE* [%]	*RMSE* [mm/d]
Young	0.11	1.87	0.92	19.08	3.32
Friedrichs	0.13	1.42	1.38	13.71	2.45
Young+Friedrichs	0.13	1.47	1.33	14.27	2.54
Meteoservis	0.22	1.26	2.41	13.54	2.52

After correction:

Sensor group	*bias* [mm/d]	*MAE* [mm/d]	*rbias* [%]	*rMAE* [%]	*RMSE* [mm/d]
Young	-0.44	1.65	-4.45	16.49	2.96
Friedrichs	0.22	1.31	2.13	12.67	2.3
Young+Friedrichs	0.15	1.34	1.45	13.06	2.37
Meteoservis	0.18	1.25	2.02	13.45	2.48

Table 4.4: Quality parameters for corrected stations only (average), grouped by sensor type.

In both analyses, the MAE, $rMAE$ and $RMSE$ improved significantly for all sensor groups. Thus, the prediction error has decreased and all sensor groups show a higher agreement with the reference (ANBS median). Hence, the data have a significantly higher homogeneity. Note that a spatial representation of the improvement is given by grid data comparison in the next subsection. However, it also reveals, with exception of the Meteoservis and the combined Friedrichs + Young sensor group, the latter only when all stations are considered, that the $bias$ and $rbias$ parameters have slightly worsened.

While the differences in the Friedrichs and the Friedrichs + Young group are minor ($< 0.1\,\mathrm{mm\,d^{-1}}$ for $bias$ and < 1 pp. for $rbias$), the Young group appears to have a stronger negative bias. Since only very few Young sensors were corrected, it seems likely that this is due to a possible overcorrection of station 139. The respective Young sensor faced a strong positive bias and was considerably corrected downwards (cf. Table 4.2). It is conceivable that the now slightly negative bias was triggered by this. However, this also implies that the previously strong positive bias has averaged out in the group.

It should be noted, that the homogeneity for this and all other stations has nevertheless improved because the prediction error decreased or equivalently, the agreement with the reference improved. However, for the two groups mentioned, the magnitude and direction of the deviation changed slightly. Whether and to what extent certain stations, such as 139, should therefore be corrected again is being investigated separately in Section 4.6.

4.4 Comparative analysis with a focus on extreme precipitation

4.4.1 Mean annual precipitation and differences in monthly precipitation

Figure 4.6 shows the averaged annual precipitation (2007-2021) for the uncorrected data version v7.1 (right panel) and for the corrected version v8 (left panel) in a 200 m x 200 m resolution. Clearly visible dark spots, indicating stations with a strong negative bias, have significantly been reduced. Examples are in particular station 44, 144 and 11 (cf. Figure 2.1). Moreover, the general spatial distribution of precipitation appears to be significantly smoother, while the gradient pattern remained.

This is substantiated when comparing mean annual precipitation (μ) and the corresponding standard deviation (σ) and coefficient of variation (CV). All values are provided in Figure 4.6. Data version v8 shows a 3.53 mm higher μ value and both σ and the CV have decreased significantly, indicating higher uniformity. Despite the higher level of homogeneity, light and dark spots, indicating deviating stations, are still visible in the v8 version. Suggesting that stations have not been corrected, were insufficiently corrected, or overcorrected. A closer look and possible re-corrections are therefore considered in Section 4.6.

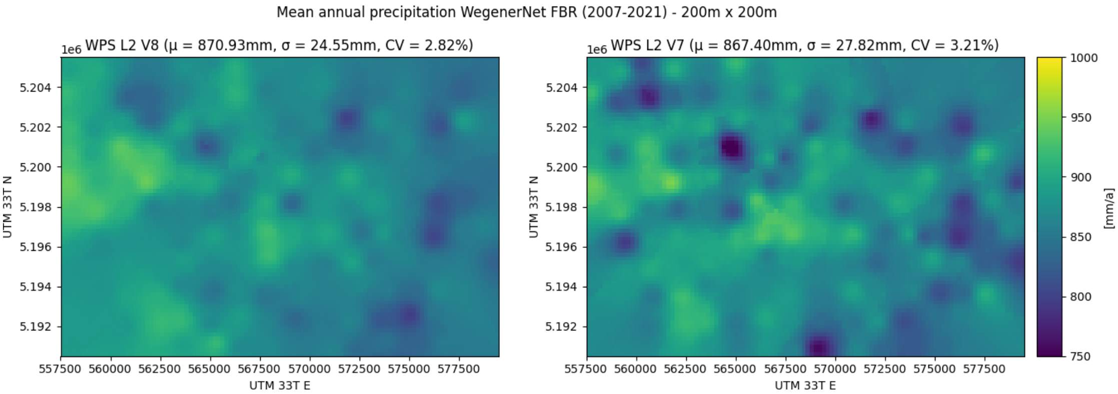

Figure 4.6: Mean annual precipitation amounts v8 vs. v7.1.

Figure 4.7 and Figure 4.8 provide the same analysis on a 1 km x 1 km grid in comparison to the ERA5 and ERA5 Land data set. In both cases μ is again lower than the respective WegenerNet value, but the σ and the CV value are smaller as well. However, a possible explanation for the uniform distribution are the minimal spatial differences in the comparative data sets visible. While both data sets indicate a northwest-southwest gradient in precipitation, albeit in slightly different magnitudes, hardly any differences are visible at grid cell level when compared to the WegenerNet data.

The comparison with the SPARTACUS data, Figure 4.9, shows a similar picture with regard to the calculated parameters. However, the comparative data set exhibits much more pronounced spatial differences, which overlap with the distribution in the WegenerNet data. Lower precipitation in the northeast and southeast and tendentially more precipitation towards the center and southwest of the Feldbach region.

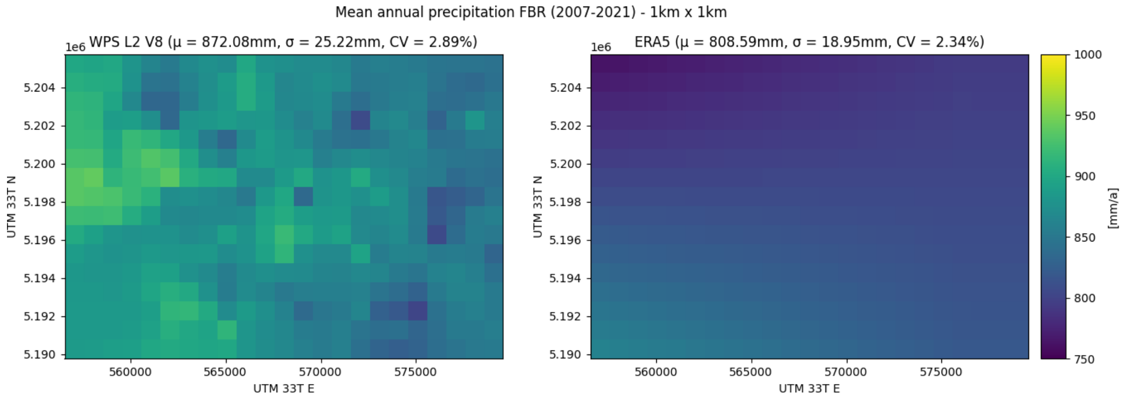

Figure 4.7: Mean annual precipitation amounts v8 vs. ERA5.

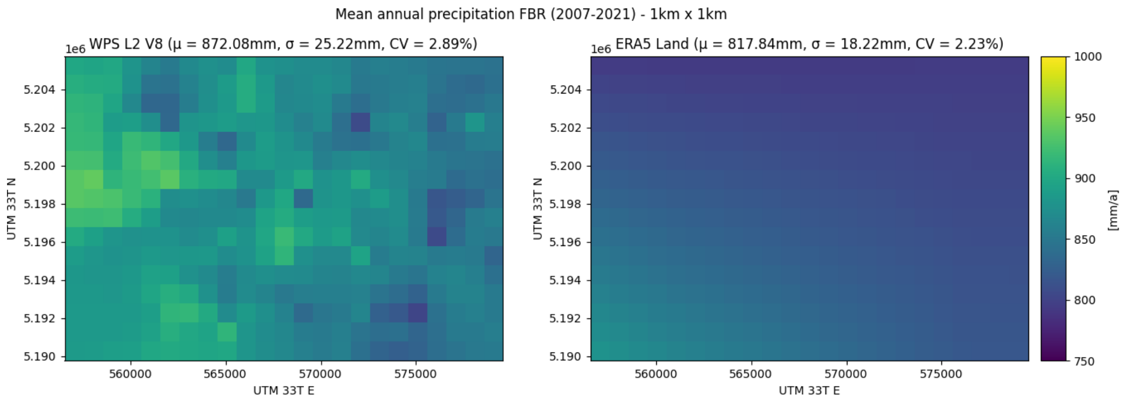

Figure 4.8: Mean annual precipitation amounts v8 vs. ERA5-Land.

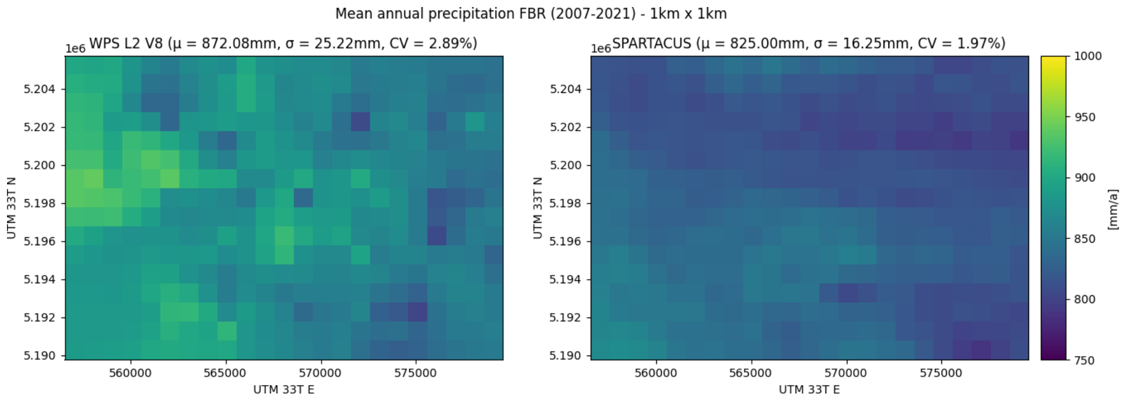

Figure 4.9: Mean annual precipitation amounts v8 vs. SPARTACUS.

Regarding mean annual precipitation, it can be concluded that the corrected data are significantly more homogeneous and smoother compared to the previous version v7.1. The comparative data sets considered show a lower regional mean value and distribution parameters, but also significantly less spatial differences and thus information content.In order to take a closer look at differences to the previous data version v7.1, the difference and relative difference in monthly precipitation sums are analyzed in Figure 4.10. Two main changes become visible.

First, the precipitation amount has increased in most summer months due to the corrections. However, these increases remain well below 5 %, albeit with five exceptional months in 2010-2012. In addition, it becomes clear that this applies more sharply to the period up to 2016. This is due to the fact that the transition to Meteoservis sensors was completed in this year, which faced fewer and smaller corrections. Second, many winter months show significantly less precipitation. This is due to an update of the WPS solid precipitation detection and interpolation algorithm, introduced in version v8. This is therefore not to be seen as an effect of the present correction but due to the improvement in the handling of solid precipitation.

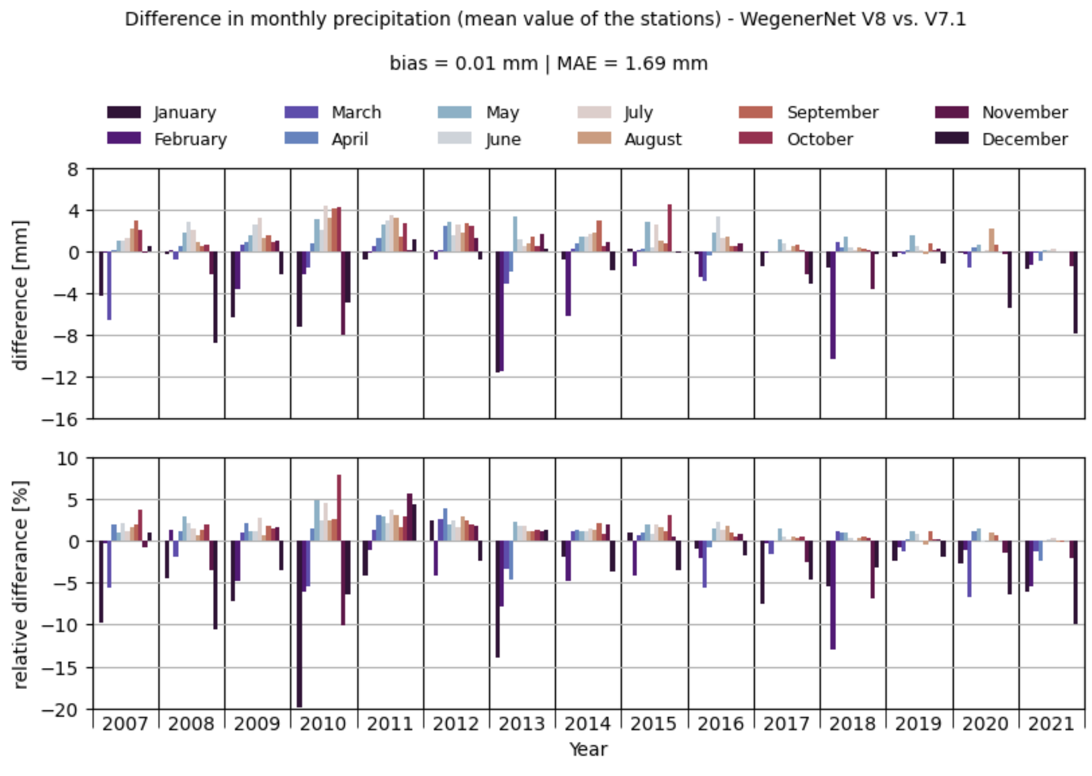

Figure 4.10: Difference in monthly precipitation amounts v8 vs. v7.1.

4.4.2 Differences in extreme precipitation

Analyses of changes in the information content of extreme precipitation events as a result of homogenization, as well as respective differences to the comparative data sets, are conducted using four different measures. Each of these measures is analyzed concerning the region and two selected locations within the FBR. The latter is intended to also demonstrate changes at grid cell level. The two locations selected are Feldbach and Fehring. Feldbach was chosen as it is the location of one of two ZAMG stations within the FBR, of which the data are included in both the INCA and SPARTACUS model data sets. Fehring, on the other hand, was chosen because it is afield from the ZAMG stations such that the weight in the INCA and SPARTACUS data is expected to be smaller. This allows a differentiated comparison between the datasets, as well as an investigation of the influence of station proximity on the model-driven datasets INCA and SPARTACUS.

The first measure is the maximum 24 hour precipitation sum per month (24HMMax), analyzed from April to October. Thereby the 24HMMax difference between the v8 data and the respective comparative data set is examined. Note that consequently, the WegenerNet v8 data determines the date where the respective 24HMMax is located. The second measure is analogous to 24HMMax, but examines the maximum amount of precipitation per hour during a month, denoted as 1HMMax. For each comparative data set, the date where the 1HMMax is located is determined by the v8 data, but the exact time (hour) on the specific day remains a degree of freedom. Thus, the sum of the strongest hour in each set on the determined day are used to calculate the 1HMMax difference.

The last two measures examine the exceedance of the 95th percentile of 24- and 1-hour precipitation totals per month from April to October. The percentiles were calculated using daily (> 0.99 mm) and hourly (> 0.33 mm) v8 grid data covering 15 years (2007-2021). The calculated values are $31.50\,\mathrm{mm\,d^{-1}}$ and $7.30\,\mathrm{mm\,h^{-1}}$, respectively. In addition to the amount of exceedance, defined as measured millimeters above the percentile per month, the difference from the WegenerNet v8 data is also considered.

Figure 4.11 shows the 24HMMax difference (top) between the WegenerNet v8 and v7.1 data version. Except for a few month, the difference is positive, indicating that the correction in general lead to an increase of the 24HMMax amounts. The provided relative difference reveals that this increase, except for 4 month, is less than +5 %. Furthermore the increase is more pronounced up to the year 2016. This is consistent with stronger corrections for sensors in operation prior to the 2016 replacement with Meteoservis sensors.

Regarding the change in the 1HMMax difference (bottom), the picture is similar as to be expected. The corrections resulted in higher 1HMMax values in the new data version, with most values increasing by no more than 0.25 mm. The differences, except for 5 values, do not, consequently, exceed the 5% mark. Again, the differences appear more pronounced by 2016, which is due to the stronger correction of the non-meteoservis sensors.

For the selected locations Feldbach and Fehring regarding the 24HMMax measure, Figure 4.12, the picture is different. While in Feldbach the correction has resulted in significantly higher values almost over the entire period, Fehring was subject to a significant downward correction, resulting in negative 24HMMax differences up until 2016, followed by a weak positive trend. Feldbach therefore faced a notable negative bias before correction, while in Fehring, before the Meteoservis sensors where operative, a positive bias was present.

The corresponding analysis of the 1HMMax differences in Figure 4.13 shows the same pattern. In Feldbach, an upward correction led to higher values almost over the entire period, while in Fehring there was predominantly a downward correction until 2016 and an upward correction from then until the present, although with smaller magnitude.

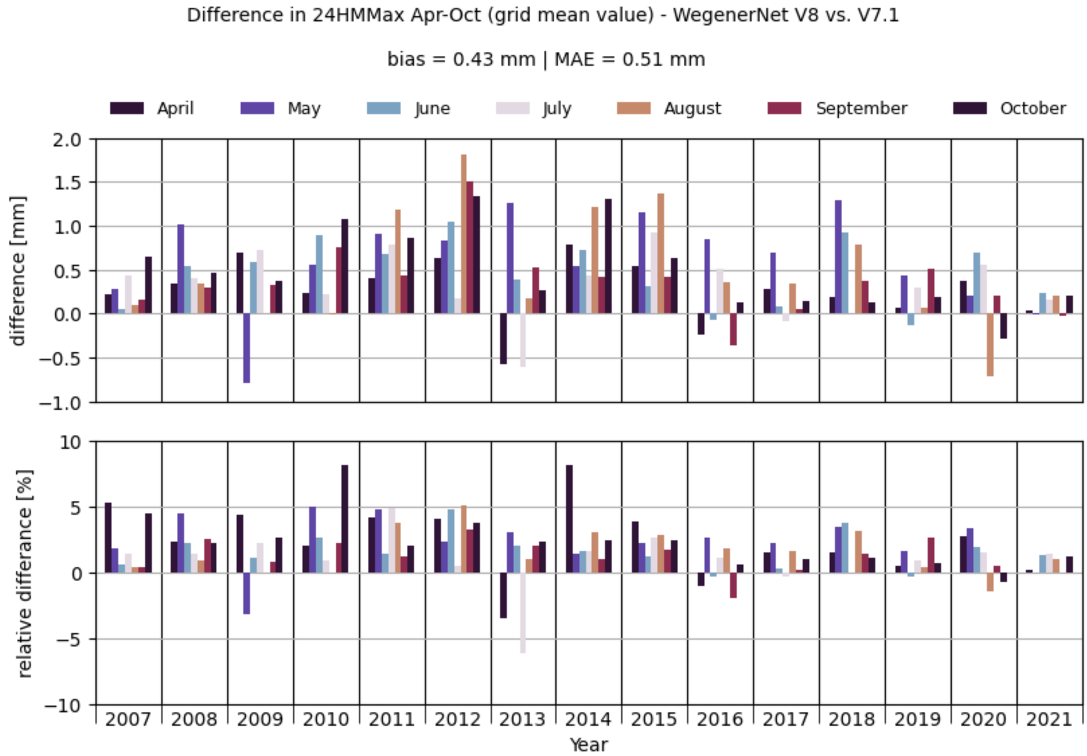

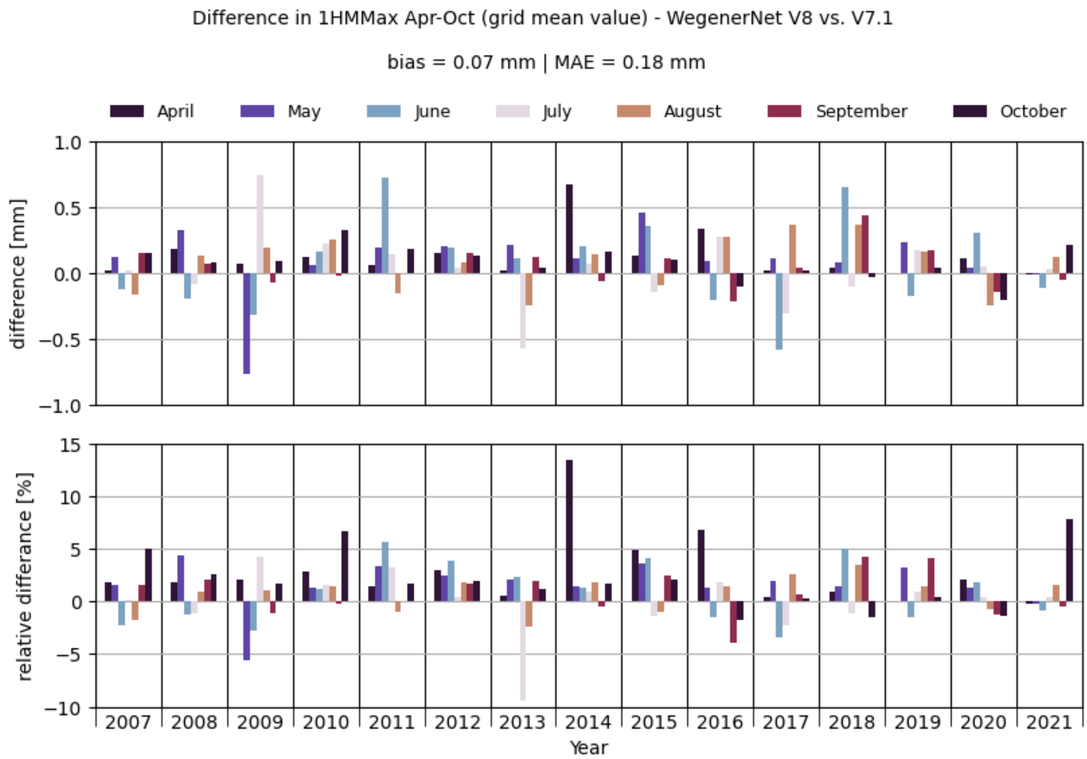

Figure 4.11: 24HMMax (top) and 1HMMax (bottom) difference FBR - WegenerNet v8 vs. v7.1.

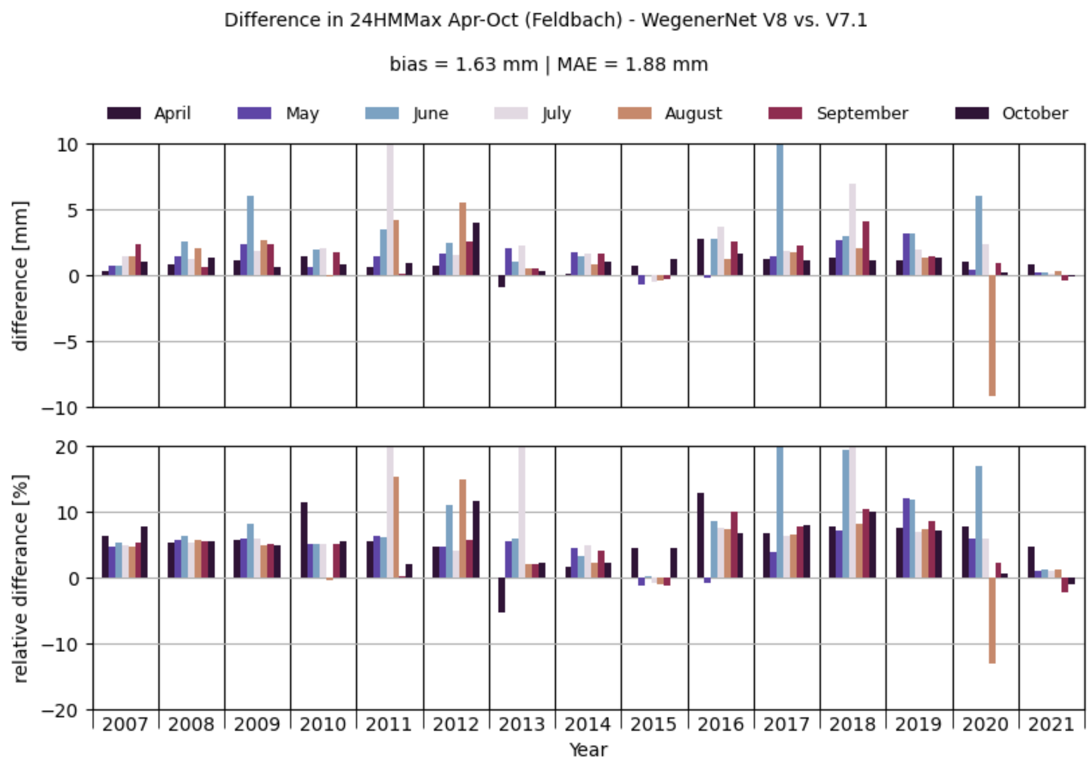

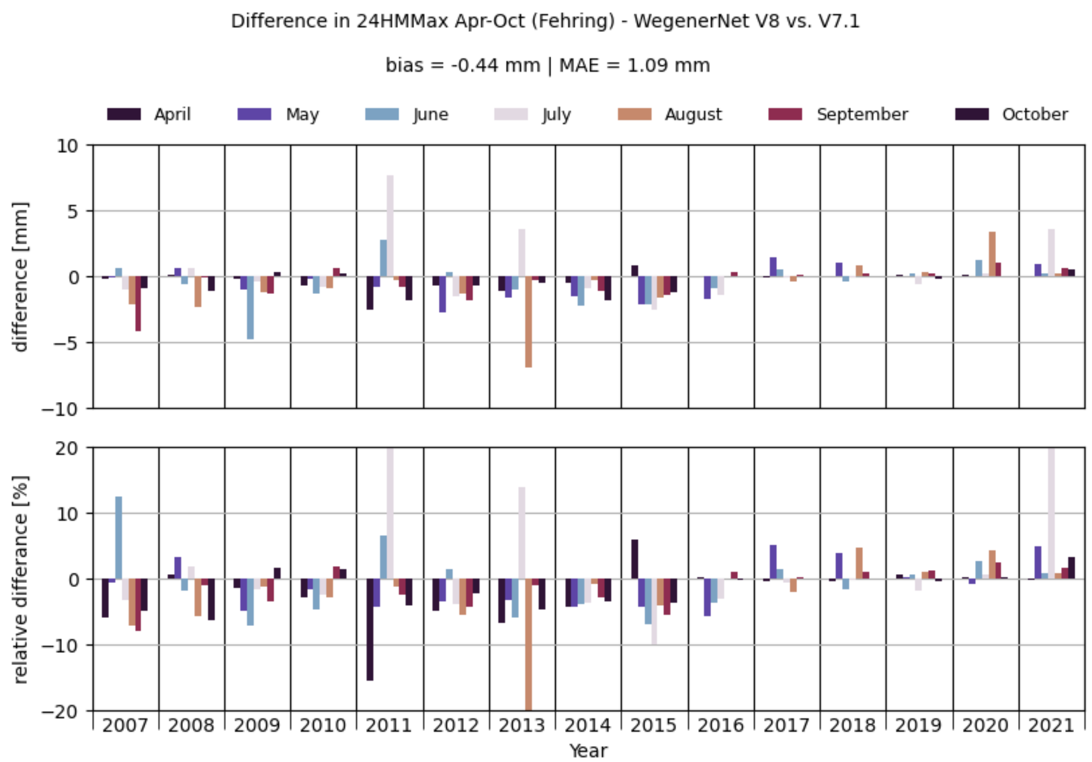

Figure 4.12: 24HMMax difference Feldbach/Fehring - WegenerNet v8 vs. v7.1.

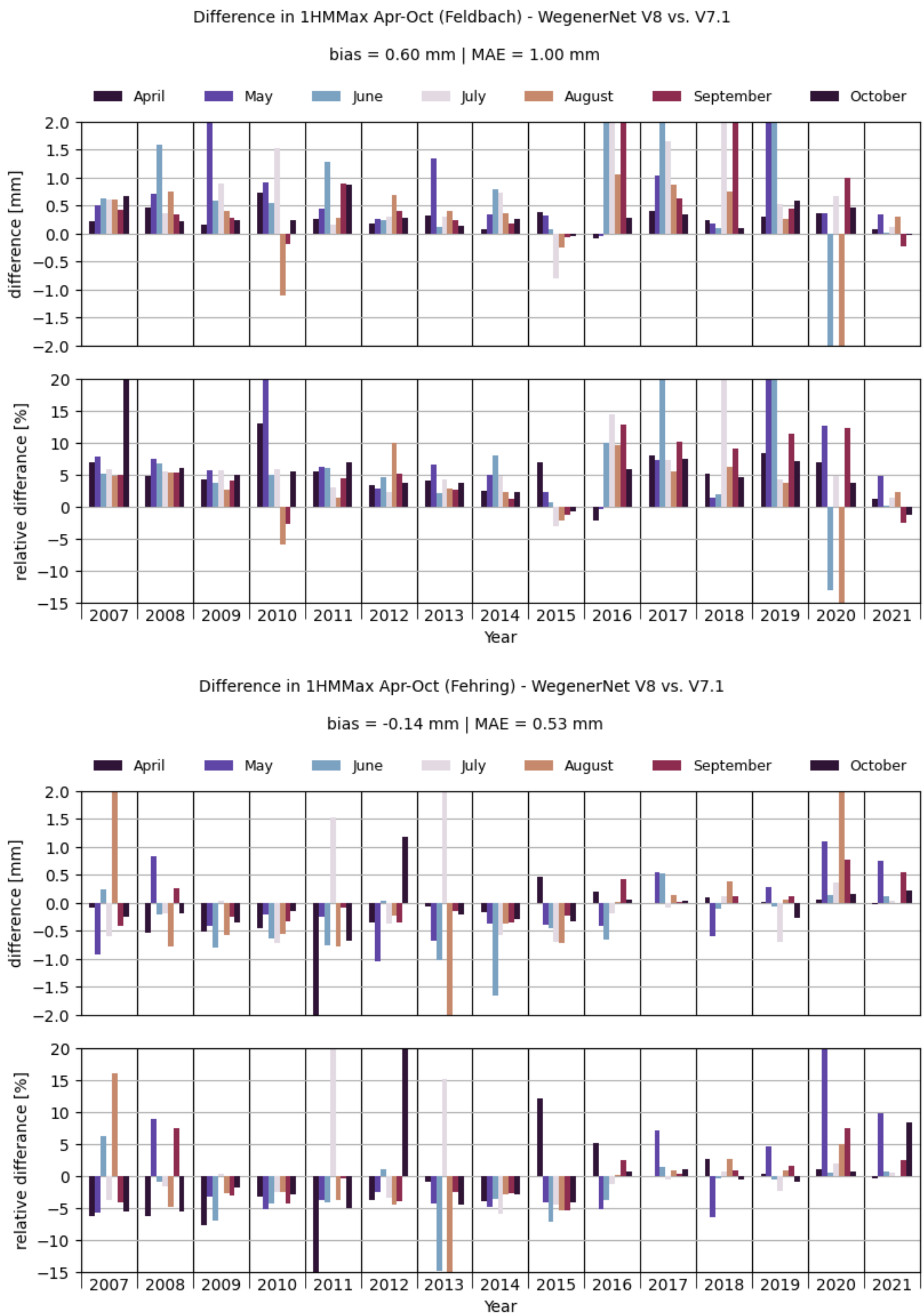

Figure 4.13: 1HMMax difference Feldbach/Fehring - WegenerNet v8 vs. v7.1.

While the differences from the v7.1 data version are generally small, a different picture emerges when analyzing the ERA5 and ERA5 land data in Figure 4.14. For almost all months, the absolute differences in 24HMMax are positive, with most being below $20\,\mathrm{mm\,d^{-1}}$. A look at the relative difference shows that this negative deviation is strong in both data sets, with many months exceeding the 100% mark. This means that heavy precipitation events in the region that lead to the 24HMMax in the v8 data are often represented much less intense or not at all in the considered data sets.

As an example, this is shown for ERA5 Land in Figure 4.15 and Figure 4.16 for June 2018 and August 2021, respectively. These figures include the precipitation total in the region on the day the 24HMMax was recorded (third panel) and the day before and after (second and fourth panel, respectively) as well as, for reference, the monthly precipitation total (first panel). All data are plotted on a 1 km x 1 km grid. Analyzing Figure 4.15, the WegenerNet v8 data display a regional mean of $26.29\,\mathrm{mm\,d^{-1}}$ on June 21, 2018 (24HMMax). The ERA5 land dataset, on the other hand, shows only $1.70\,\mathrm{mm\,d^{-1}}$. Therefore, the strongest 24-hour precipitation event in June 2018 is not fully represented in the ERA5 dataset.

However, when looking at the monthly total, it can be seen that the difference resulting from the discrepancy is averaged out. As a result, the monthly precipitation mean (first panel in Figure 4.15) is larger than the value in the WegenerNet v8 data. Examining the case of August 2021 (Figure 4.16) in the same way, the situation is similar except that the difference in 24HMMax does not even out over the month and persists, as can be seen from the average precipitation values for the entire month.
Regarding the 24HMMax difference to ERA5 (Figure 4.17) and ERA5 Land (Figure 4.18) in Feldbach and Fehring, the picture is similar to the region. However, strong deviations, where the comparative data set does not show a 24-hour precipitation sum of comparable magnitude to the 24HMMax of the v8 data, seem to occur more frequently in Feldbach than in Fehring, especially in the years up to 2010. Furthermore, the absolute difference is also significantly smaller in Fehring. As in the analysis for the region, there are no structural differences between ERA5 and ERA5 Land, although the differences in the ERA5 Land data are marginally smaller.

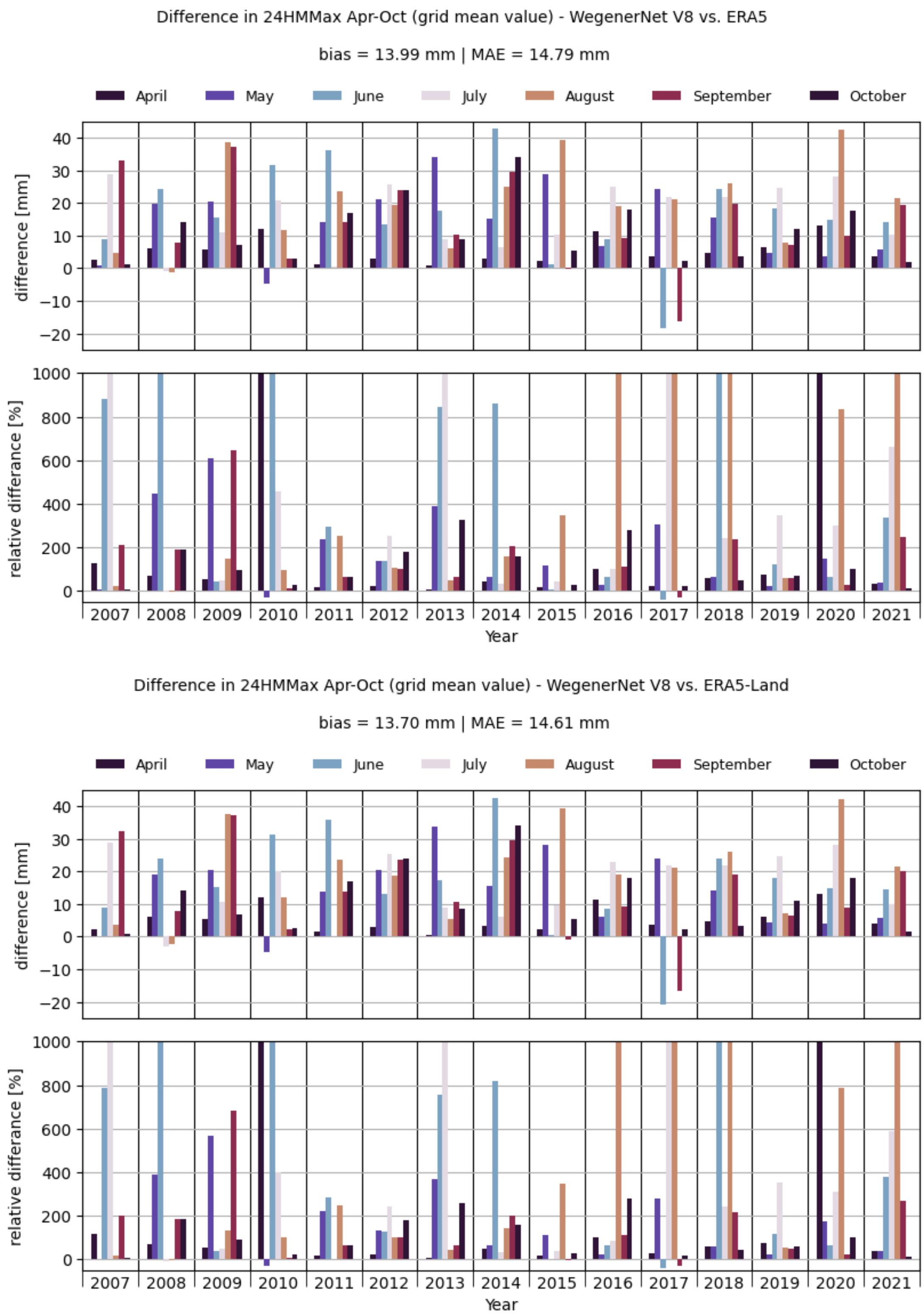

Figure 4.14: 24HMMax difference FBR - WegenerNet v8 vs. ERA5 and ERA5 Land.

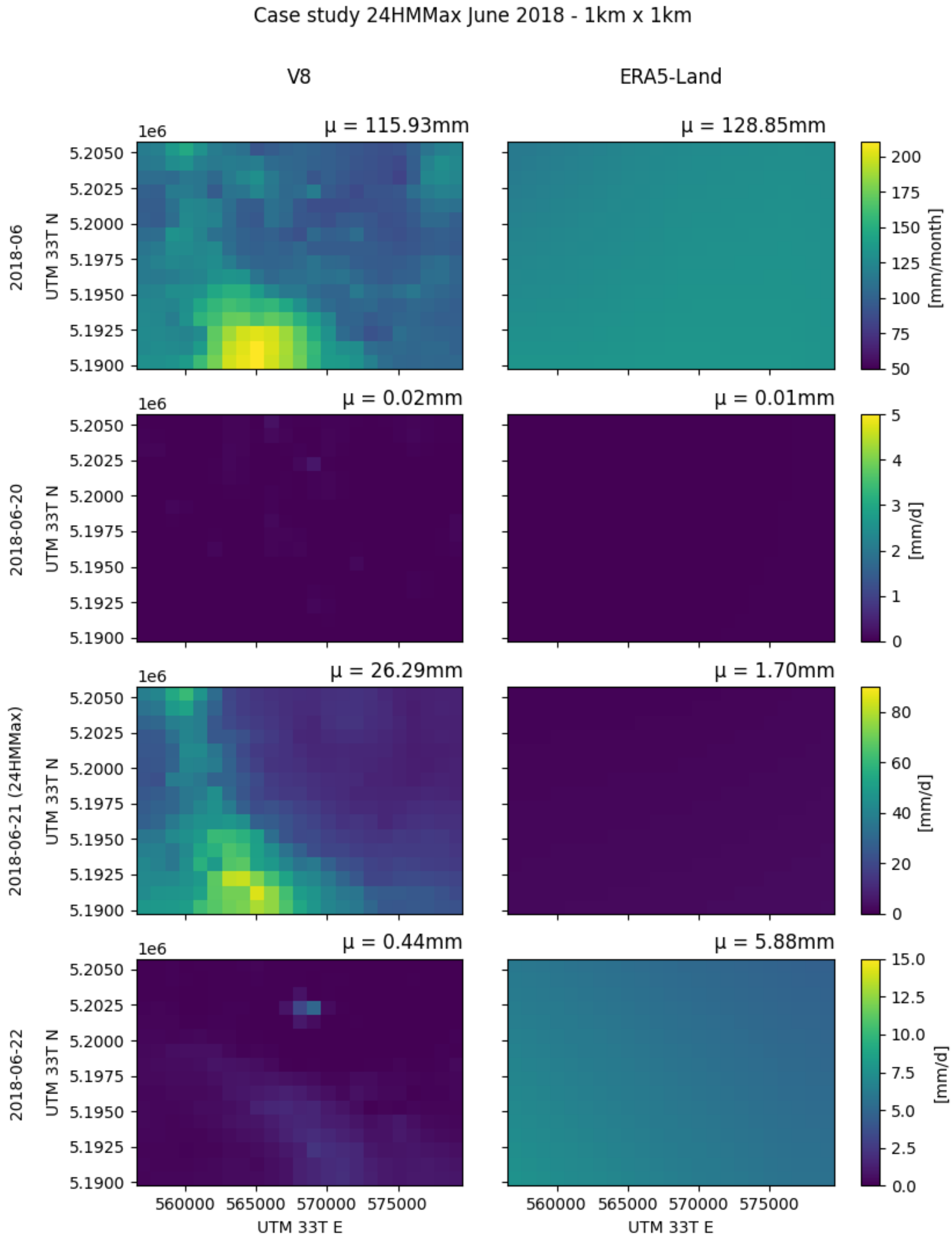

Figure 4.15: 24HMMax case study: June 2018 - WegenerNet v8 vs. ERA5-Land.
first row: Monthly mean *second row*: Day before 24HMMax
third row: Day of 24HMMax *fourth row*: Day after 24HMMax

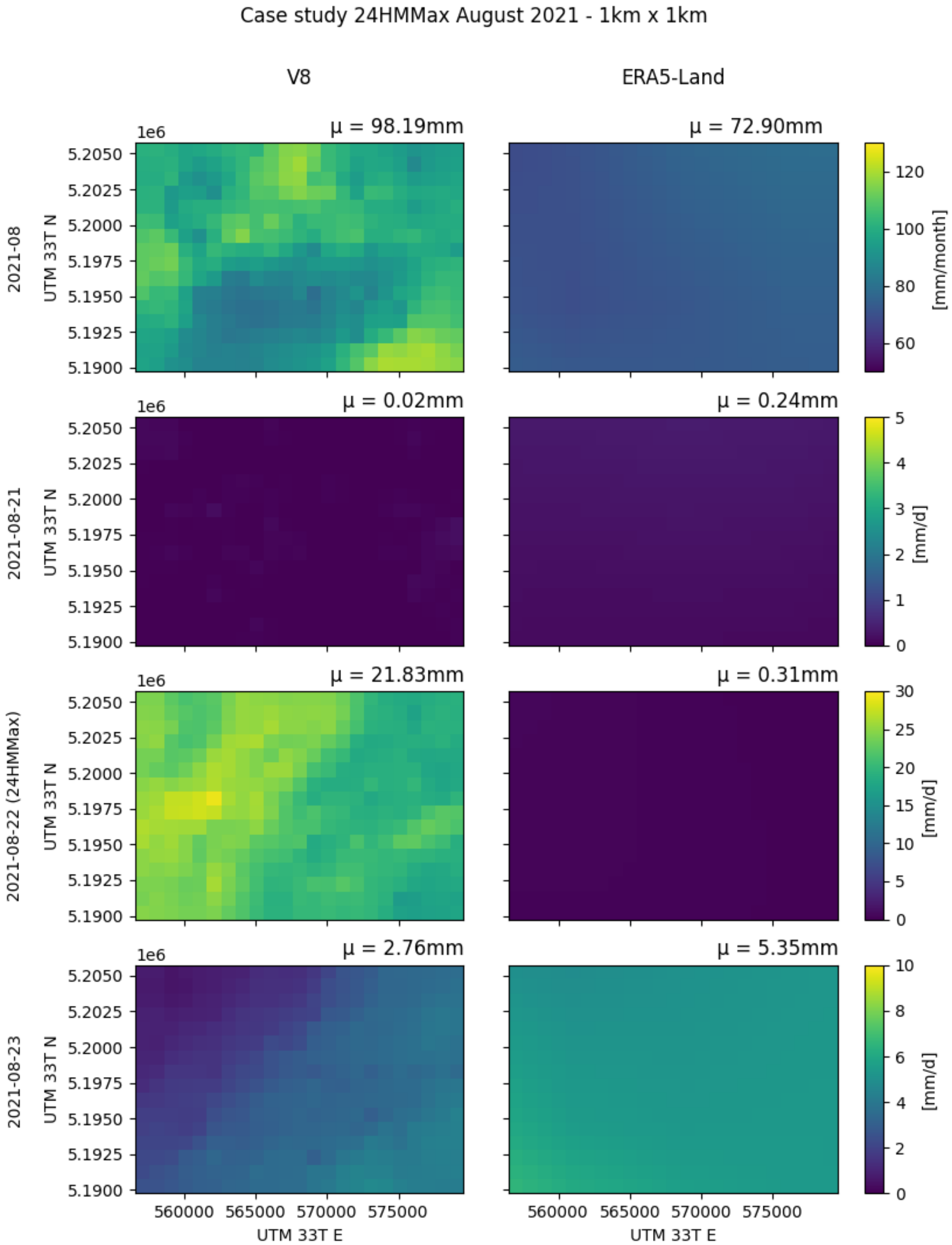

Figure 4.16: 24HMMax case study: August 2021 - WegenerNet v8 vs. ERA5-Land.
first row: Monthly mean *second row*: Day before 24HMMax
third row: Day of 24HMMax *fourth row*: Day after 24HMMax

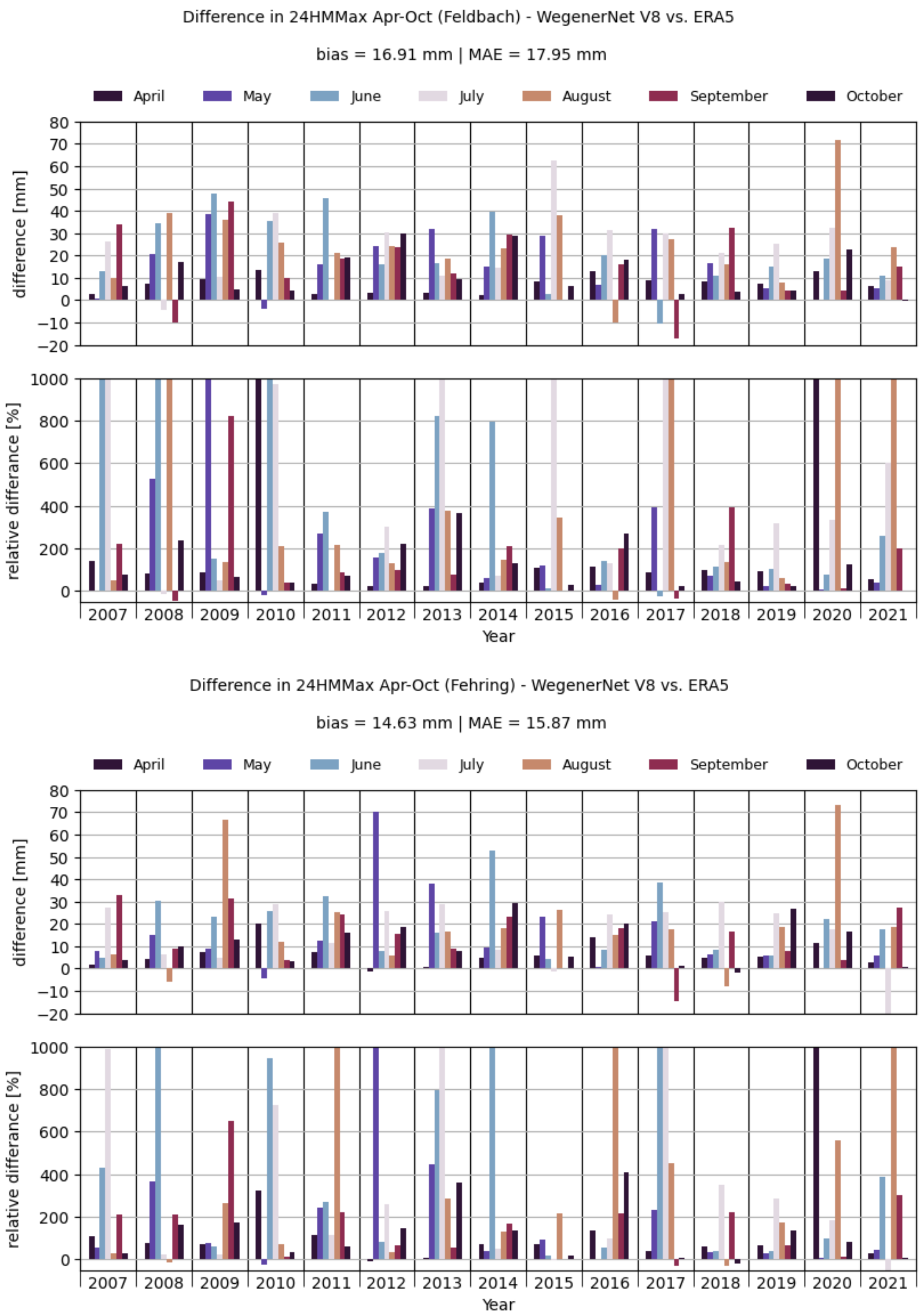

Figure 4.17: 24HMMax difference Feldbach/Fehring - WegenerNet v8 vs. ERA5.

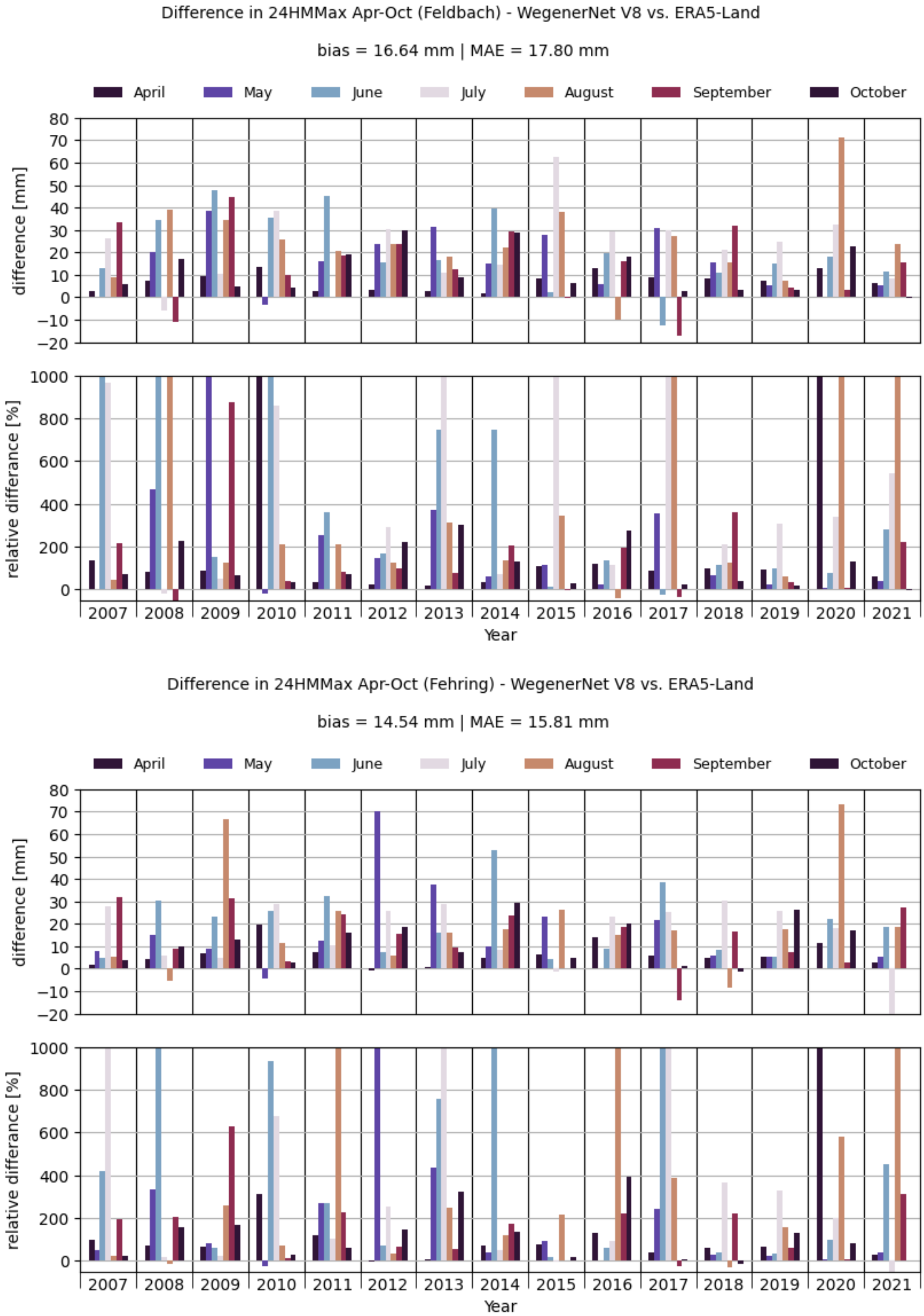

Figure 4.18: 24HMMax difference Feldbach/Fehring - WegenerNet v8 vs. ERA5-Land.

The comparative analysis of the v8 data with the SPARTACUS data shows differences to the comparison with the ERA5 and ERA5 land datasets. This can be attributed to the higher spatial resolution of the SPARTACUS data, which leads to a higher agreement with the WegenerNet data. This is evident when analyzing the 24HMMax differences of the region in Figure 4.19. The SPARTACUS data also show a negative difference for most months, but the differences are mostly well below $10\,\mathrm{mm\,d^{-1}}$. The relative difference for most months is less than +25 %.

Nevertheless, there are four months in which the relative 24HMMax difference exceeds the 100% mark. This suggests that the SPARTACUS dataset fails to reflect certain 24HMMax extreme precipitation events in a similar manner as the ERA5 and ERA5 land datasets. However, these discrepancies occur much less frequently. Again, two of these events are examined in detail in two case studies. Figure 4.20 thereby analyzes the 24HMMax event in May 2009. While the WegenerNet data provide a regional mean of $24.17\,\mathrm{mm\,d^{-1}}$, the SPARTACUS data estimate is $5.65\,\mathrm{mm\,d^{-1}}$. The difference is almost exactly the same as the difference in monthly totals (first panel), i.e., the difference is not offset by generally higher values in the SPARTACUS data and remains.
Similarly, this can be seen for the July 2017 24HMMax event in Figure 4.21, with a similarly large difference on that particular day.

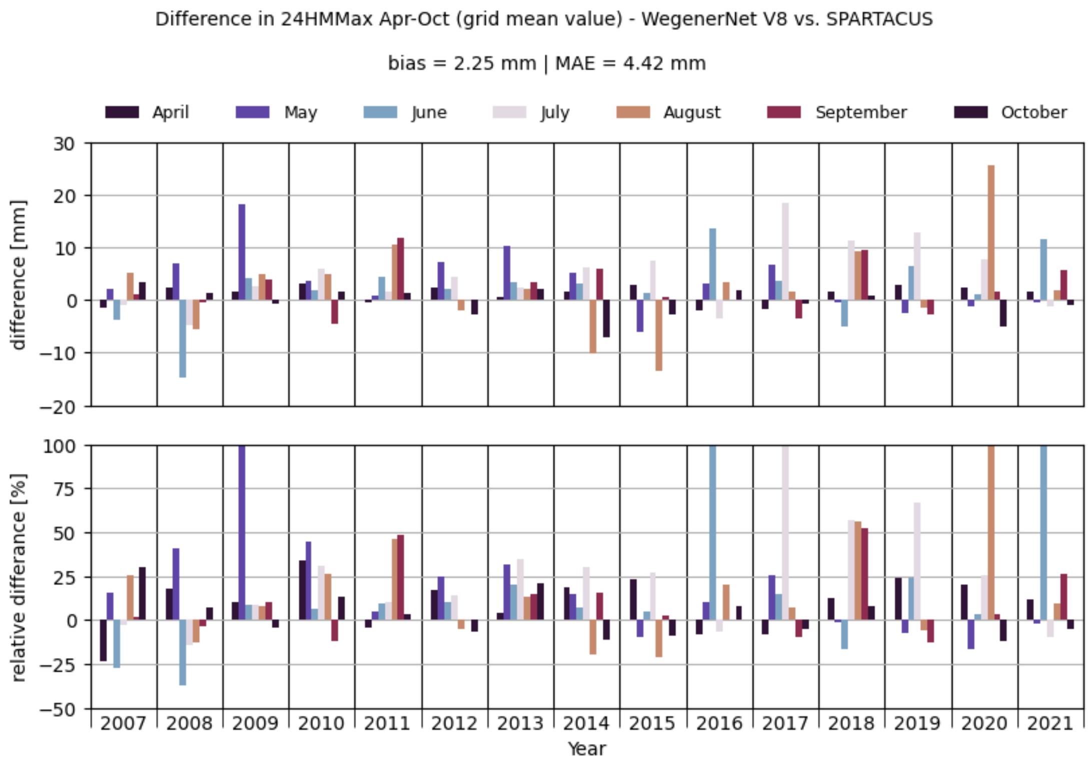

Figure 4.19: 24HMMax difference FBR - WegenerNet v8 vs. SPARTACUS.

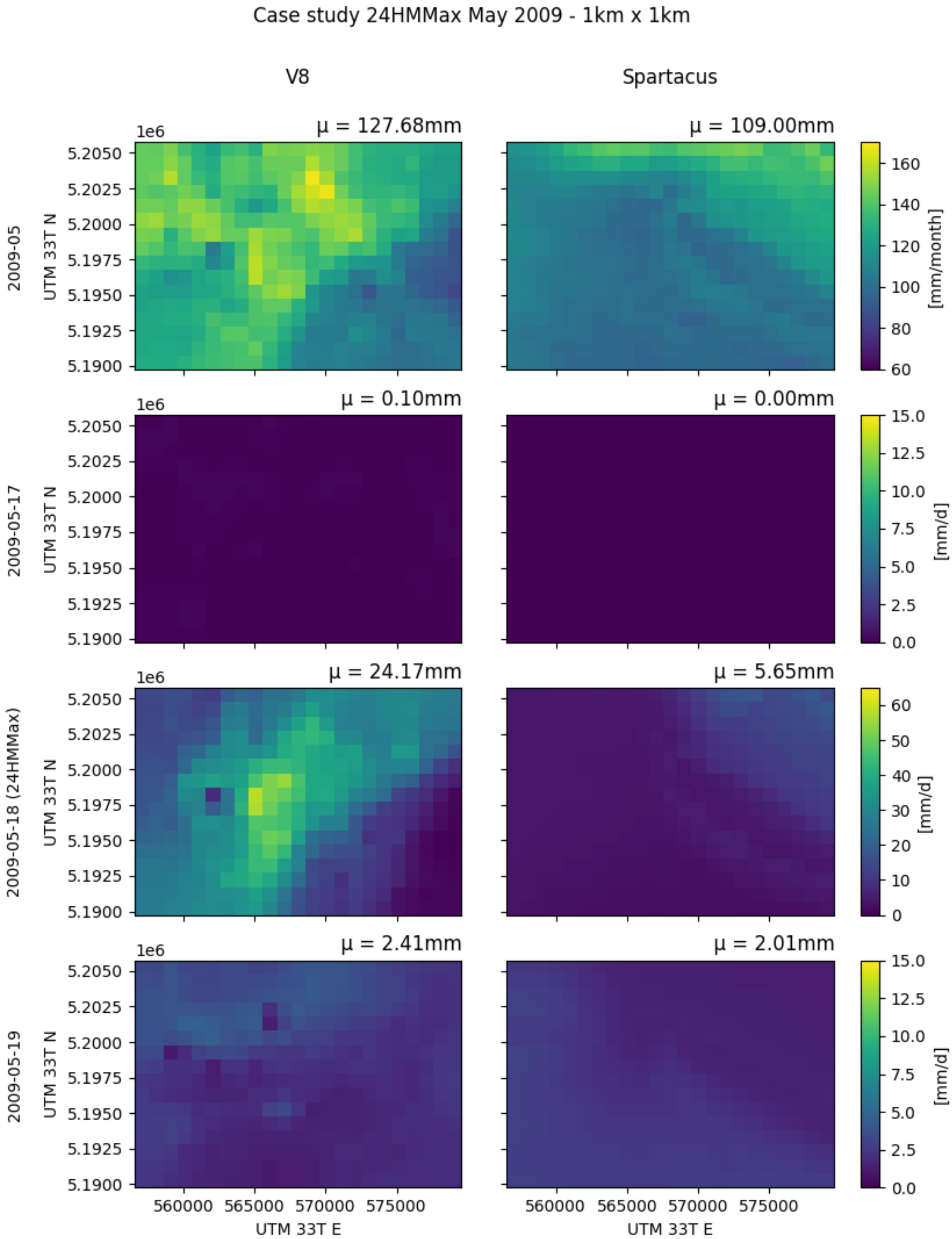

Figure 4.20: 24HMMax case study: May 2009 - WegenerNet v8 vs. SPARTACUS.
first row: Monthly mean *second row*: Day before 24HMMax
third row: Day of 24HMMax *fourth row*: Day after 24HMMax

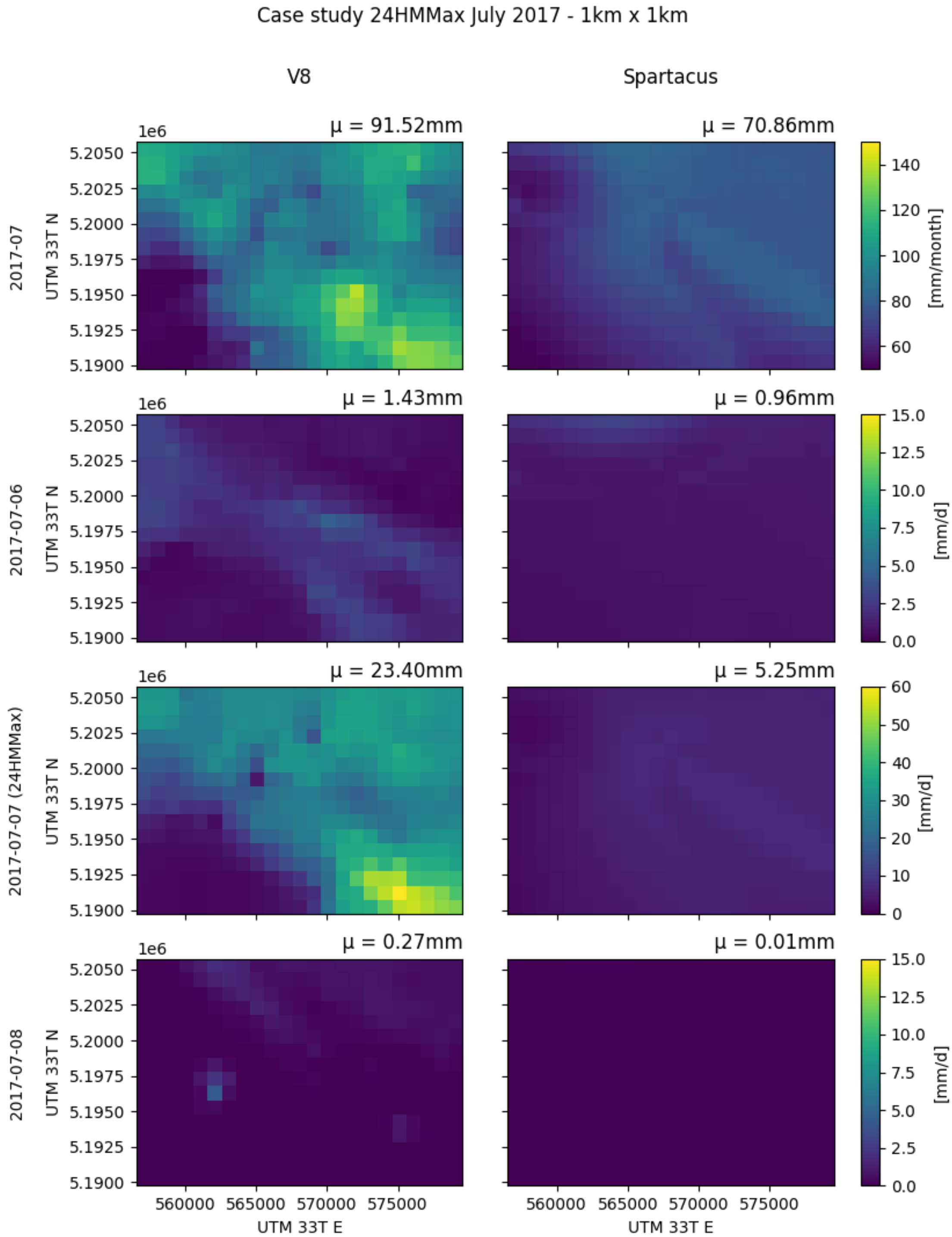

Figure 4.21: 24HMMax case study: July 2017 - WegenerNet v8 vs. SPARTACUS.
first row: Monthly mean *second row*: Day before 24HMMax
third row: Day of 24HMMax *fourth row*: Day after 24HMMax

Regarding the 24HMMax difference between the v8-WegenerNet data and SPARTACUS in Feldbach and Fehring, Figure 4.22, the picture is similar to the regional observation. However, the number of 24HMMax mismatches with a deviation of more than 100% is higher in both locations (Fehring (13) and Feldbach (10)). It is also noticeable that the SPARTACUS data in Feldbach, in contrast to Fehring, shows a solely negative monthly bias for the years 2010-2013 (positive difference). In all other years and at both sites, negative and positive biased months are present. However, with a strong tendency towards negative bias.

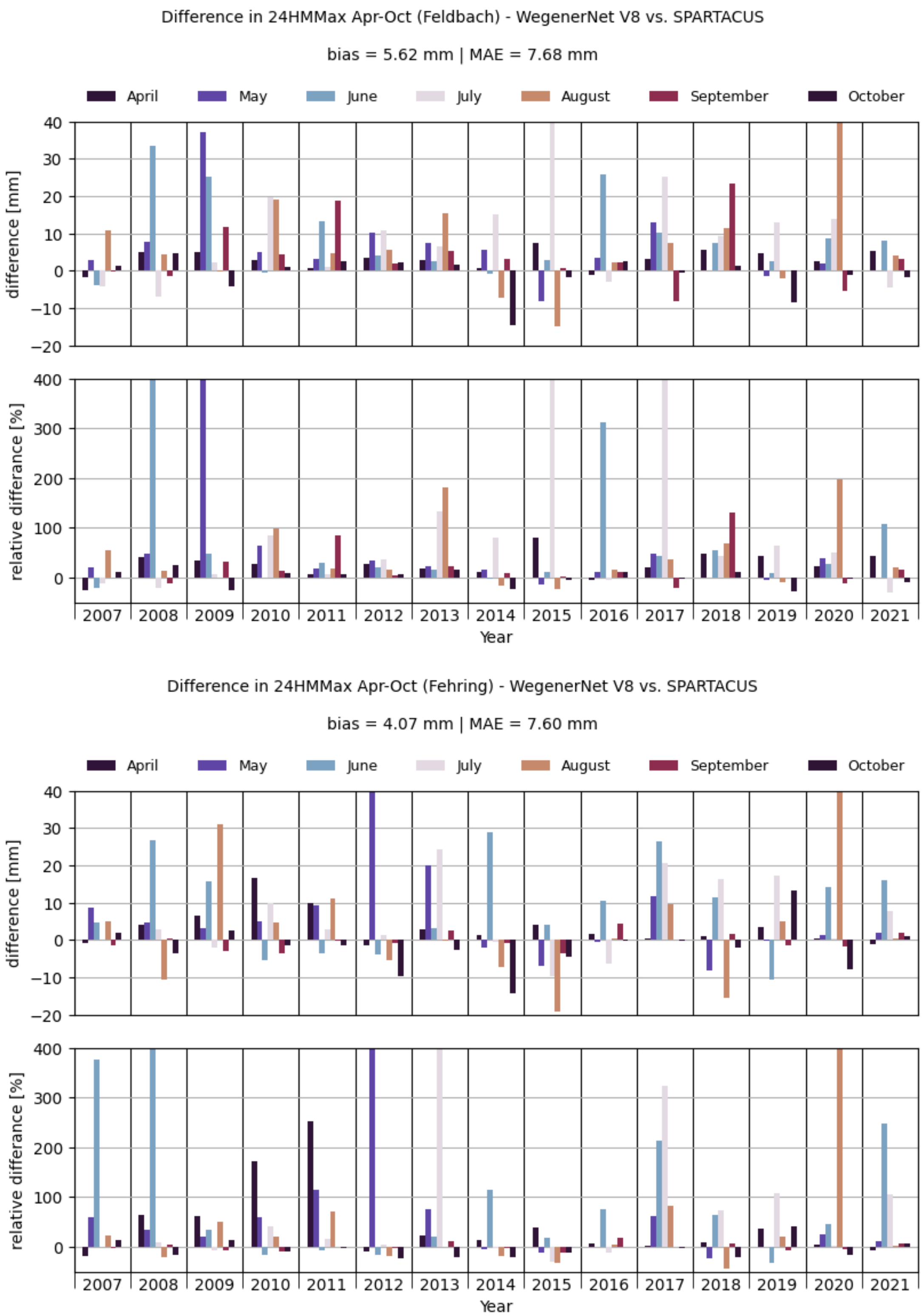

Figure 4.22: 24HMMax difference Feldbach/Fehring - WegenerNet v8 vs. SPARTACUS.

A comparative analysis of the 1HMMax data from WegenerNet v8 and the INCA dataset in Figure 4.23 shows that the INCA data are subject to a substantial negative bias, with very few negative differences visible until about 2013. Thereafter, the negative differences are more prominent, with the positive differences generally being more pronounced. In addition, it is noticeable that similar to the other comparative datasets, single hourly precipitation extremes are not depicted in the INCA dataset. This is evident when analyzing the 1HMMax difference in April 2009, May 2011 to 2013, and July 2015 in Figure 4.23. In which cases, the relative difference is well above the 100% mark.
Figure 4.24 provides the 1HMMax differences for Feldbach and Fehring. While the INCA data show a negative bias at both locations, it is much stronger in Fehring with many differences beeing above +50%. Also, differences where the INCA dataset does not reflect certain 1HMMax extreme precipitation events are much more frequent in this location. This applies in particular to the years 2007 to 2012. In general, as in the region as a whole, the bias in the INCA data appears to be stronger in both regions by 2013.

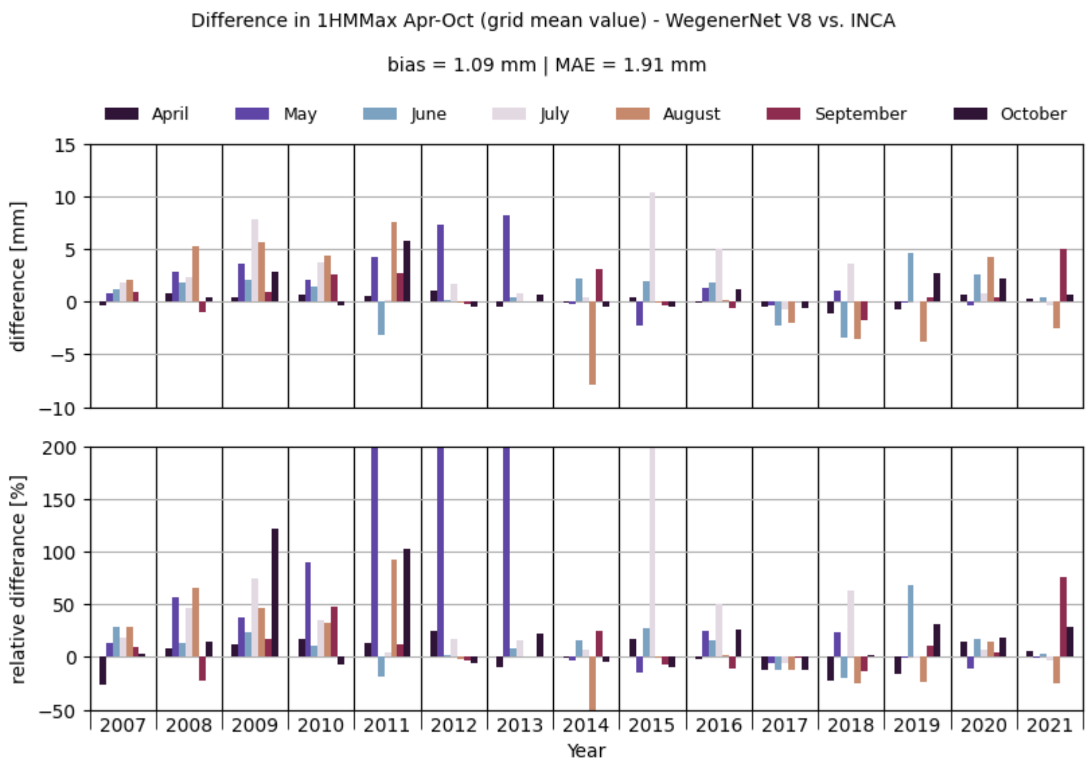

Figure 4.23: 1HMMax difference FBR - WegenerNet v8 vs. INCA.

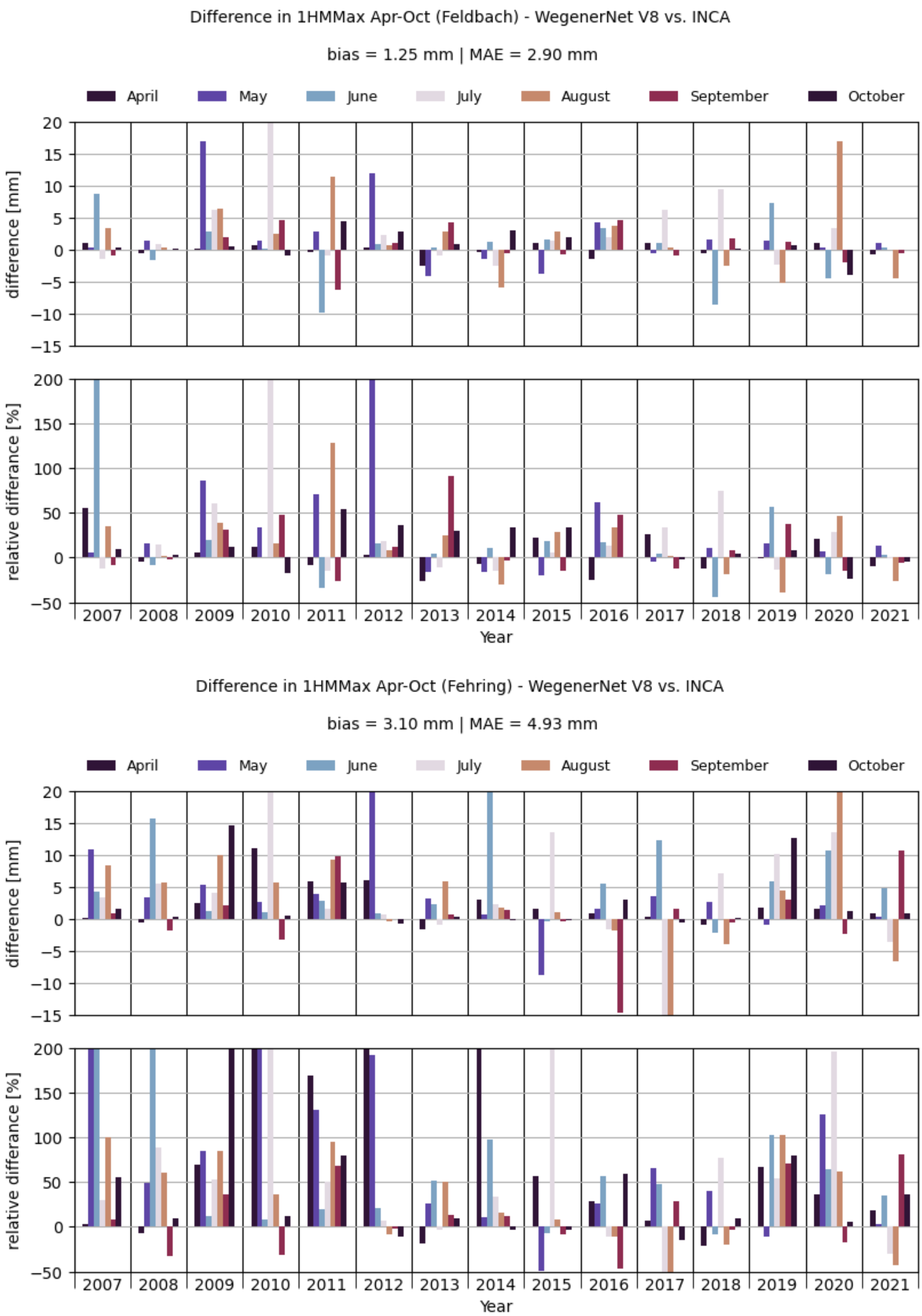

Figure 4.24: 1HMMax difference Feldbach/Fehring - WegenerNet v8 vs. INCA.

Analyzing the amount of exceedance of the 95th percentile of the 24-hour totals in mm per month for the FBR region, the WegenerNet data show the highest values compared to the other data sets, as can be seen in Figure 4.25. The difference between the v7.1 and v8 data versions is small and does not exceed 1.5 mm, as seen in Figure 4.28. Thus, homogenization resulted in higher precipitation amounts of the heaviest 5% of all 24-hour precipitation totals. This is further highlighted by the predominantly positive differences between the v8 and v7.1 data versions in Figure 4.28.

While the ERA5 and ERA5Land datasets show only a few months with exceedance, where the highest values are in August 2009 and September 2017, the SPARTACUS data show a similar pattern to the WegenerNet data, albeit with lower values. The latter is evident in Figure 4.25. As with the 24HMMax differences, the agreement of the SPARTACUS dataset with the WegenerNet data is much higher compared to the ERA5 and ERA5 Land data, most likely due to the higher spatial resolution and the weight of direct measurements obtained from the ZAMG stations located in the region. Although less pronounced, a negative bias is nevertheless clearly visible in the SPARTACUS data as well.
Two years, 2009 and 2021, are particularly noteworthy. For both June and August 2009, the highest exceedance values in the last 15 years are observed. This is visible in all considered data sets except for the ERA5 & ERA5 Land data where this only holds for August. In 2021, on the other hand, no exceedance was observed in the WegenerNet and Spartacus data, while the ERA5 & ERA5 land data indicate about 15 to 20 mm for July of that year.
For the sites Feldbach and Fehring, the following can be stated regarding the exceedance amounts (Figure 4.26 and Figure 4.27, respectively) and the differences to the v8 data version (Figure 4.29 and Figure 4.30, respectively). Analyzing the differences, Feldbach was subject to a negative bias prior correction, so that the difference between v8 and v7.1 was almost entirely positive. Fehring, on the other hand, was subject to a positive bias before correction until 2016, when it was corrected downward (see Figure 4.30). Since the corrections for the pre-2016 sensors (non-Meteoservis) were stronger, this is consistent. However, since the mentioned differences are of small magnitude, the overall difference to the comparative datasets, at both sites, is not significantly different from the analysis for the region.

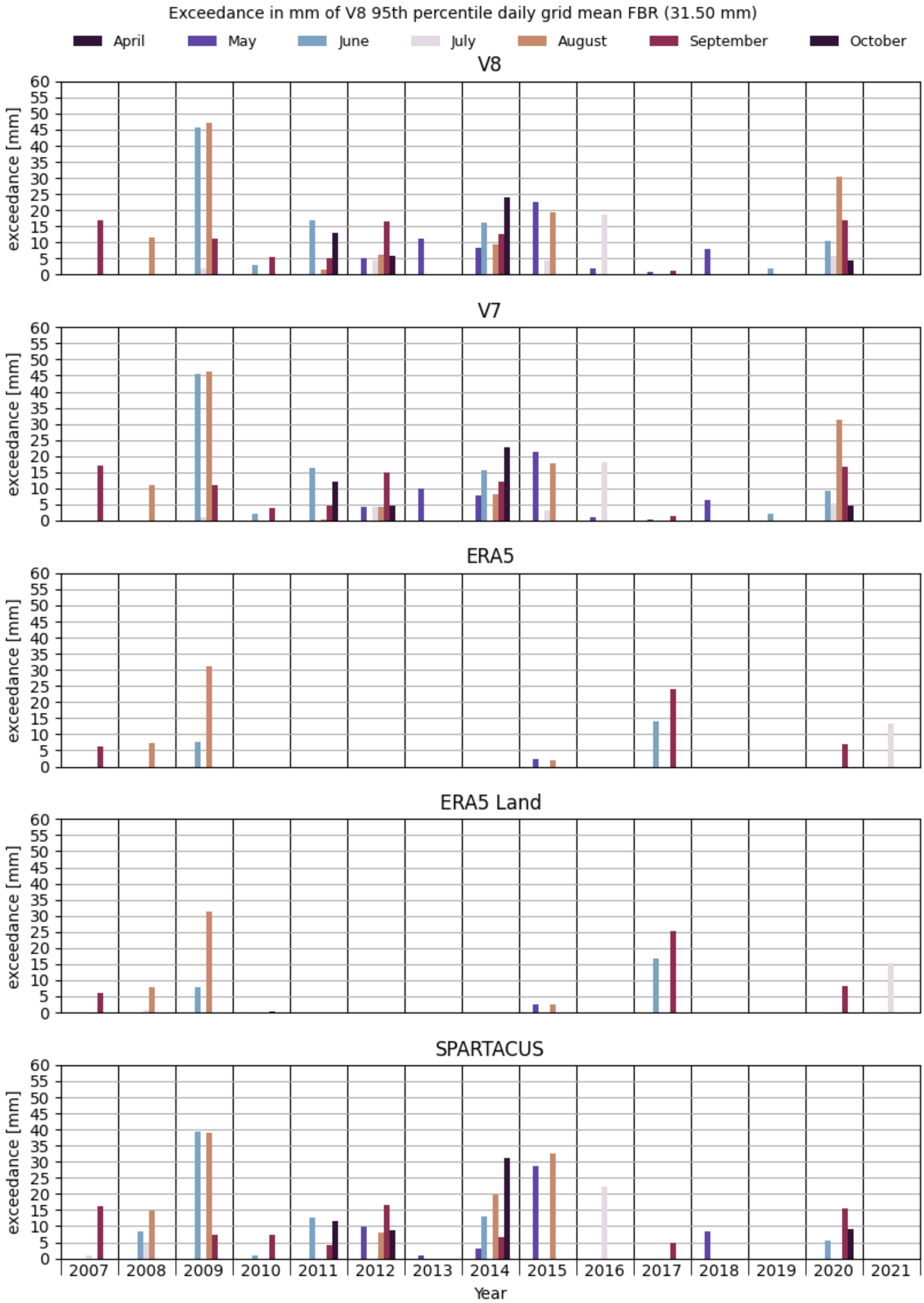

Figure 4.25: Precipitation exceedance amount - 24H / whole Region.

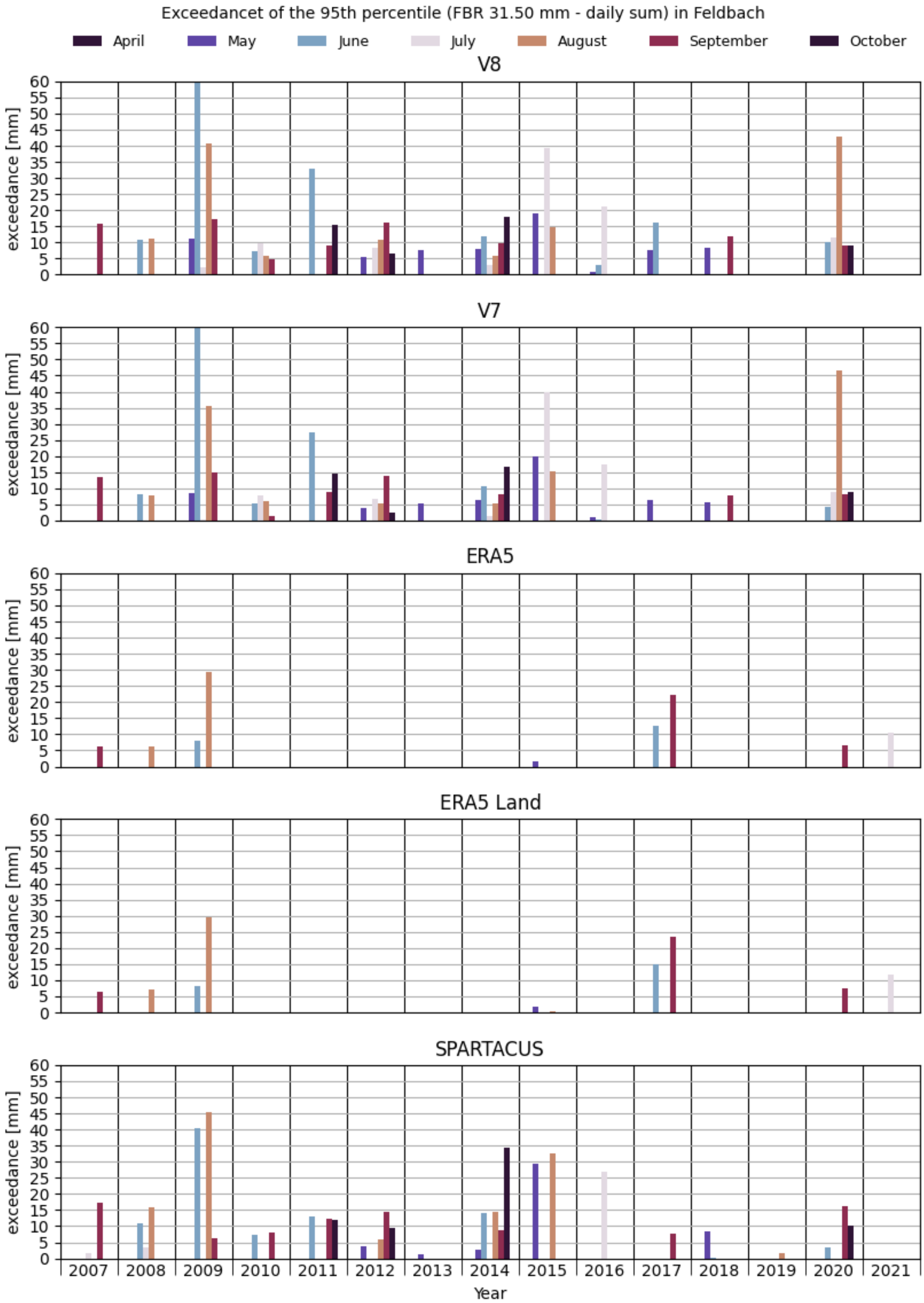

Figure 4.26: Precipitation exceedance amount - 24H / Feldbach station.

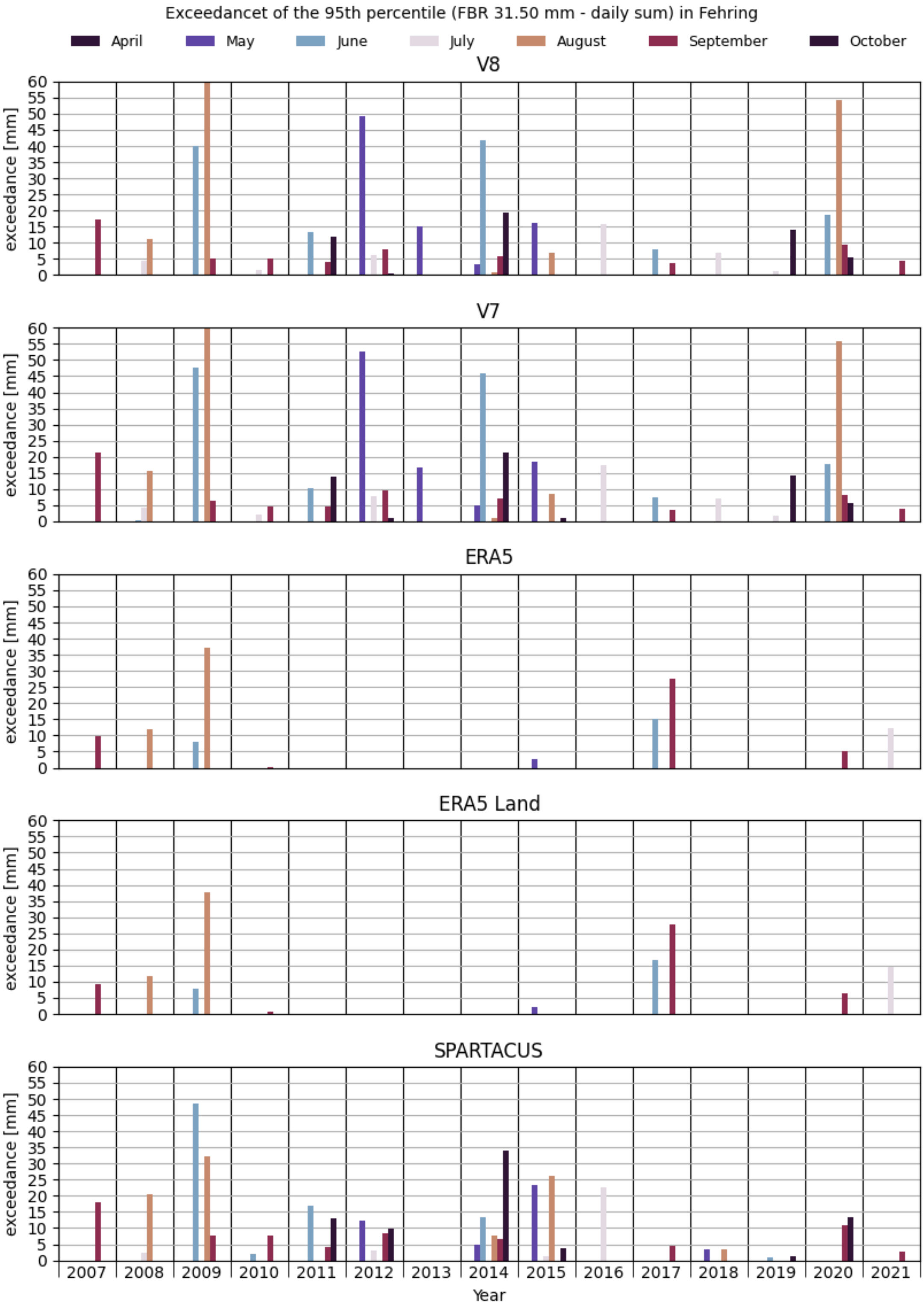

Figure 4.27: Precipitation exceedance amount - 24H / location Fehring station.

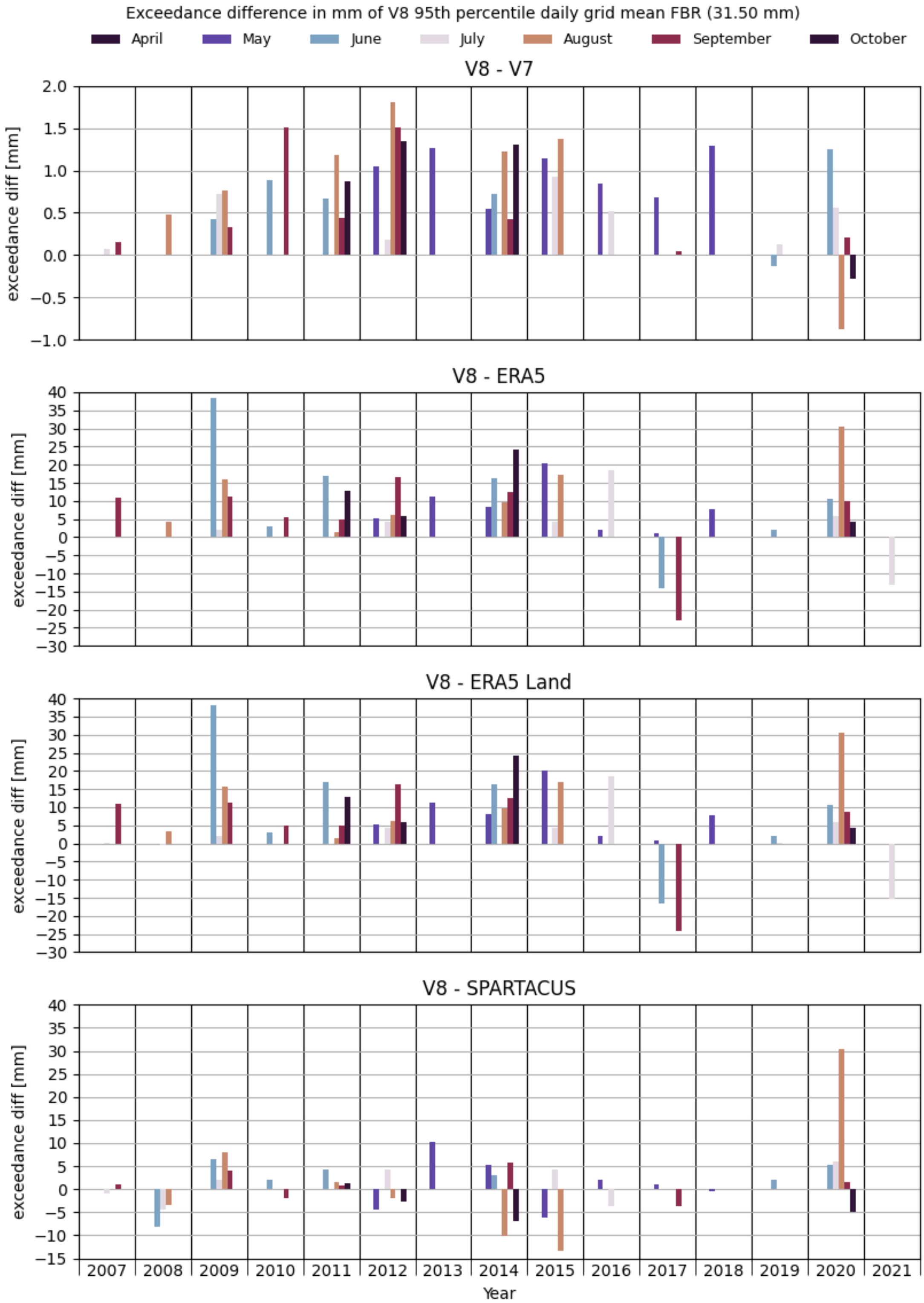

Figure 4.28: Precipitation exceedance difference - 24H / whole Region.

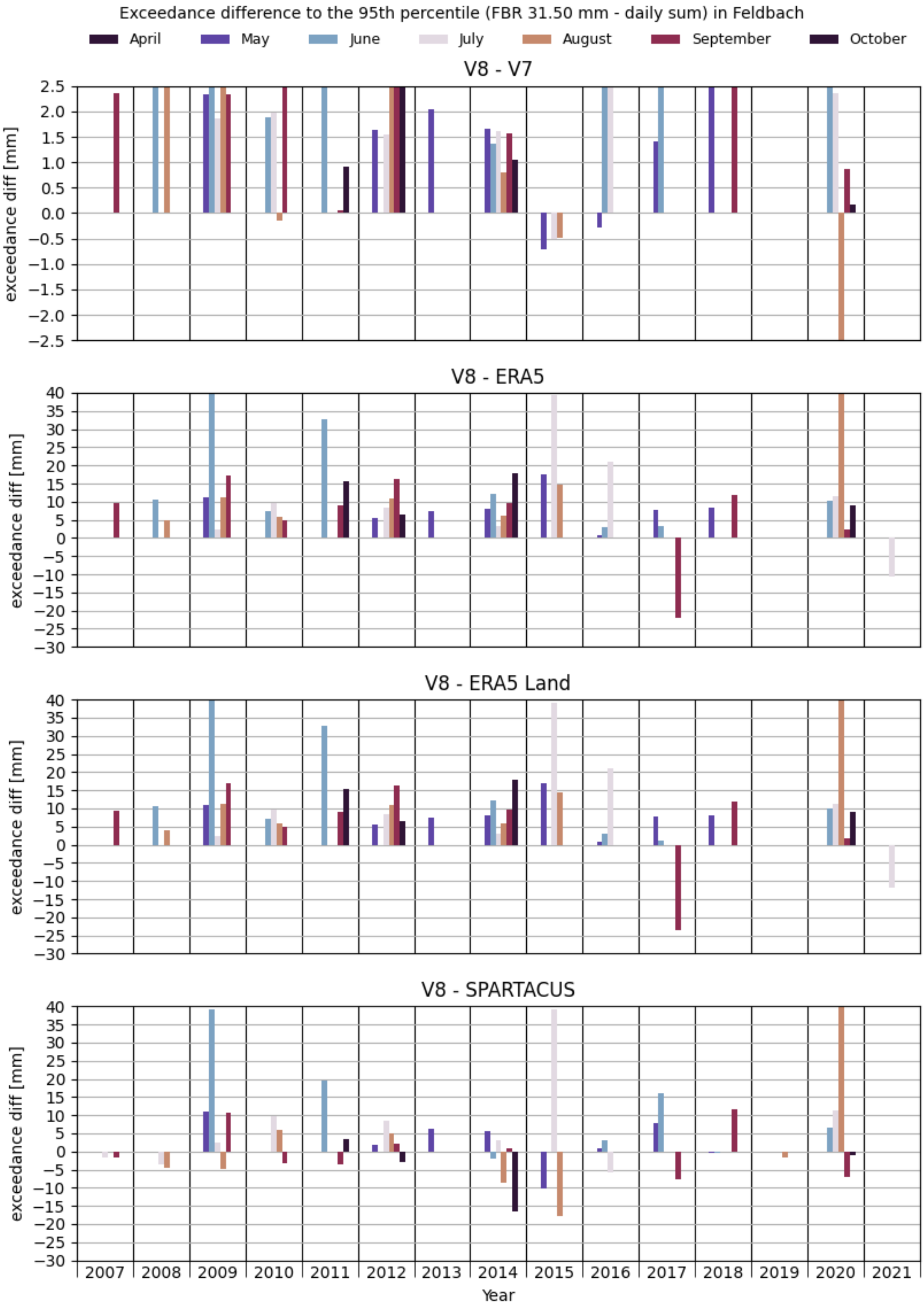

Figure 4.29: Precipitation exceedance difference - 24H / Feldbach station.

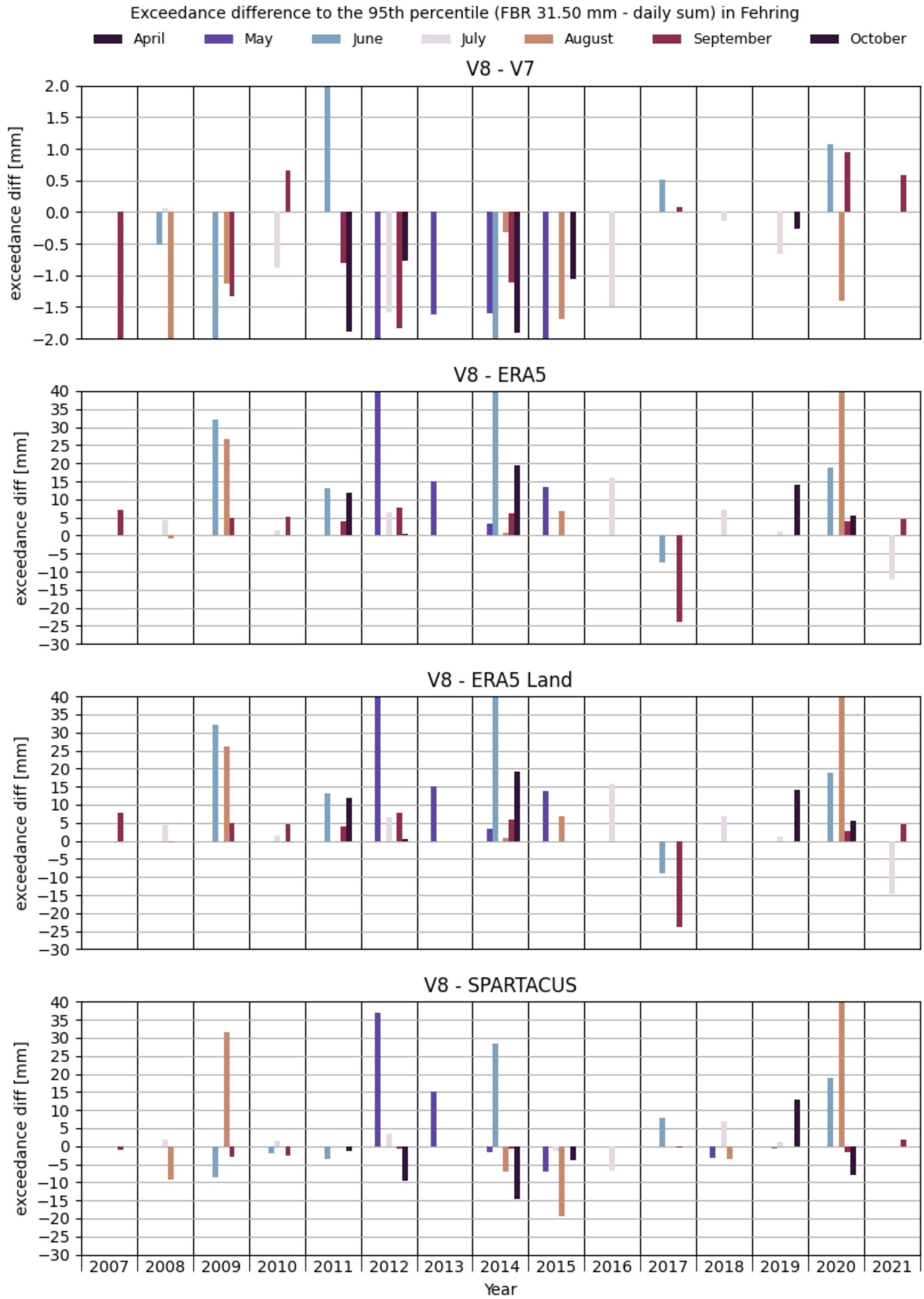

Figure 4.30: Precipitation exceedance difference - 24H / Fehring station.

Analyzing the amount of exceedance of the 95th percentile of 1-hour totals in milli meter per month for the FBR region, the WegenerNet data show higher values compared to the INCA dataset, as seen in Figure 4.31. The difference between the v8 and v7.1 data versions is small and does not exceed 1.5 mm with one exception, as seen in Figure 4.34. Thus, as with the 24-hour totals, homogenization resulted in higher precipitation amounts of the heaviest 5% of all 1-hour precipitation totals and is highlighted by the predominantly positive differences between the v8 and v7.1 data versions in Figure 4.34.

The INCA data show a similar pattern to the WegenerNet data (see Figure 4.31). However, when analyzing the differences between the WegenerNet v8 data and the INCA data in Figure 4.34, it is clear that the INCA data show less mm per month of exceedance than the WegenerNet data for almost all months until 2013. From 2014 onward, no clear bias is observed. The month of August 2020 is particularly notable in both data sets, with the highest observed exceedance amount.

For Feldbach and Fehring, similar to the 24HMMax analysis, the following can be stated regarding the exceedance amounts (Figure 4.32 and Figure 4.33, respectively) and the differences to the v8 data version (Figure 4.35 and Figure 4.36, respectively). Feldbach was subject to a negative bias prior correction, so that the difference between v8 and v7.1 is almost entirely positive (see fig. 4.35). Fehring, on the other hand, was subject to a positive bias before correction until 2016, when it was corrected downward (see Figure 4.36). The letter is consistent with stronger corrections of pre-2016 sensors (non-Meteoservis).

When comparing with the INCA data, it can be seen for Feldbach that the WegenerNet v8 data mostly show higher exceedance amounts until 2013. From there on, no clear trend can be seen. In comparison to Fehring, however, it becomes clear, especially for the differences (see Figure 4.35 and Figure 4.36), that the deviations in Fehring are significantly larger and more scattered. However, a trend toward negative bias in the Inca data up to the year 2013 can also be observed.

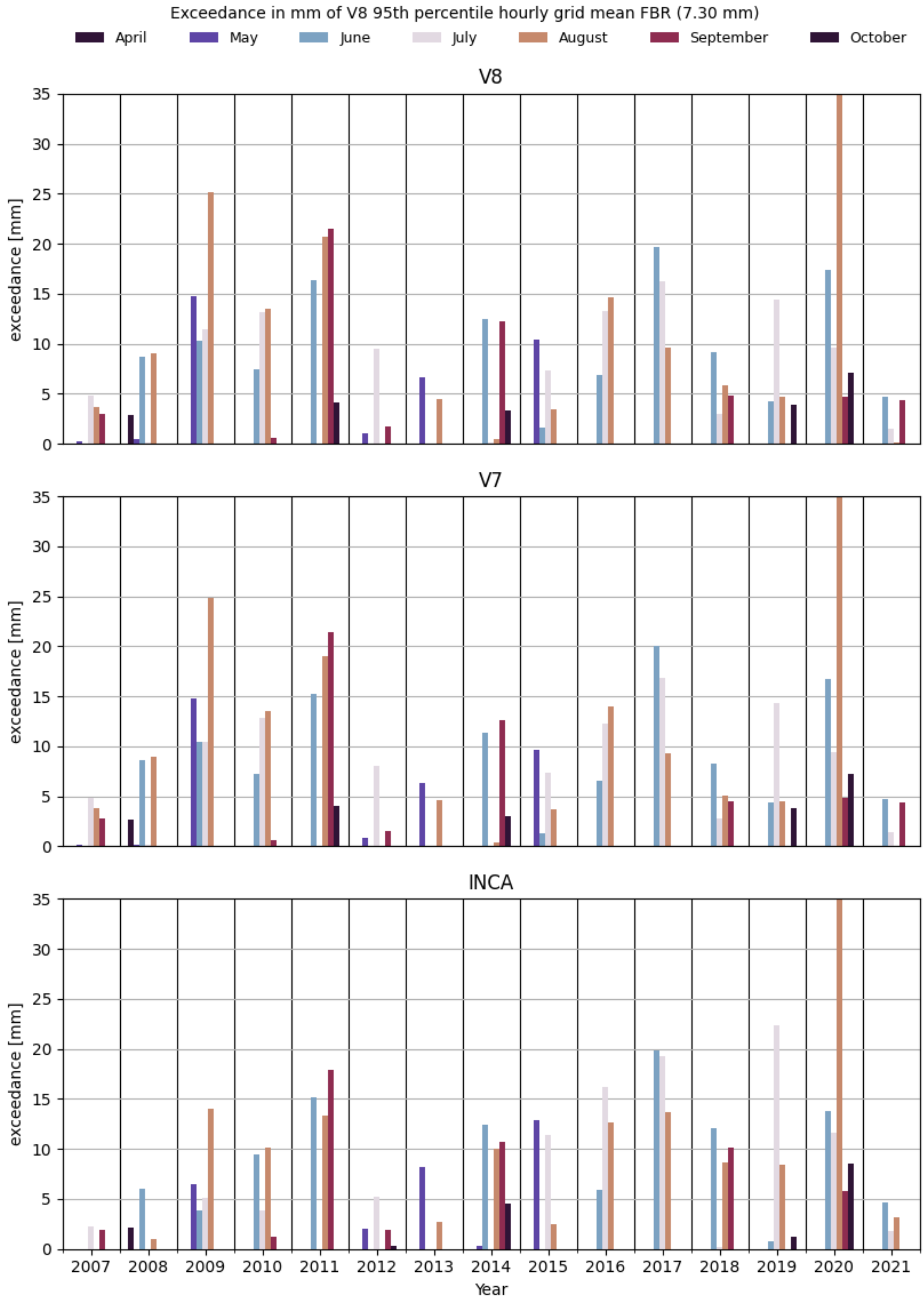

Figure 4.31: Precipitation exceedance amount - 1H / whole Region.

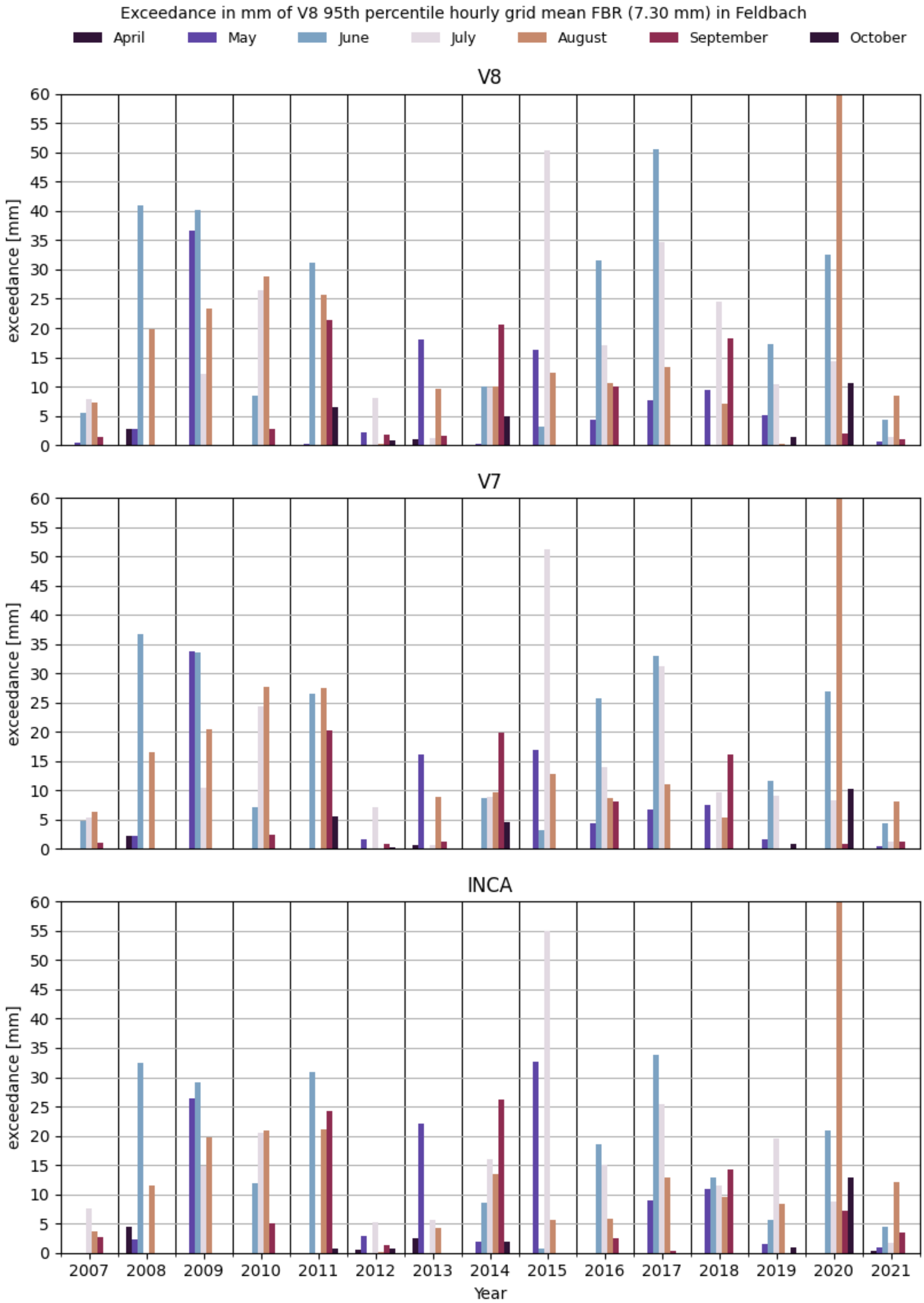

Figure 4.32: Precipitation exceedance amount - 1H / Feldbach station.

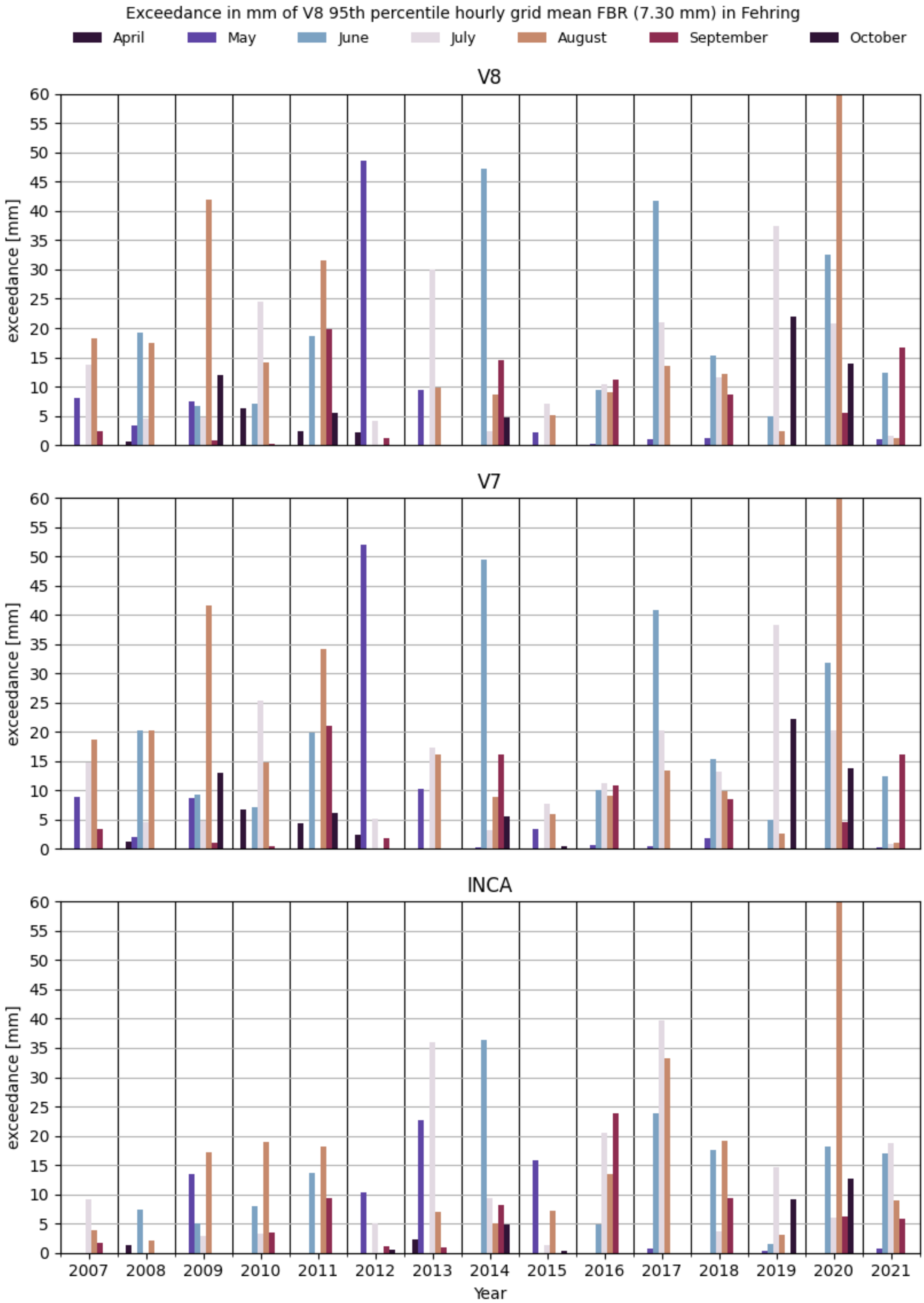

Figure 4.33: Precipitation exceedance amount - 1H / Fehring station.

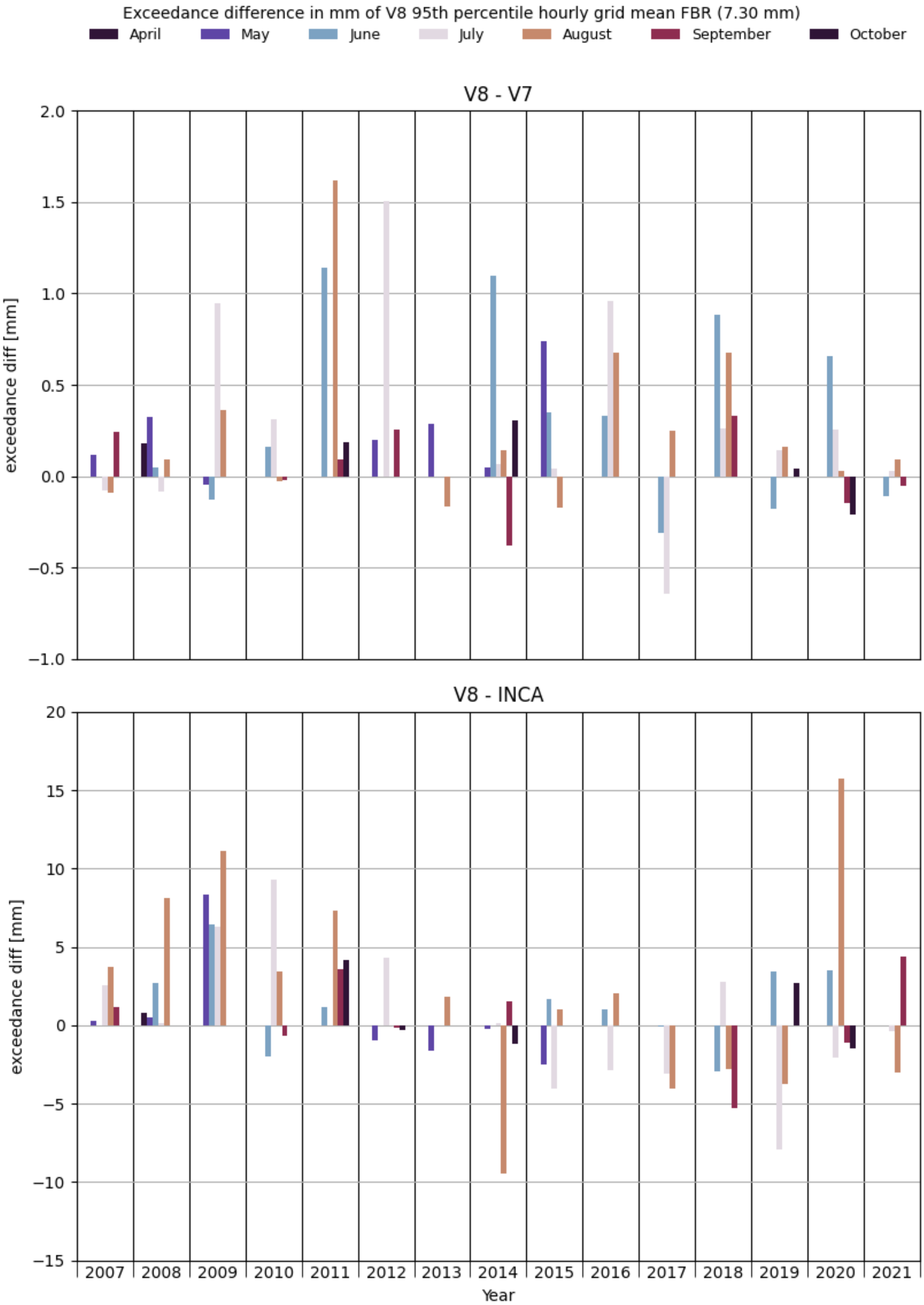

Figure 4.34: Precipitation exceedance difference - 1H / whole Region.

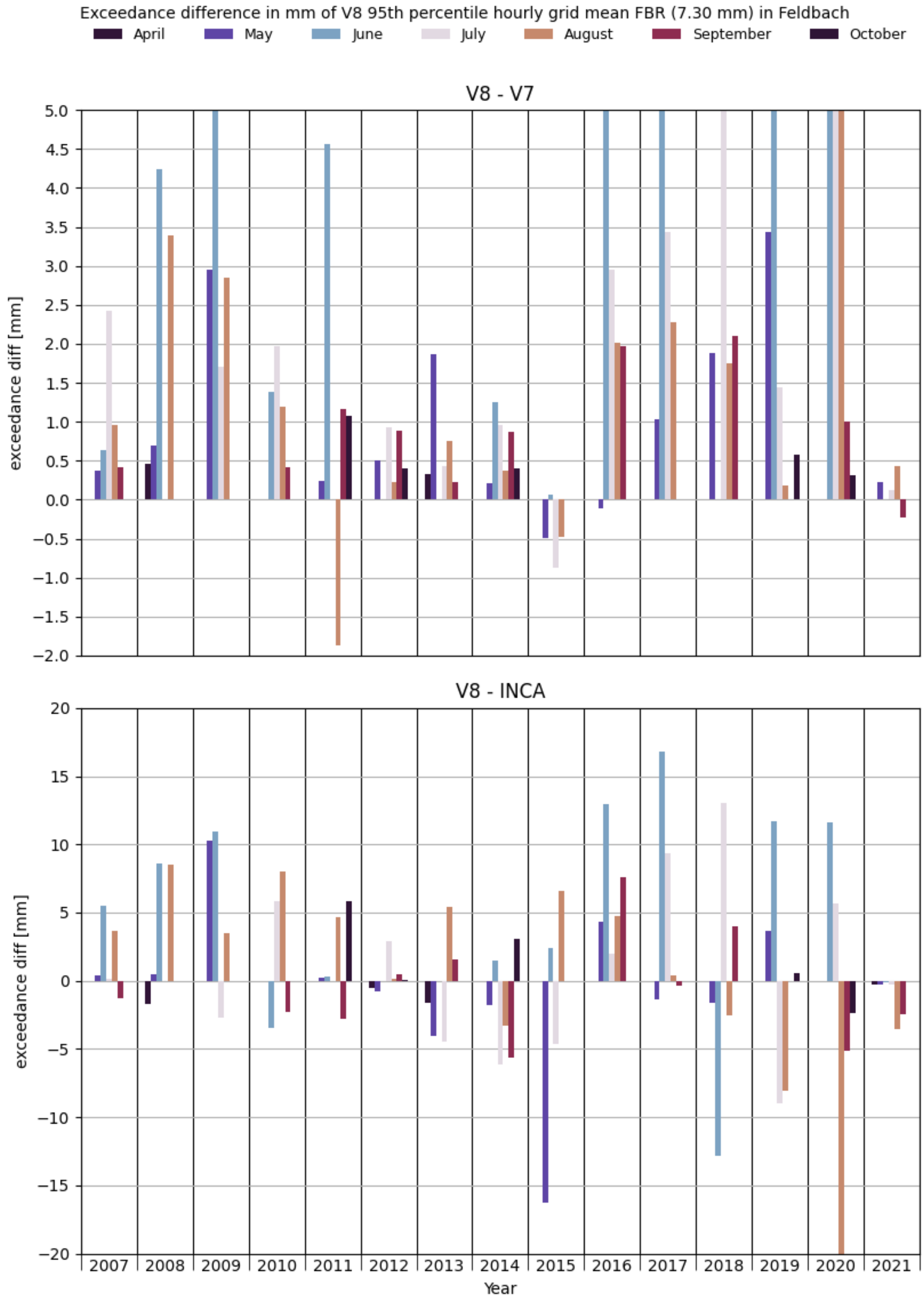

Figure 4.35: Precipitation exceedance difference - 1H / Feldbach station.

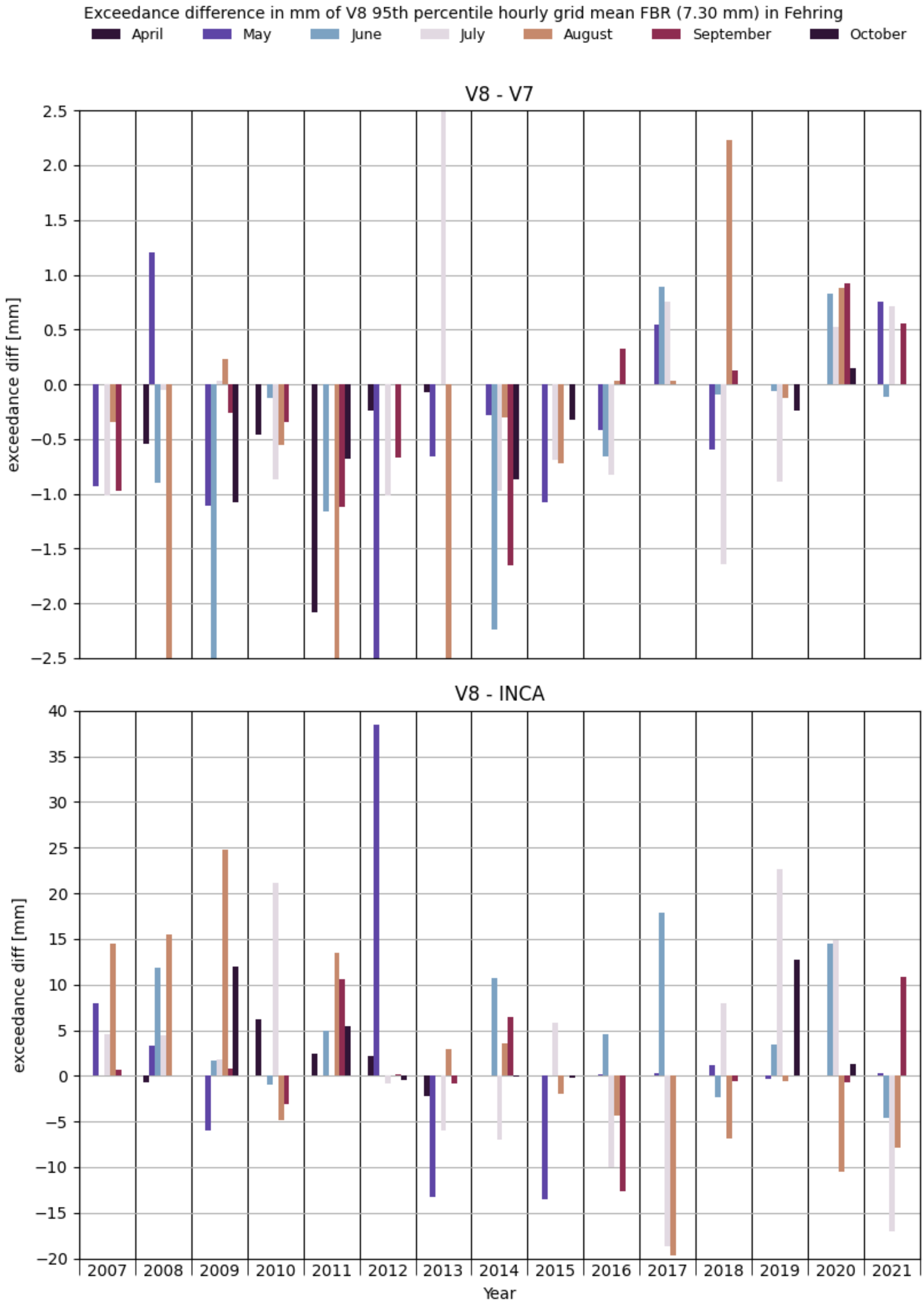

Figure 4.36: Precipitation exceedance difference - 1H / Fehring station.

4.5 Limitations of the analyses

The applied homogenization methods are subject to two main constraints. First, the breakpoint detection algorithm is not stable against repetition for higher order breakpoints close to the acceptance threshold in dependence of the bootstraps. Second, the correction of ANBS stations can lead to over correction in some cases.
The first described problem was also found in the analysis of Ebner (2017) but was significantly improved by Scheidl et al. (2020) in updating the acceptance criterion in the algorithm to Equation (3.4), making it independent of single boot strap outliers. While this minimized the repeatability issues described in detail by Scheidl et al. (2020), the present implementation still contains repeatability problems for higher order breakpoints close to the set threshold.

However, this weakness is accepted for several reasons. First, the focus in this analysis is on first-order breakpoints (primary BP). Second- and third-order BPs to further divide the respective time series were rarely applied and thus needed. Second, the graphical representation of the sum function visualizes all conspicuous points in the time series as well as all bootstraps, regardless of acceptance, so cross checks are possible. Third, breakpoints due to sensor changes are double-checked by the regression analysis anyway. Nevertheless, improvement is conceivable through a higher number of bootstraps or a filter for bootstrap outliers, but can be computationally expensive.
The second weakness can be described as follows. If a station shows no need for correction after the regression analysis (deviation of the slope between before and after sensor change is not more than 0.05), this may not be the case after correction in some cases. Since the ANBS stations are used as a reference, corrections may occur for them as well. Thus, if only a few data points are responsible for not exceeding the 5% mark due to the distribution of scatter points in the regression analysis, a slight change in these data points due to the ANBS correction may be sufficient to overcome the deviation threshold after the correction. Therefore, a second regression analysis after correction is recommended to detect such overcorrections and to counteract them if necessary.

4.6 Re-correction of the precipitation data

Due to the limitation described in the previous chapter and the remaining of conspicuous stations when analyzing grid decadal data, see Figure 4.6 and Figure 4.38, the regression analysis was carried out a second time on the v8 data, and correction factors were obtained in the same manner as outlined in Section 4.2. To avoid unrealistic changes to the probability distribution of the rain rates, a histogram analysis was used to check if the obtained correction factors are acceptable. The correction is considered acceptable, if the distribution of heavy precipitation ($\geq$ 2 mm / 5 min), faces no strong distortion by the correction and is an improvement in comparison to the uncorrected data and the reference. As reference, a Meteoservis time series of an ANBS station with a slope close to 1.0 was used. Figure 4.37 shows the histogram for example station 34. The correction factors proposed for this station before (top) and after (bottom) the sensor change resulted in a convergence of the corrected data (green) to the reference (gray) compared to the uncorrected data (blue) for most bins. Since the distribution is shifted, this is not true for all bins.

Overall, however, the distribution is closer to the reference in most bins and is therefore accepted. To further ensure that overcorrection does not occur and regional differences are not distorted, the results are compared to the decadal mean of annual precipitation in the region, see panel (a) in Figure 4.38. Stations that overestimate or underestimate precipitation compared to their neighbors (dark red and blue dots), e.g., station 34 and 57, are visible and can be cross-checked with the results of the regression analysis. Only if a station appears suspicious in fig. 4.38 panel (a) the proposed and quantified correction factor by the regression analysis is accepted. If a station appears conspicuous in Figure 4.38 but does not exceed the threshold for correction according to the result of the regression analysis, it is corrected nevertheless. However, this remains an exception. In the case that the regression analysis specifies a correction factor for a station and time series that has already been corrected, the final correction factor is calculated as follows:

$$x = (1 + y) * (1 + z) - 1 \tag{4.1}$$

where

$$x = \text{final correction factor}$$
$$y = \text{preliminary correction factor}$$
$$z = \text{re-correction factor}$$

By applying the correction factors obtained in this manner, a further improvement in the homogeneity of the data can be achieved. The previously dark red and dark blue spots in panel (a) of Figure 4.38, have largely disappeared after the re-correction, see panel (b). This demonstrates that the still existing strongly deviating stations have now also been corrected and an even more homogeneous pattern has emerged overall. Furthermore, the regional differences remain largely intact, giving no indication of overcorrection.

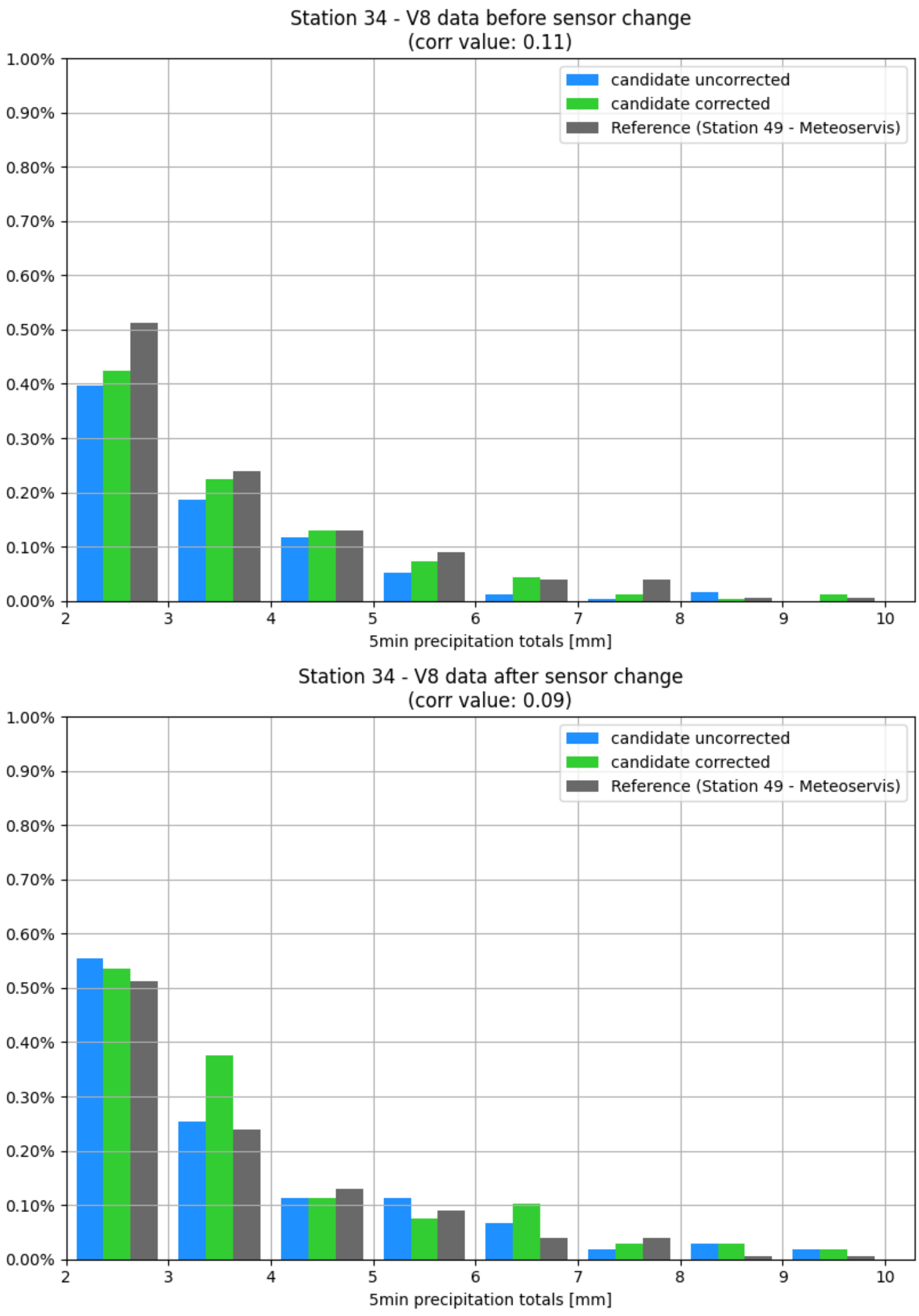

Figure 4.37: Partial histogram of example station 34 (bins $\geq$ 2 mm / 5 min).

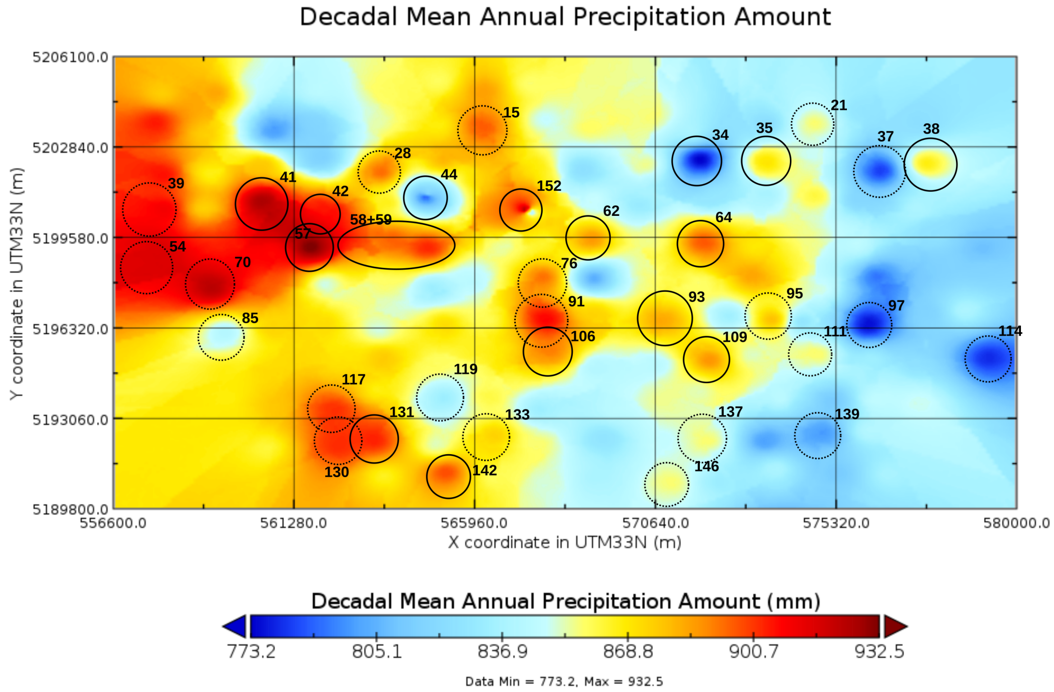

(a) Before re-correction

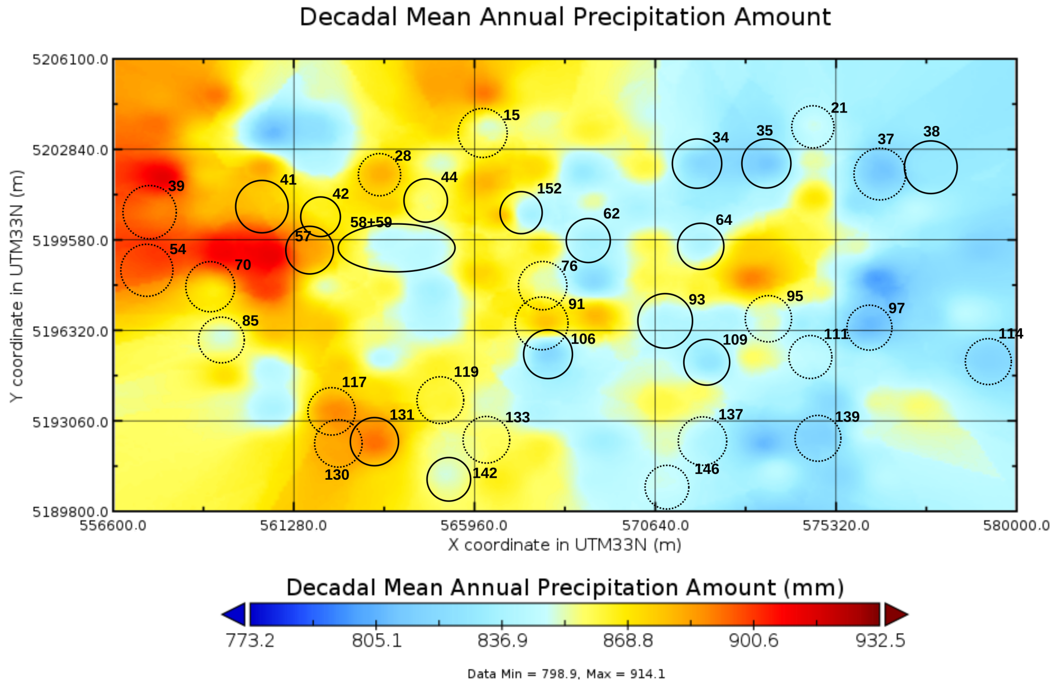

(b) After re-correction

Figure 4.38: Decadal mean annual precipitation amount (v8 Data) and conspicuous stations before (a) and after (b) the re-correction.

The final correction values we recommend for homogenizing the WegenerNet v8 data, merging the preliminary factors of Table 4.2 and the obtained re-correction factors as described above, are provided in Table 4.5 below.

Station	Begin	End	Correction factor
3	2007-01-01	2016-07-05	0.09
4	2007-01-01	2011-04-12	-0.06
4	2011-04-12	2016-07-06	-0.12
5	2007-01-01	2011-05-15	0.09
6	2007-01-01	2016-07-08	-0.04
7	2007-01-01	2016-07-08	0.08
8	2009-05-24	2016-07-08	-0.05
9	2016-07-05	2099-12-31	-0.06
10	2007-01-01	2016-07-05	0.16
10	2016-07-05	2099-12-31	-0.05
11	2007-01-01	2013-10-07	0.05
13	2007-01-01	2016-07-06	0.05
15	2007-01-01	2016-07-08	0.03
15	2016-07-08	2099-12-31	-0.06
16	2009-05-22	2016-07-08	-0.08
17	2007-01-01	2011-07-02	0.06
18	2007-01-01	2015-05-07	-0.05
19	2007-01-01	2011-08-09	-0.09
20	2014-07-10	2016-08-08	-0.06
21	2016-08-19	2099-12-31	-0.05
22	2018-06-08	2018-09-01	-0.15
22	2018-09-01	2099-12-31	-0.08
23	2007-01-01	2011-08-27	-0.11
24	2007-01-01	2016-07-05	0.06
25	2016-07-05	2099-12-31	-0.06
27	2007-01-01	2016-07-04	-0.09
28	2016-07-09	2099-12-31	-0.06
29	2007-01-01	2099-12-31	-0.05
30	2007-01-01	2010-05-13	0.03
31	2014-10-01	2016-07-09	-0.08
32	2008-04-29	2013-10-07	0.06
34	2007-01-01	2016-07-09	-0.04
34	2016-07-09	2099-12-31	0.09
35	2016-08-08	2099-12-31	-0.09
35	2007-01-01	2016-08-08	-0.08
36	2015-02-22	2016-08-09	-0.05
37	2007-04-01	2013-10-18	-0.04
37	2013-10-10	2018-05-16	0.06
38	2016-08-09	2099-12-31	-0.06
39	2016-07-05	2019-05-09	0.04
39	2019-05-09	2099-12-31	-0.09
40	2007-01-01	2009-07-05	-0.08
40	2009-07-05	2016-07-05	0.12
41	2007-01-01	2016-07-06	-0.08
41	2016-07-06	2099-12-31	-0.06
42	2007-01-01	2013-08-24	0.11
42	2013-08-24	2016-07-06	0.03
42	2016-07-06	2099-12-31	-0.06
44	2007-01-01	2011-07-22	0.19
44	2011-07-22	2013-10-08	0.34
44	2013-10-08	2018-06-12	0.23
44	2018-06-12	2099-12-31	0.12
45	2016-08-27	2099-12-31	-0.05
46	2007-01-01	2016-08-29	0.06
47	2007-01-01	2015-03-02	-0.07
48	2007-01-01	2016-07-05	-0.09
50	2007-01-01	2016-08-29	0.08
51	2007-01-01	2016-08-09	0.07
52	2012-07-14	2015-03-02	0.05
53	2007-01-01	2016-08-09	-0.11
54	2016-07-05	2099-12-31	-0.06
57	2007-01-01	2016-07-06	-0.07
57	2016-07-06	2099-12-31	-0.06
58	2016-08-22	2099-12-31	-0.09
58	2007-01-01	2016-08-22	-0.06
59	2007-01-01	2016-08-22	0.01
59	2016-08-22	2099-12-31	-0.06
60	2018-05-29	2021-12-17	0.14
61	2007-01-01	2013-05-05	0.06
61	2013-05-05	2016-08-28	0.05
62	2012-11-12	2016-08-27	-0.03
62	2007-01-01	2012-11-12	-0.08
62	2016-08-27	2099-12-31	-0.06
64	2007-01-01	2016-07-05	-0.04
64	2016-07-05	2099-12-31	-0.07
66	2007-01-01	2016-08-29	-0.08
68	2011-04-12	2016-08-09	-0.06
69	2007-01-01	2016-08-09	0.07
70	2012-02-19	2016-08-22	-0.07
70	2016-08-22	2099-12-31	-0.09
71	2007-01-01	2011-06-23	0.12
71	2011-06-23	2016-08-22	0.05
72	2007-01-01	2013-10-05	-0.05
75	2007-01-01	2016-08-24	-0.09
76	2007-01-01	2016-08-28	-0.05
76	2016-08-28	2099-12-31	-0.07
77	2007-01-01	2014-01-14	-0.08
77	2017-10-11	2099-12-31	-0.07
78	2007-01-01	2014-07-25	0.07
78	2014-07-25	2016-08-27	0.25
80	2018-06-06	2099-12-31	-0.05
82	2007-01-01	2009-06-27	-0.07
83	2007-01-01	2016-08-10	-0.1
84	2017-06-10	2099-12-31	-0.06
85	2007-01-01	2013-05-05	0.23
85	2012-07-29	2013-05-05	0.15
87	2012-10-01	2016-08-22	-0.08
88	2016-01-06	2016-08-22	-0.05
88	2016-08-22	2099-12-31	-0.07
89	2007-01-01	2012-10-29	-0.06
89	2012-10-29	2016-08-24	-0.11
89	2016-08-24	2099-12-31	-0.05
90	2007-01-01	2016-08-28	-0.09
91	2013-06-24	2016-08-21	-0.12
93	2016-08-29	2018-07-15	-0.13
93	2007-01-01	2016-08-29	-0.07
93	2018-07-15	2099-12-31	-0.06
95	2007-01-01	2016-08-29	-0.07
96	2007-01-01	2016-08-27	0.08
97	2007-01-01	2016-08-27	0.08
98	2007-01-01	2010-08-08	-0.03
98	2010-08-08	2016-08-21	0.07
101	2018-09-23	2021-12-15	-0.24
101	2013-10-16	2018-09-23	-0.06
103	2007-01-01	2099-12-31	-0.05
104	2016-08-24	2099-12-31	-0.06
105	2007-01-01	2010-03-22	0.05
105	2014-10-23	2016-06-28	0.05
106	2007-01-01	2016-08-28	-0.07
106	2016-08-28	2099-12-31	-0.07
107	2007-01-01	2014-09-26	0.05
107	2017-07-01	2099-12-31	-0.07
109	2016-08-29	2099-12-31	-0.06
111	2007-01-01	2016-08-26	-0.05
111	2016-08-26	2099-12-31	-0.06
112	2007-01-01	2008-06-20	-0.05
113	2008-06-30	2014-11-14	0.05
113	2014-11-14	2016-08-23	0.17
114	2007-01-01	2016-08-23	0.1
115	2016-08-23	2099-12-31	-0.05
116	2007-01-01	2012-07-24	0.08
116	2016-08-23	2099-12-31	-0.06
117	2016-08-25	2099-12-31	-0.05
119	2007-01-01	2008-11-30	-0.07
119	2018-02-08	2019-09-02	-0.13
119	2019-09-02	2099-12-31	-0.04
119	2008-11-30	2016-08-28	0.05
120	2016-08-28	2099-12-31	-0.05
121	2007-01-01	2016-08-25	-0.06
123	2007-01-01	2016-08-29	-0.05
125	2016-08-24	2099-12-31	-0.05
126	2008-06-23	2016-08-23	0.1
126	2017-07-24	2099-12-31	-0.07
127	2009-10-01	2016-08-23	0.08
128	2007-01-01	2016-08-23	-0.06
129	2011-09-18	2016-08-08	0.08
130	2016-08-25	2099-12-31	-0.07
131	2007-04-03	2009-12-22	-0.09
131	2016-08-25	2099-12-31	-0.05
133	2007-04-03	2016-08-25	-0.05
134	2014-06-03	2016-08-25	-0.06
135	2007-01-01	2010-08-15	-0.16
137	2016-08-26	2017-12-10	-0.06
137	2007-01-01	2016-08-26	-0.06
139	2007-01-01	2012-04-22	-0.25
139	2012-04-22	2013-10-21	-0.03
142	2007-01-01	2016-08-25	0.05
142	2016-08-25	2019-08-02	-0.13
143	2007-01-01	2007-08-10	-0.13
143	2014-02-11	2016-08-25	-0.07
145	2007-01-01	2009-01-16	0.09
145	2009-01-16	2016-08-26	0.2
146	2016-08-28	2099-12-31	-0.05
148	2007-01-01	2016-08-24	0.05
152	2014-06-03	2020-08-23	-0.19
7730	2015-07-10	2018-08-10	0.06
7730	2018-08-10	2099-12-31	-0.06
7731	2007-01-01	2013-10-16	-0.29

Table 4.5: Final correction factors.

5 Conclusion

Most regions of the northern hemisphere have experienced a climate change-driven increase in one- and five-day heavy precipitation since the 1950s, with the proportion of stations with significant increases varying widely among regions (IPCC 2021, Sun et al. 2021). Simultaneously, losses in assets due to hydrological events are increasing (Munich Re 2020). High-resolution precipitation data are therefore of great value. The high density ground weather station network WegenerNet Feldbach Region (FBR) provides such data continuously since 2007. Inhomogeneities are inevitable when providing precipitation data from many stations with high temporal resolution.

The main purpose of this thesis consequently was to improve the quality of the data by homogenization and to compare the information content of extreme precipitation in the data to the standard data sets SPARTACUS, ERA5, ERA5-Land, and INCA.
By adapting the method of Scheidl et al. (2020) resp. Taylor (2000) to the homogenization of precipitation data, breakpoints in the WegenerNet L2 v7.1 daily data were detected by comparing the time series of all stations with those of selected neighboring stations. The primary breakpoints identified are summarized in Table 4.1. Based on these breakpoints, a regression analysis was performed to quantify the deviation from selected neighboring stations, referred to as Agreeing Neighboring Stations (ANBS). These values were used as linear correction factors to homogenize the WegenerNet data L2 v7.1.

It was found that especially sensors installed before 2016 and thus in operation before a major upgrade of most stations, changing Friedrichs and Young to Meteoservis sensors, needed correction. This finding supports the argument for the switch to Meteoservis gauges as primary sensors. The application of the proposed correction factors leads to a quantifiable quality improvement, for details see Section 4.3 and Section 4.4. As a result the data are significantly more homogeneous. In general, the correction results in an increase in precipitation amounts compared to the uncorrected data when analyzing the grid mean annual precipitation over 15 years, see Figure 4.6, and the differences in monthly precipitation amounts, see Figure 4.10. This trend is more pronounced through 2016, as sensors that were in operation prior to the switch to Meteoservis faced a significant negative bias.

In order to ensure that no overcorrection was introduced, and because it became apparent, e.g. in Figure 4.38, that some stations still deviated strongly from the neighboring stations, the used methods were applied again on the corrected data in Section 4.6. The merged correction factors of the preliminary values and the ones obtained in the re-correction are proposed as quality improvement for the new WegenerNet data version

L2 v8 and are documented in Table 4.5.

When analyzing the differences from the standard datasets regarding the mean annual precipitation amount over 15 years in the FBR (Section 4.4), it was found that the comparative datasets all underestimate precipitation. Furthermore, little spatial differences are present in the ERA5 and ERA5-land data. Spatial patterns are however evident in the SPARTACUS data that overlap with the pattern in the WegenerNet data.

With respect to the comparative analysis between v8 and v7.1 extreme precipitation, the following can be stated. Compared to the uncorrected v7.1 data, there are only small differences. However, since most sensors showed a negative bias, all relevant parameters, 24HMMax, 1HMMax, and the analyzed exceedance amounts tend to show slightly higher values after correction.

In the ERA5 and ERA5-Land data, a negative bias is consistently seen in the 24HMMax measure. In certain months, the deviation from the WegenerNet data is more than 100 %. Hence, individual 24-hour extreme precipitation events are not accurately represented in these data sets. The difference between ERA5 and ERA5-Land is small, but the ERA5-Land data agrees consistently better with the WegenerNet data. For the SPARTACUS data however, the agreement with the WegenerNet data is clearly more significant, which can be explained by the higher spatial resolution compared to the ERA5 and ERA5-Land data. Nevertheless, it is also evident here that individual 24-hour extreme precipitation events are not or only inadequately represented compared to the WegenerNet data, with intensity differences of well over 100 %.

Concerning the 1HMMax parameter, the INCA data showed a negative bias compared to the WegenerNet data up to the year 2013 (this is consistent with the findings of Ghaemi et al. (2021)). Thereafter, this bias is significantly less pronounced. In addition, although less common, there are mismatches where a 1HMMax event is not reflected in the INCA data, similar to the other data sets and the 24HMMax measure. Concerning the exceedance of the 95th percentile of the 24-hour amounts, the ERA5 and ERA5-Land data showed hardly any exceedance amount. In contrast, the SPARTACUS data showed a very similar distribution of the quantities over time compared to the WegenerNet data. However, the exceedance amounts are lower than in the WegenerNet data. With regard to the exceedance of the 95th percentile of the 1-hour precipitation amounts, the INCA data showed no bias after 2013 and a very similar picture to the WegenerNet data. Before that, however, as with the 1HMMax values, a slightly negative bias can be identified.

If extreme precipitation events are to be analyzed at the regional level or for specific locations with the analyzed datasets as a basis, it is advisable to crosscheck events or the period under observation with nearby ground stations. Events that occur on small spatial scales, but lead to significant precipitation amounts in the region, are not always represented in model-based and/or reanalysis data, according to the evidence provided in this thesis.

List of Figures

List of Tables

Bibliography

Ebner, S. (2017), Analysis and Homogenization of WegenerNet Temperature and Humidity Data and Quality Evaluation for Climate Trend Studies, Sci. Rep. No.70-2017, ISBN 978-3-9503918-9-3, Wegener Center Verlag, Graz, Austria. `https://static.uni-graz.at/fileadmin/urbi-zentren/Wegcenter/9.WegCenterVerlag/2017/WCV-SciRep-No70-SEbner-Aug2017.pdf`.

Fuchsberger, J., Kirchengast, G., Bichler, C., Leuprecht, A. & Kabas, T. (2021), *WegenerNet climate station network Level 2 data version 7.1 (2007–2020)*, Wegener Center for Climate and Global Change, University of Graz. `https://doi.org/10.25364/WEGC/WPS7.1:2021.1`.

Fuchsberger, J., Kirchengast, G. & Kabas, T. (2021), 'Wegenernet high-resolution weather and climate data from 2007 to 2020', *Earth System Science Data* **13**, 1307–1334.

Ghaemi, E., Foelsche, U., Kann, A. & Fuchsberger, J. (2021), 'Evaluation of Integrated Nowcasting through Comprehensive Analysis (INCA) precipitation analysis using a dense rain-gauge network in southeastern Austria', *Hydrol. Earth Syst. Sci.* **25**(8), 4335–4356.

Haiden, T., Kann, A., Wittmann, C., Pistotnik, G., Bica, B. & Gruber, C. (2011), 'The integrated nowcasting through comprehensive analysis (inca) system and its validation over the eastern alpine region', *Weather and Forecasting* **26**, 166–183.

Hersbach, H., Bell, B., Berrisford, P., Biavati, G., Horányi, A., Sabater, J. M., Nicolas, J., Peubey, C., Radu, R., Rozum, I., Schepers, D., Simmons, A., Soci, C., Dee, D. & Thépaut, J.-N. (2018), *ERA5 hourly data on single levels from 1979 to present*, Copernicus Climate Change Service (C3S) Climate Data Store (CDS). `https://doi.org/10.24381/cds.adbb2d47`,.

Hersbach, H., Bell, B., Berrisford, P., Hirahara, S., Horányi, A., Muñoz-Sabater, J., Nicolas, J., Peubey, C., Radu, R., Schepers, D., Simmons, A., Soci, C., Abdalla, S., Abellan, X., Balsamo, G., Bechtold, P., Biavati, G., Bidlot, J., Bonavita, M., De Chiara, G., Dahlgren, P., Dee, D., Diamantakis, M., Dragani, R., Flemming, J., Forbes, R., Fuentes, M., Geer, A., Haimberger, L., Healy, S., Hogan, R. J., Hólm, E., Janisková, M., Keeley, S., Laloyaux, P., Lopez, P., Lupu, C., Radnoti, G., de Rosnay, P., Rozum, I., Vamborg, F., Villaume, S. & Thépaut, J.-N. (2020), 'The era5 global reanalysis', *Quarterly Journal of the Royal Meteorological Society* **146**(730), 1999–2049.

Hiebl, J. & Frei, C. (2018), 'Daily precipitation grids for austria since 1961—development and evaluation of a spatial dataset for hydroclimatic monitoring and modelling', *Theoretical and Applied Climatology* **132**, 327–345.

IPCC (2021), Summary for policymakers, *in* 'Climate Change 2021: The Physical Science Basis. Contribution of Working Group I to the Sixth Assessment Report of the Intergovernmental Panel on Climate Change', Cambridge University Press.

Kabas, T. (2012), WegenerNet Klimastationsnetz Region Feldbach: Experimenteller Aufbau und hochauflösende Daten für die Klima- und Umweltforschung, Sci. Rep. No.47-2012, ISBN 978-3-9503112-4-2, Wegener Center Verlag, Graz, Austria. `http://wegcwww.uni-graz.at/publ/wegcreports/2012/WCV-WissBer-No47-TKabas-Jan2012.pdf`.

Kirchengast, G., Kabas, T., Leuprecht, A., Bichler, C. & Truhetz, H. (2014), 'WegenerNet: A Pioneering High-Resolution Network for Monitoring Weather and Climate', *Bull. Am. Meteorol. Soc.* **95**(2), 227–242.

Meteoservis (2022), MR3(xx) a MR3H(xx) Rain Gauges. `https://www.meteoservis.cz/en/63-TB-RAIN-GAUGES/78-MR3-xx-and-MR3H-xx` [Accessed: October 9, 2022].

Munich Re (2020), '*Natural disaster risks: Losses are trending upwards*'. `https://www.munichre.com/en/risks/natural-disasters-losses-are-trending-upwards.html` [Accessed: October 9, 2022].

Muñoz Sabater, J. (2019), *ERA5-Land hourly data from 1981 to present*, Copernicus Climate Change Service (C3S) Climate Data Store (CDS). `https://doi.org/10.24381/cds.e2161bac`.

Nerini, D., Zulkafli, Z., Wang, L. P., Onof, C., Buytaert, W., Lavado-Casimiro, W. & Guyot, J. L. (2015), 'A comparative analysis of trmm-rain gauge data merging techniques at the daily time scale for distributed rainfall-runoff modeling applications', *Journal of Hydrometeorology* **16**, 2153–2168.

O, S., Foelsche, U., Kirchengast, G. & Fuchsberger, J. (2018), 'Validation and correction of rainfall data from the wegenernet high density network in southeast austria', *Journal of Hydrology* **556**, 1110–1122.

O, S., Foelsche, U., Kirchengast, G., Fuchsberger, J., Tan, J. & Petersen, W. A. (2017), 'Evaluation of gpm imerg early, late, and final rainfall estimates using wegenernet gauge data in southeastern austria', *Hydrology and Earth System Sciences* **21**, 6559–6572.

Scheidl, D., Fuchsberger, J. & Kirchengast, G. (2020), Analysis of wegenernet temperature and humidity data and recommendations for long-term homogeneity, WegenerNet Sci. Rep. No.01-2020, Graz, Austria. `https://wegenernet.org/downloads/Scheidl-etal_2020_TQ_homogenization.pdf`.

Sharifi, E., Steinacker, R. & Saghafian, B. (2016), 'Assessment of gpm-imerg and other precipitation products against gauge data under different topographic and climatic conditions in iran: Preliminary results', *Remote Sensing* **8**(2), 135.

Sun, Q., Zhang, X., Zwiers, F., Westra, S. & Alexander, L. V. (2021), 'A global, continental, and regional analysis of changes in extreme precipitation', *Journal of Climate* **34**(1), 243–258.

Szeberényi, K. (2014), Analysis of WegenerNet Precipitation Data and Quality Evaluation for Case Studies and Climatologies, Sci. Rep. No.58-2014, ISBN 978-3-9503608-5-1, Wegener Center Verlag, Graz, Austria. `http://wegcwww.uni-graz.at/publ/wegcreports/2014/WCV-SciRep-No58-KSzeberenyi-Mar2014.pdf`.

Taylor, W. (2000), Change-Point Analysis: A Powerful New Tool For Detecting Changes, Taylor Enterprises, Inc. `https://variation.com/wp-content/uploads/change-point-analyzer/change-point-analysis-a-powerful-new-tool-for-detecting-changes.pdf` [Accessed: October 9, 2022].

Theodor Friedrichs & Co (2022), Precipitation Sensor 7041.0000 BG. `http://www.th-friedrichs.de/assets/ProductPage/ProductDownload/E7041.pdf` [Accessed: October 9, 2022].

Young (2022), Model 52202 Tipping Bucket Rain Gauge. `https://www.youngusa.com/wp-content/uploads/2008/01/5220228081429.pdf` [Accessed: October 9, 2022].